

Durham E-Theses

The crystal structures of some coordination compounds of group II metals

Moseley, P. T.

How to cite:

Moseley, P. T. (1968) *The crystal structures of some coordination compounds of group II metals*, Durham theses, Durham University. Available at Durham E-Theses Online:
<http://etheses.dur.ac.uk/8775/>

Use policy

The full-text may be used and/or reproduced, and given to third parties in any format or medium, without prior permission or charge, for personal research or study, educational, or not-for-profit purposes provided that:

- a full bibliographic reference is made to the original source
- a [link](#) is made to the metadata record in Durham E-Theses
- the full-text is not changed in any way

The full-text must not be sold in any format or medium without the formal permission of the copyright holders.

Please consult the [full Durham E-Theses policy](#) for further details.

THE CRYSTAL STRUCTURES OF SOME COORDINATION
COMPOUNDS OF GROUP II METALS

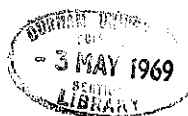
by

P.T. Moseley, B.Sc.

A Thesis Submitted for the Degree of
Doctor of Philosophy

University College, Durham

September, 1968.



PREFACE

This thesis describes research in chemical crystallography carried out in the Chemistry Department of the University of Durham between October, 1965 and September, 1968.

I wish to express my sincere thanks to Dr. H.M.M. Shearer, under whose direction this research was undertaken, for his invaluable guidance and encouragement. I am also indebted to Professor G.E. Coates for the interest he has shown, and to Dr. N.A. Bell for the provision of crystals of one of the compounds.

I gratefully acknowledge the award of a Science Research Council Studentship.

CONTENTS

<u>PREFACE</u>	ii
----------------	----

SUMMARY

CHAPTER ONE

THE DETERMINATION OF CRYSTAL STRUCTURES

1.1	The Crystal Lattice	1
1.2	The Diffraction of X-rays by a Crystal Lattice	2
1.3	The Structure Factor	3
1.4	The Temperature Factor	7
1.5	Fourier Series	9
1.6	The Patterson Function	12
1.7	The Heavy Atom Method	13
1.8	Structure Refinement	15
1.9	Accuracy of parameters derived from least squares refinement	18
1.10	Termination of Series Effects and Absorption Errors	19
	Bibliography	22

CHAPTER TWO

SOME ASPECTS OF THE ORGANOMETALLIC AND HYDRIDE CHEMISTRY OF ZINC
AND MAGNESIUM

2.1	Introduction	23
2.2	Internal Co-ordination Complexes of Magnesium and Zinc Alkyls	23

2.2.i	Complexes with 1-atom donor groups	
	a) From reactions with amines	26
	b) From reactions with alcohols	28
	c) From reactions with thiols	29
	d) Halides	32
2.2.ii	Complexes with 2-atom donor groups	33
2.3	The Constitution of Ethylzinc Halides in solution	37
2.4	The Reaction of Grignard Reagents with Ketones	41
2.5	Zinc and Magnesium Hydrides	46

CHAPTER THREE

THE CRYSTAL STRUCTURE OF ETHYLZINC IODIDE

3.1	Introduction	48
3.2	Preparation	49
3.3	Crystal Data	50
3.4	Data Collection	51
3.5	Structure Determination	
	a) Heavy Atom Positions	52
	b) Carbon Atom Positions	55
3.6	Structure Refinement	57
3.7	Test of the Space Group	61
3.8	Description of Structure	61
3.9	The Polymerisation of Unsolvated Alkyl group IIb Halides	70

CHAPTER FOUR

THE CRYSTAL STRUCTURE OF THE DIETHYL ETHER COMPLEX OF TERTIARY-
BUTOXYMAGNESIUM BROMIDE

4.1	Introduction	75
4.2	Crystal Data	76
4.3	Data Collection and Correction	77
4.4	The Patterson Function	77
4.5	Light Atom Positions	79
4.6	Refinement	80
4.7	Description and Discussion of Structure	85
4.8	Stereochemistry of Compounds $(\text{Bu}^t\text{OMBr}\cdot\text{OEt}_2)_2$ (where M is Mg or Be)	96

CHAPTER FIVE

THE CRYSTAL STRUCTURE OF DIMERIC 2-DIMETHYLAMINOETHYLMETHYL-
AMINOZINC HYDRIDE

5.1	Introduction	100
5.2	Crystal Data	100
5.3	Data Collection and Correction	101
5.4	Patterson Function	103
5.5	Light Atom Positions	104
5.6	Refinement	104
5.7	Absorption Correction	108
5.8	Description and Discussion of Structure	113
5.9	The Zinc-Hydrogen Bond	123

APPENDIX 1

Isothermal Molecular Weight Measurement 126

APPENDIX 2

Computer Programmes 130

REFERENCES

131

LIST OF TABLES

TABLE 3a.	EtZnI, Least-Squares Totals and Weighting Analysis	59
TABLE 3b.	EtZnI, Final Values of Atomic Co-ordinates and their Standard Deviations, Final Values of Anisotropic Temperature Parameters and their Standard Deviations	60
TABLE 3c.	EtZnI, Final Values of the Observed and Calculated Structure Factors	74
TABLE 3d.	EtZnI, Bond Lengths and their Standard Deviations, Bond Angles and their Standard Deviations	66
TABLE 3e.	EtZnI, Non-bonding Intermolecular Contacts Less than 4.33\AA	68
TABLE 4a.	$(\text{Bu}^t\text{OMgBr.OEt}_2)_2$, Final Values of Atomic Co-ordinates and their Standard Deviations	82
TABLE 4b.	$(\text{Bu}^t\text{OMgBr.OEt}_2)_2$, Final Values of Anisotropic Temperature Parameters and their Standard Deviations	83
TABLE 4c.	$(\text{Bu}^t\text{OMgBr.OEt}_2)_2$, Least-Squares Totals and Weighting Analysis	84
TABLE 4d.	$(\text{Bu}^t\text{OMgBr.OEt}_2)_2$, Final Values of the Observed and Calculated Structure Factors	99
TABLE 4e.	$(\text{Bu}^t\text{OMgBr.OEt}_2)_2$, Summary of Mean Planes through the Oxygen atoms and the atoms bonded to Oxygen	87

TABLE 4f.	$(\text{Bu}^t\text{OMgBr.OEt}_2)_2$, Bond Lengths and their Standard Deviations	89
TABLE 4g.	$(\text{Bu}^t\text{OMgBr.OEt}_2)_2$, Bond Angles with their Standard Deviations	90
TABLE 4h.	Intramolecular Non-bonding Contacts Less than $4\overset{\circ}{\text{A}}$	93
TABLE 5a.	$(\text{HZnN}(\text{Me})\text{C}_2\text{H}_4\text{NMe}_2)_2$, Final Values of Atomic Co-ordinates and their Standard Deviations	106
TABLE 5b.	$(\text{HZnN}(\text{Me})\text{C}_2\text{H}_4\text{NMe}_2)_2$, Final Values of Anisotropic Temperature Parameters and their Standard Deviations	107
TABLE 5c.	$(\text{HZnN}(\text{Me})\text{C}_2\text{H}_4\text{NMe}_2)_2$, Least-Squares Totals and Weighting Analysis	109
TABLE 5a.*	$(\text{HZnN}(\text{Me})\text{C}_2\text{H}_4\text{NMe}_2)_2$, Atomic Co-ordinates and their Standard Deviations derived from data corrected for absorption	111
TABLE 5b.*	$(\text{HZnN}(\text{Me})\text{C}_2\text{H}_4\text{NMe}_2)_2$, Anisotropic Temperature Parameters and their Standard Deviations derived from data corrected for absorption	112
TABLE 5d.	$(\text{HZnN}(\text{Me})\text{C}_2\text{H}_4\text{NMe}_2)_2$, Final Values of the Observed and Calculated Structure Factors	125
TABLE 5e.	$(\text{HZnN}(\text{Me})\text{C}_2\text{H}_4\text{NMe}_2)_2$, Equations of Least-Squares Planes referred to the Crystal Axes	115
TABLE 5f.	$(\text{HZnN}(\text{Me})\text{C}_2\text{H}_4\text{NMe}_2)_2$, Bond Lengths and their Standard Deviations	116

TABLE 5g.	(HZnN(Me)C ₂ H ₄ NMe ₂) ₂ , Bond Angles with their Standard Deviations	117
TABLE 5h.	(HZnN(Me)C ₂ H ₄ NMe ₂) ₂ , Intramolecular and Inter- molecular Non-bonding Contacts less than 4 ^o Å	121

LIST OF FIGURES

ETHYLZINC IODIDE

Figure 3.1	Patterson Function	54
Figure 3.2	Fragment of the Ethylzinc Iodide Polymer	62
Figure 3.3	Bond Lengths and Angles	65
Figure 3.4	Projection on the 010 plane	69
Figure 3.5	Relationship between the polymer and a theoretical tetrameric alternative	73

DIMERIC DIETHYL ETHER COMPLEX OF TERTIARYBUTOXYMAGNESIUM BROMIDE

Figure 4.1	Perspective drawing of $(\text{Bu}^t\text{OMgBr}\cdot\text{OEt}_2)_2$	86
Figure 4.2	Some Bond Lengths and Angles	91
Figure 4.3	Projection on the 010 plane	95

DIMERIC 2-DIMETHYLAMINOETHYLMETHYLAMINOZINC HYDRIDE

Figure 5.1	Perspective drawing of $(\text{HZnN}(\text{Me})\text{C}_2\text{H}_4\text{NMe}_2)_2$	114
Figure 5.2	Some Bond Lengths and Angles	118
Figure 5.3	Projection on the 010 plane	122

ISOTHERMAL MOLECULAR WEIGHT MEASUREMENT

Figure A1	Apparatus	127
Figure A2	Variation of Volumes during Isopiestic Distillation	129

SUMMARY

X-ray diffraction techniques have been used to examine the structural chemistry of three compounds of Group II metals. The crystal structures of all three compounds were solved by the heavy atom method and refined, with three dimensional data, by the method of least squares.

Ethylzinc Iodide

Ethylzinc iodide crystallizes, solvent-free from ethyl iodide, in the orthorhombic space group Pnma. The unit cell dimensions are $a = 21.17$, $b = 4.33$, $c = 5.38\text{\AA}$ and the unit cell contains four units of $\text{C}_2\text{H}_5\text{ZnI}$ which are situated on mirror planes at $y = 0.25$ and 0.75 .

Each iodine atom is at a distance of 2.64\AA from a zinc atom lying on the same mirror plane, the I-Zn-C angle in the plane being midway between the tetrahedral and linear values. In addition, each iodine atom is 2.91\AA from two other zinc atoms, which lie on adjacent mirror planes half a unit-cell length above and below it respectively.

The overall picture is of a co-ordination polymer, the iodine-zinc linkages giving rise to a layer structure which extends in two dimensions.

The Dimeric Diethyl Ether Complex of t-ButoxyMagnesium Bromide

A product of the addition reaction between acetone and methylmagnesium bromide crystallizes from ether in a ~~monoclinic~~^{clinic} cell. The

space group is $P2_1/c$; cell dimensions are $a = 9.68$, $b = 11.10$, $c = 15.10\text{\AA}$, $\beta = 129.13^\circ$.

There are two units of $(\text{Bu}^t\text{OMgBr.OEt}_2)_2$ in the unit cell and the molecule is dimeric in the crystal as it is in solution in both benzene and ether. The dimer contains a four-membered Mg_2O_2 ring.

The magnesium-oxygen bond length in the ring (1.91\AA) is less than the bond length (2.01\AA) between magnesium and the ether oxygen, and the oxygen atoms in both types of environment, although three-coordinate, have trigonal configurations.

Dimeric 2-dimethylaminoethylmethylaminozinc Hydride

The crystals of $(\text{HZnN}(\text{Me})\text{C}_2\text{H}_4\text{NMe}_2)_2$ are monoclinic, space group $P2_1/c$. The cell dimensions are $a = 6.372$, $b = 11.316$, $c = 11.977\text{\AA}$, $\beta = 111.75^\circ$, $Z = 2$ units of $(\text{HZnN}(\text{Me})\text{C}_2\text{H}_4\text{NMe}_2)_2$. The molecule is dimeric, both in benzene solution and in the solid phase.

A four-membered Zn_2N_2 ring links the two halves of the dimer round a centre of symmetry and a second, albeit weaker, dative bond, involving the second nitrogen atom, results in the formation of five-membered rings and brings the co-ordination number of the metal atoms to four.

The zinc-hydrogen bond is terminal and is principally covalent in character.

Chapter One

The Determination of Crystal Structures

1.1 The Crystal Lattice

Crystals are composed of groups of atoms repeated at regular intervals, with the same orientation, in three dimensions. If an arbitrary origin is chosen then it will be possible to find many further points in space which have an environment identical to the origin. These points define a lattice which can be described in terms of three non-coplanar vectors \underline{a} , \underline{b} , and \underline{c} . The parallelepiped defined by \underline{a} , \underline{b} , and \underline{c} is termed the "unit cell". This is said to be primitive if it contains no interior lattice points, and non-primitive otherwise.

Any three integers x , y , z then define another lattice vector $x\underline{a} + y\underline{b} + z\underline{c}$, terminating in the lattice point (x, y, z) . A rational plane through the origin (known as a lattice plane) has the equation $hx + ky + lz = 0$ where h , k , l are three integers known as Miller indices (hkl) . Integer solutions of the above equation define lattice points lying in the plane. The equation $hx + ky + lz = 1$ defines a lattice plane parallel to $hx + ky + lz = 0$ and characterized by the same arrangement of lattice points. It is generated from $hx + ky + lz = 0$ by a translation made up of a normal component and a tangential component and both planes are characterized by the same repeat vector.

A set of parallel planes

$$hx + ky + lz = 0, \pm 1, \pm 2, \dots$$

may be generated, which between them contain all the lattice points.

For a plane to have a high density of lattice points however, the Miller indices (which correspond to the reciprocals of the axial intercepts) must be relatively small. It is such planes which tend to form the faces of crystals and this is expressed in the law of Rational Indices which states that the ratio of the indices of a crystal face are rational and, in general, small whole numbers.

1.2 The Diffraction of X-rays by a Crystal Lattice.

In 1912, at the suggestion of Laue, the diffraction of X-rays by a crystal lattice was demonstrated by Friederich and Knipping. Their results established the wave-like property of X-rays and showed crystals to be periodic arrangements of matter with separations on the molecular scale.

The crystal lattice as defined above is important in the context of this phenomenon since it decides completely the conditions for diffraction. The relationship between a crystal lattice and the scattered radiation was recognised by W.L. Bragg and, in 1913, was expressed by him in the law which bears his name

$$n\lambda = 2d \sin\theta$$

Thus the resultant beam diffracted by a crystal lattice behaves as if it were reflected from the lattice planes with Miller indices (hkl) and with d as the interplanar spacing. In order to describe the whole 3-dimensional diffraction pattern it is necessary to consider

three sets of planes perpendicular to \underline{a} , \underline{b} , and \underline{c} respectively such that the interplanar spacings along each individual direction \underline{a} , \underline{b} or \underline{c} are equal. Each plane corresponds to a particular value of h , k and l .

The intersections of these planes represent the end points of vectors \underline{a}^* , \underline{b}^* and \underline{c}^* that satisfy the conditions for maximum intensity diffraction and delineate a lattice of points which is termed the "reciprocal lattice".

The reciprocal lattice is defined by the vectors \underline{a}^* , \underline{b}^* and \underline{c}^* where

$$\underline{a} \cdot \underline{a}^* = \underline{b} \cdot \underline{b}^* = \underline{c} \cdot \underline{c}^* = 1$$

Each point in this lattice corresponds to a "reflection" from the plane with Miller indices (hkl) and is at a distance $\frac{1}{d(hkl)}$ along a vector \underline{R} in the direction normal to the plane (hkl) where

$$\underline{R} = h \underline{a}^* + k \underline{b}^* + l \underline{c}^*$$

1.3 The Structure Factor.

In the simplest case all the atoms in a crystal are located with their mean positions at points on a single lattice. Most crystals are much more complicated however and can be represented only by placing within each unit cell of the lattice a certain arrangement of atoms. We may still regard any one set of corresponding atoms in the different cells as lying upon a lattice and thus a crystal with N

atoms in the unit cell can be regarded as based upon N identical interpenetrating lattices. X-rays scattered by these different lattices will differ in phase according to their separations and so if there is a large number of atoms in the unit cell complicated relationships may be expected between the intensities of their various orders of diffraction.

Suppose that the unit cell of a crystal contains N atoms situated at positions x_n, y_n, z_n where x_n, y_n and z_n are expressed as fractions of the unit cell edges. The position of the nth atom, P, in the unit cell can thus be represented by a vector \underline{r}_n , where

$$\underline{r}_n = x_n \underline{a} + y_n \underline{b} + z_n \underline{c}$$

The path difference between the waves scattered by the atom at P and those that would be scattered by an atom at the origin is proportional to \underline{r}_n . The atom at P can be assumed to lie on a plane parallel to (hkl) whose perpendicular distance from the origin will be given by the projection of \underline{r} on the vector \underline{R} describing the normal to the plane (hkl)

Thus if ϕ_n is the phase of the wave scattered by the element of volume round P then

$$\begin{aligned} \frac{\phi_n}{2\pi} &= \underline{R} \cdot \underline{r}_n \\ &= (\underline{h}\underline{a}^* + \underline{k}\underline{b}^* + \underline{l}\underline{c}^*)(x_n \underline{a} + y_n \underline{b} + z_n \underline{c}) \end{aligned}$$

$$= (hx_n + ky_n + lz_n)$$

$$\text{and } \phi_n = 2\pi(hx_n + ky_n + lz_n)$$

Hence the expression for the complete wave scattered by the nth lattice is

$$f_n \exp 2\pi i(hx_n + ky_n + lz_n)$$

where f_n is the atomic scattering factor of the nth atom. The complete wave scattered by a crystal containing N atoms per unit cell is given by a vector:

$$F(hkl) = \sum_{n=1}^N f_n \exp.2\pi i(hx_n + ky_n + lz_n)$$

where the quantity F is known as the structure factor, and is a function of h, k, l. The modulus of F is termed the Structure Amplitude and is defined as the ratio of the amplitude of the radiation scattered in the order h, k, l by the contents of the unit cell to that scattered by a single electron at the origin under the same conditions.

The atomic scattering factor represents the characteristic scattering power of an atom and its value may be found using a knowledge of the distribution of the electrons about the atom. It is generally quoted as the ratio of the scattering power of the atom compared with that of a single electron in the same direction. In atoms the electrons occupy a finite volume and phase differences occur

between rays scattered in different parts of this volume. Interference between these waves causes the scattering factor to decrease with increasing θ .

The structure factor F is a complex quantity and may be expressed in terms of its real and imaginary components:

$$F(hkl) = A(hkl) + iB(hkl)$$

$$\text{where } A(hkl) = \sum_{n=1}^N f_n \cos 2\pi(hx_n + ky_n + lz_n)$$

$$B(hkl) = \sum_{n=1}^N f_n \sin 2\pi(hx_n + ky_n + lz_n)$$

The structure amplitude is then given by $|F(hkl)|^2 = (A^2 + B^2)$ and the phase constant, $\alpha(hkl) = \tan^{-1} \frac{B}{A}$.

When the space group has a higher symmetry than $P1$ the summation over all atoms n is usually split into a summation over symmetry related atoms followed by a summation over the members of the asymmetric unit. For space-groups with a centre of symmetry at the origin $B(hkl) = 0$.

For each space group, the international Tables, Volumes I gives simplified forms of the trigonometric summations over symmetry related atoms. These expressions however are not directly applicable to atoms which are subject to general anisotropic vibrations.

A more fundamental treatment of the structure factor is possible by consideration of each element of volume of the unit cell separately. Thus if $\rho(x,y,z)$ is the electron density at the point (x,y,z) , the amount of scattering matter in the volume element $Vdx dy dz$ is $\rho V dx dy dz$, and the structure factor equation may be written

$$F(hkl) = \int_{x=0}^1 \int_{y=0}^1 \int_{z=0}^1 V \rho(x,y,z) \exp. 2\pi i(hx + ky + lz) dx dy dz$$

1.4 The Temperature Factor.

At all temperatures atoms have a finite amplitude of oscillation ^{frequency} (about 10^{13} sec^{-1}) which is much smaller than the frequency of X-rays (about 10^{18} sec^{-1}) so that to a beam of X-rays at any one instant the atoms appear to be stationary but displaced from their true mean positions in the lattice. Thus in producing a given X-ray reflection, atoms in neighbouring unit cells which should scatter in phase will scatter slightly out of phase, the total effect being an apparent reduction in the scattering factor of the atoms by an amount which increases with angle. With certain assumptions about the nature of the atomic vibrations the form of the variation of scattering factor with angle can be allowed for; - if the atomic scattering factor referred to previously is f_0 then the factor to be used in practice is

$$f = f_0 \exp.(-B \sin^2 \theta / \lambda^2)$$

where θ is the Bragg angle and B is a constant given by $B = 8\pi^2 \overline{u^2}$ if the mean square displacements $\overline{u^2}$ are the same in all directions.

In general the thermal displacement will not be isotropic and for the purposes of accurate crystal-structure investigation may be described in terms of an ellipsoidal distribution. The vibrations are described by a symmetrical tensor \underline{U} which has six independent components. The mean square amplitude of vibration in the direction of a unit vector $\underline{l} = (l_1, l_2, l_3)$ is

$$\overline{u^2} = \sum_{i=1}^3 \sum_{j=1}^3 U_{ij} l_i l_j$$

$$\text{or } \overline{u^2} = U_{11} l_1^2 + U_{22} l_2^2 + U_{33} l_3^2 + 2U_{23} l_2 l_3 \\ + 2U_{31} l_3 l_1 + 2U_{12} l_1 l_2,$$

where U and l are defined with respect to the reciprocal lattice axes \underline{a}^* , \underline{b}^* and \underline{c}^* . The component of U in the (1,0,0) direction parallel to \underline{a}^* is

$$\overline{u^2} = U_{11} \text{ and so on.}$$

In this anisotropic case the transform of the smearing function is

$$q(\underline{s}) = \exp.[-2\pi^2(\sum \sum U_{ij} s_i s_j)]$$

where $\underline{s} = (s_1, s_2, s_3)$ is the reciprocal lattice vector. If the units

of U_{ij} are \AA^2 , the units of s_i are \AA^{-1} .

At a reciprocal lattice point $\underline{s} = (h\underline{a}^* + k\underline{b}^* + l\underline{c}^*)$ the transform of the smearing function may be written

$$q(hkl) = \exp[-2\pi^2 (U_{11} h^2 \underline{a}^{*2} + U_{22} k^2 \underline{b}^{*2} + U_{33} l^2 \underline{c}^{*2} + 2U_{31} kl \underline{b}^* \underline{c}^* + 2U_{31} lh \underline{c}^* \underline{a}^* + 2U_{12} hk \underline{a}^* \underline{b}^*)]$$

and the scattering factor f_T for an atom in anisotropic thermal vibration is given by the product $f_T(hkl) = f(hkl)q(hkl)$.

1.5 Fourier Series

Since a crystal is periodic in three dimensions it can be represented by a three-dimensional Fourier series

$$\rho(x,y,z) = \sum_{h'} \sum_{k'} \sum_{l'=-\infty}^{\infty} C(h',k',l') \exp.2\pi i(h'x + k'y + l'z)$$

each Fourier coefficient C having integral indices h' , k' and l' allotted to it.

This value for the electron density may be substituted in the structure factor equation

$$F(hkl) = \int_0^1 \int_0^1 \int_0^1 \sum_{h'} \sum_{k'} \sum_{l'=-\infty}^{\infty} C(h',k',l') \exp.2\pi i(h'x + k'y + l'z)$$

$$\exp.2\pi i(hx + ky + lz)V \, dx \, dy \, dz.$$

Now the exponential functions in this expression are both periodic and the integral of their product over a single complete period is zero in general; only if $h = -h'$, $k = -k'$, $l = -l'$ does the periodicity disappear and the expression take a non-zero value, then

$$F(h,k,l) = \int_0^1 \int_0^1 \int_0^1 C(h',k',l) V dx dy dz$$

and therefore $F(h,k,l) = C(\bar{h},\bar{k},\bar{l})V$

The three-dimensional Fourier synthesis can now be written

$$\rho(x,y,z) = \frac{1}{V} \sum_h \sum_k \sum_{l=-\infty}^{\infty} F(hkl) \exp.[2\pi i(hx + ky + lz)]$$

since the Fourier coefficients are directly related to the corresponding structure factors.

The above expression for electron density is not suitable for quantitative evaluation since it contains complex quantities. The equation may be rewritten

$$\rho(x,y,z) = \frac{1}{V} \sum_h \sum_k \sum_{l=-\infty}^{\infty} A(hkl) \cos 2\pi(hx + ky + lz) \\ + B(hkl) \sin 2\pi(hx + ky + lz)$$

where A and B are the two components of the structure factor, F.

In view of the fact that $A(\bar{h},\bar{k},\bar{l}) = A(hkl)$, $B(\bar{h},\bar{k},\bar{l}) = -B(hkl)$ and taking into account that the term $F(000)$ is its own conjugate,

further simplification is possible:

$$\rho(xyz) = \frac{1}{V} \left(F(000) + 2 \sum_{h=0}^{\infty} \sum_{k, l=-\infty}^{\infty} A(hkl) \cos 2\pi(hx + ky + lz) + B(hkl) \sin 2\pi(hx + ky + lz) \right)$$

or

$$\rho(xyz) = \frac{1}{V} \left(F(000) + 2 \sum_{h=0}^{\infty} \sum_{k, l=-\infty}^{\infty} |F(hkl)| \cos 2\pi(hx + ky + lz) - \alpha(hkl) \right)$$

where $\alpha(hkl)$ is the phase angle for the reflection hkl .

This is a general expression which describes the electron density in all crystals but by making use of space-group symmetry in combining symmetry related reflections further simplifications are possible.

The expression for electron density in terms of the independent structure factors only is given for each space group, in International Tables Volume I.

To make use of such expressions in solving crystal structures a complete knowledge of the relevant structure factors is necessary. The structure amplitudes are experimentally observable quantities but the corresponding phase angles are not and their valuation constitutes a problem of varying magnitude from one structure analysis to another.

1.6 The Patterson Function

One of the devices employed to solve the phase problem depends on a summation suggested by Patterson who defines a function

$$P(u,v,w) = v \int_0^1 \int_0^1 \int_0^1 \rho(x,y,z)\rho(x+u,y+v,z+w)dx dy dz$$

When the values for the electron densities are inserted, the Patterson function reduces to the form in which it is more usually quoted

$$P(u,v,w) = \frac{1}{v} \sum_h \sum_k \sum_{l=-\infty}^{\infty} |F(hkl)|^2 \exp.2\pi i(hu + kv + lw)$$

which can be summed without ambiguity since the quantities $|F|^2$ are directly derivable from the X-ray intensities. The significance of this summation is that when the distribution of $P(u,v,w)$ is plotted through the unit cell, maxima occur at the point (uvw) when the vector $\underline{r} = u\underline{a} + v\underline{b} + w\underline{c}$ represents a vector joining two atoms, i.e. when $\rho(xyz)$ and $\rho(x+u,y+v,z+w)$ are both large. The heights of the peaks depend on the electron densities of the atoms giving rise to them, and thus a heavy atom in the structure will give rise to relatively high Patterson peaks and it will often be possible to discover the position of such an atom from these peaks.

A large peak occurs at the origin of the Patterson function due to the vectors between all the atoms and themselves.

1.7 The Heavy Atom Method

If, as described above, the positions of the heavy atoms in a structure are fixed by scrutiny of the Patterson function, then structure factors may be calculated based on the heavy atom contributions and used to compute an F_o synthesis which should reveal at least some of the lighter atom positions. In theory this process may be repeated using structure factors phased on the increasing number of located atoms until the positions of all of the atoms are known. In practice however it may not be possible to detect hydrogen atoms for reasons mentioned below.

The assumption that the phase angles based on the heavy atoms alone are the correct ones for the various reflections will normally give a Fourier synthesis which is a close approximation to the complete structure. Formally this result can be represented by writing the structure factor for a crystal with one heavy atom in the unit cell as

$$F(h,k,l) = f_H \exp.2\pi i(hx_H + ky_H + lz_H) + \sum_n f_n \exp.2\pi i(hx_n + ky_n + lz_n)$$

where f_H is the scattering factor of the heavy atom, whose positional parameters are x_H , y_H , and z_H . If f_H is much greater than f_n , then the first term will tend to be much greater than the second, since the summation, being due to several atoms, will usually be relatively small. It is unnecessary, and indeed undesirable that f_H should be

greater than $\sum f_n$ - that is, that the heavy atom should scatter more than all the other atoms together. If f_H is too large, the Fourier synthesis may show only the heavy atom and some difficulty will be found in accurately locating the lighter atoms.

As a rough guide, for successful use of the method, the sum of the squares of the atomic numbers of the heavy atoms and of the light atoms should be approximately equal. This is seen by considering the equation

$$\overline{I(hkl)} = \sum_j f_j^2$$

which shows that, on the average, the contribution of any one atom to the diffracted intensity depends on the square of its scattering factor.

Sim (1961) gives a graph showing the proportion of correct signs in terms of a ratio r , where

$$r = \frac{\sum f_H^2}{\sum f_L^2}$$

f_H and f_L being the scattering factors of the heavy and light atoms respectively, which for this purpose must be taken as proportional to the atomic numbers.

The signs of those structure factors to which the heavy atom makes only a small contribution are uncertain and Woolfson (1956) has

suggested that each term used for the Fourier synthesis should be weighted according to the contribution of the heavy atom to the structure factor.

A major difficulty which arises surprisingly often is the problem of pseudosymmetry. When the space group is non-centrosymmetric or if the heavy atom is located on or near a symmetry element, the symmetry of a higher space group may be simulated and the phases deduced from the heavy atom position alone give false information about the structure.

1.8 Structure Refinement

After an initial structure has been obtained it is desirable to adjust the atomic parameters so as to give the best agreement between the observed structure amplitudes and the calculated structure factors. The method of least-squares refinement was employed in the case of the structure analyses to be described.

Suppose the parameters to be evaluated are p_1, p_2, \dots, p_n , then the structure factor is some function of these parameters.

$$|F_c| = f(p_1, p_2, \dots, p_n)$$

A similar expression obtains for the observed structure amplitude

$$|F_o| = f(p_1 + \epsilon_1, p_2 + \epsilon_2, \dots, p_n + \epsilon_n)$$

where $\epsilon_1, \epsilon_2, \dots, \epsilon_n$ are the shifts required to give the true

structural parameters.

If the starting structure is a good approximation then ϵ_1 , $\epsilon_2, \dots, \epsilon_n$ will all be small and F_o may be expanded in a Taylor series to the first order

$$|F_o| = f(p_1, p_2, \dots, p_n) + \sum_{i=1}^n \frac{\partial f(p_1, p_2, \dots, p_n)}{\partial p_i} \epsilon_i$$

that is $|F_o| = |F_c| + \sum_{i=1}^n \frac{\partial |F_c|}{\partial p_i} \epsilon_i$

or $|F_o| - |F_c| = \sum_{i=1}^n \frac{\partial |F_c|}{\partial p_i} \epsilon_i$

An equation of this type may be derived for each reflection. Each F_o is subject to random errors of observation and suitable values of ϵ_i have to be found to give the best fit between F_o and F_c . Error theory predicts that the most acceptable set of ϵ_i is that which minimises some function of the difference, $(|F_o| - |F_c|)$ with respect to the structure parameters,

normally $M = \sum_{hkl} w(|F_o| - |F_c|)^2 = \sum_{hkl} w\Delta^2$

where the sum is taken over the set crystallographically independent

planes and $w(hkl)$ is a weight for each term.

The criterion that $\sum w\Delta^2$ should be a minimum leads to a set of simultaneous equations, the 'normal equations',

$$\sum_{h,k,l} w\Delta \frac{\partial |F_c|}{\partial p_i} = \sum_{h,k,l} w \left(\frac{\partial |F_c|}{\partial p_i} \right)^2 \epsilon_i + \sum_{h,k,l} w \frac{\partial |F_c|}{\partial p_i} \left\{ \sum_{j \neq i} \frac{\partial |F_c|}{\partial p_j} \epsilon_j \right\}$$

There are n of the equations for $j = 1, \dots, n$ to determine the n parameters. They may be written out as

$$\sum w \left(\frac{\partial |F_c|}{\partial p_1} \right)^2 \epsilon_1 + \sum w \left(\frac{\partial |F_c|}{\partial p_1} \right) \left(\frac{\partial |F_c|}{\partial p_2} \right) \epsilon_2 + \dots = \sum w\Delta \frac{\partial |F_c|}{\partial p_1}$$

$$\sum w \left(\frac{\partial |F_c|}{\partial p_1} \right) \left(\frac{\partial |F_c|}{\partial p_2} \right) \epsilon_1 + \sum w \left(\frac{\partial |F_c|}{\partial p_2} \right)^2 \epsilon_2 + \dots = \sum w\Delta \frac{\partial |F_c|}{\partial p_2}$$

etc.

Alternatively the normal equations may be expressed in matrix form

as
$$\sum_i a_{ij} \epsilon_i = b_j$$

where
$$a_{ij} = \sum_{hkl} w \frac{\partial |F_c|}{\partial p_i} \frac{\partial |F_c|}{\partial p_j}, \quad b_j = \sum_{hkl} w\Delta \frac{\partial |F_c|}{\partial p_j}$$

It is the normal equations which must be set up and solved to refine a structure by the least squares method.

For structures involving a large number of atomic parameters it is frequently impracticable to calculate all the terms of the normal equation matrix a_{ij} . In such cases it is necessary to consider approximations in which many off-diagonal elements of a_{ij} (i.e. when $i \neq j$) are neglected. For three-dimensional data a "block-diagonal approximation" (Cruickshank et al., 1961) has been found useful which normally makes use of a chain of 9 x 9 matrices for the co-ordinates and anisotropic vibration parameters of each atom with a 2 x 2 matrix for the scale and overall isotropic vibration parameter. If the vibrations are isotropic the coordinate matrices will be 4 x 4.

The full matrix method was possible for the structures described herein however and advantage was taken of this opportunity. The full matrix method yielded more reliable estimates of the standard deviation (see below) and, in one case, probably gave convergence in the least possible computing time.

1.9 Accuracy of parameters derived from least-squares refinement.

The best choice of weights, yielding parameters of the lowest variance, is $w = \frac{1}{\sigma^2}$. In general with the full a_{ij} matrix for the normal equations, the variance of parameter i is

$$\sigma^2(p_i) = (a^{-1})_{ii}$$

where $(a^{-1})_{ii}$ is an element of the matrix inverse to a_{ij} .

If the relative weights only are known, such that $w = \frac{k}{\sigma^2}$, the experimental standard deviation (e.s.d.) is given by

$$\sigma^2(p_i) = (a^{-1})_{ii} \left(\sum w\Delta^2 \right) / (m-n)$$

where m is the number of observations and n is the number of parameters; - i.e. $(m-n)$ is the number of degrees of freedom.

In the block-diagonal approximation variances may be estimated using the inverses of the block matrices, but the values thus derived somewhat underestimate the true variances because of the neglect of the inter-atomic interactions in the full matrix (Hodgson and Rollett, 1963).

1.10 Termination of series effects and Absorption errors.

Although an infinite number of terms ought to be considered when a Fourier synthesis is used during a structure determination, in practice there will generally be an experimental limitation on the number of terms available. The result of including only a finite number of terms is that peaks of electron density appear surrounded by ripples which may cause other peaks in the unit cell to be displaced from their true positions. Such "termination of series" effects may be overcome by use of a difference synthesis, in which the quantity $(F_o - F_c)_{hkl}$ replaces $(F_c)_{hkl}$ as the Fourier coefficient, or by least squares refinement procedures.

Errors in X-ray data due to absorption by the specimen can change the shape of electron density maxima in a systematic way also. For

example, the use of a specimen of elliptic cross-section without correction for absorption, may lead to Fourier peak shapes very similar to those produced by anisotropic thermal vibration (Jellinek, 1958). However, Jellinek suggests that since the derivations of atomic parameters (except for hydrogen) depend mainly on the intensities of the high order reflexions while systematic errors due to absorption are largest at low values of θ a modification of the difference synthesis method should give improved results. Accurate atomic parameters (except for hydrogen) and scale factor should be determined from moderate and high angle reflexions only and then a difference synthesis involving the low order reflexions will reveal the effects of systematic errors such as absorption. It is suggested that after these errors have been appropriately corrected for (by a procedure which can be reiterated) improved resolution of the structure may be obtained from a new low-angle reflexions difference synthesis.

A more satisfactory approach is to correct the original intensity data for absorption errors. Busing and Levy (1957) have put forward a method which is well suited for automatic computation. The function to be computed is given by

$$A = \int \frac{1}{V} \exp.[-\mu(r_p + r_d)] dv$$

where v is the crystal volume, μ the linear absorption coefficient and

r_p , r_d the path lengths of the primary and diffracted beams respectively within the crystal for reflexion by the volume element dv .

In order to fix the boundaries of the crystal the n plane faces are defined by n inequalities of the form

$$a_s x + b_s y + c_s z - d_s \geq 0$$

where $s = 1, 2, \dots, n$. To satisfy these conditions the crystal must have no re-entrant angles.

The integrals are evaluated by the method of Gauss, the triple integral reducing to a summation of the form

$$\int_a^b dx \int_c^d dy \int_e^f g(x,y,z) dz \approx \sum_{i=1}^m \sum_{j=1}^n \sum_{k=1}^1 (b-a)(d-c)(f-e) R_i R_j R_k g(x_i, y_j, z_k)$$

where the R_i 's are the relative weights of the terms in the sum and are tabulated for all values of $m \leq 16$.

An analytical method of correction for absorption has also been described (de Meulenaer and Tompa, 1965). This involves the division of the crystal into a number of elementary polyhedra throughout each of which the sum of the path lengths is a linear function of the co-ordinates of the volume element. This may give better results than Busing and Levy's method when an insufficient number of sampling points ($m, n, 1$) are used in the latter case.

Bibliography

"Chemical Crystallography" by C.W. Bunn, Second Edition, Clarendon Press, Oxford (1961).

"The Crystalline State, Volume III" by H. Lipson and W. Cochran, Bell (1966).

"Crystal Structure Analysis" by M.J. Buerger, Wiley (1960).

"International Tables for X-ray Crystallography", Volume I (1952), Volume II (1959), Volume III(1962), Kynoch Press, Birmingham.

Chapter Two

Some Aspects of the Organometallic and Hydride Chemistry of Zinc and Magnesium

2.1 Introduction

This thesis is concerned with the structural chemistry of compounds containing zinc and magnesium and specifically with the chemical information which may be gleaned from the solution of the crystal structures of three such compounds. An extension is made to the information available concerning internal co-ordination complexes of organozinc compounds and a contribution is made to the discussion of the reaction between Grignard reagents and carbonyl compounds. The crystal structure of the first known crystalline zinc hydride is described.

The organometallic compounds of zinc and magnesium are well known (Coates and Wade, 1968) and it is proposed to concentrate only on aspects of the more recent developments in their chemistry.

Bearing in mind that the characteristic valency of these metals is two, their compounds exhibit a remarkable variety of structures some of which have only recently been elucidated.

2.2 Internal Co-ordination Complexes of Magnesium and Zinc Alkyls

Considerable attention has been devoted to the so-called "Internal co-ordination complexes" of group II metals which result when a metal dialkyl or diaryl compound reacts with a substance (HA) containing reactive hydrogen, to give a product of the type RMA. Such a compound if monomeric would be co-ordinatively unsaturated at the metal atom, which would itself have enhanced acceptor characteristics due to the

δ^+ δ^-
dipole M—A. If the moiety A possesses any lone pair electrons on the atom attached to metal then their donor potential will be increased for the same reason. The chemistry of compounds of this type is highly influenced by the various methods whereby the valency shells of the metal atoms may be expanded. The compounds do of course frequently associate and degrees of association of 2,3,4,5,6 and infinity have been reported in various cases.

The factors which affect the degree of association of this type of compound are now beginning to be understood though their relative importance is sometimes obscure (Beachley and Coates, 1965).

Some of the principle considerations are

a) Valence Angle Deformation

Atoms of high atomic number may tolerate deformation of their valence angles away from the values expected for their particular state of hybridisation more easily than lighter elements (Gillespie, 1960). Valence angle deformation is gradually relieved with the formation of larger cyclic oligomers and polymers.

b) Steric Influence of Bulky Substituents on the Donor Atom

Steric interference between bulky substituents appears to increase as the degree of association increases. Thus $(\text{EtZnOCHPh}_2)_3$ is trimeric while $(\text{EtZnOCPh}_3)_3$ is a dimer. These first two factors will tend to work in opposition. Complexes with bulky substituents on the donor atoms will tend towards dimeric structures. On the other hand dimers

necessarily involve considerable valence angle strain in a four-membered ring. Large oligomers will relieve valence angle strain but will bring bulky substituents into closer proximity.

c) Entropy

The effect of entropy will always be to favour the formation of dimers in preference to trimers, tetramers or more associated species since this affords the greatest number of independent molecules per unit mass.

d) The Nature of reaction intermediates

Intermolecular condensations involving polymeric intermediates are expected to result in polymeric, tetrameric or trimeric products and intramolecular condensations going through monomeric intermediates should favour the dimer as the associated species (Beachley and Coates, 1965).

Most of the work on the factors affecting degree of association has been concerned with the organic compounds of Group III elements. However sufficient information is available on the co-ordination complexes of magnesium (Coates and Heslop, 1966; Coates and Ridley, 1967; Coates et al., 1968) and zinc (Coates and Ridley, 1965; Coates and Ridley, 1966; Boersma and Noltes, 1968) to establish that the above factors are important in connection with the association of compounds of these elements also.

2.2.i Complexes with 1-atom donor groups

a) From reactions with amines

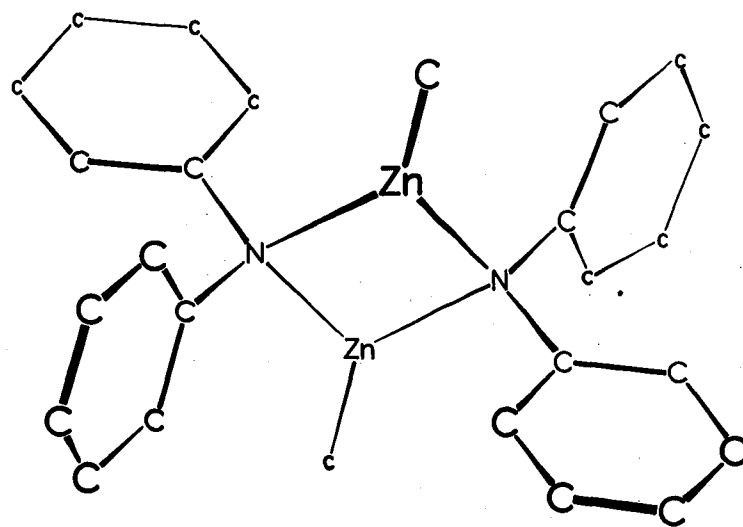
When the ligand attached to metal is a secondary amine, only one lone-pair of electrons is available on the nitrogen for co-ordination and compounds of the type $RMNR'_2$ can only associate to form open ring structures or polymers in which the metal atoms are three-co-ordinate.

Aminoberyllium alkyls have been recorded which have either dimeric or trimeric structures, the ring size in this case apparently being determined by steric effects.

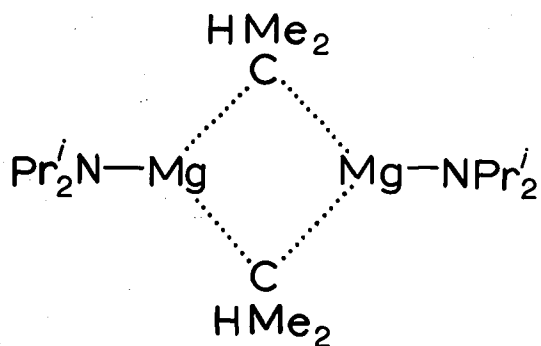
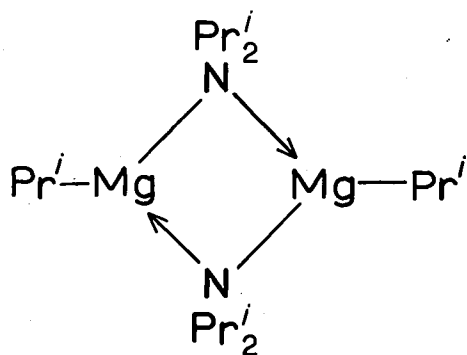
Methyl and ethyl(diphenylamino)zinc have been isolated and are dimeric in benzene solution. An X-ray structure analysis of methyl-(diphenylamino)zinc, $(MeZnNPh_2)_2$, (Shearer and Spencer, 1967) has confirmed that the molecule is dimeric in the solid phase also. The structure incorporates a four-membered Zn_2N_2 ring in which the zinc atoms are three-co-ordinate, as shown on the following page.

No trimeric aminozinc alkyls have yet been reported since the reaction of dimethylamine with dimethylzinc results in disproportionation products and only bis dimethylaminozinc $\{ (Me_2N)_2Zn \}_x$ has been isolated.

The situation with regard to aminomagnesium alkyls is more complex due both to the high tendency for alkyl groups bound to magnesium to form alkyl bridges and to the necessity of working with R_2Mg in solution in donor solvents such as diethylether and tetrahydrofuran, which are often difficult to remove from the reaction products.



An example of an ether-free aminomagnesium alkyl is available however; isopropyl(di-isopropylamino)magnesium, $(\text{Pr}^i\text{MgNPr}_2^i)_2$, may be formulated with either of the two structures shown



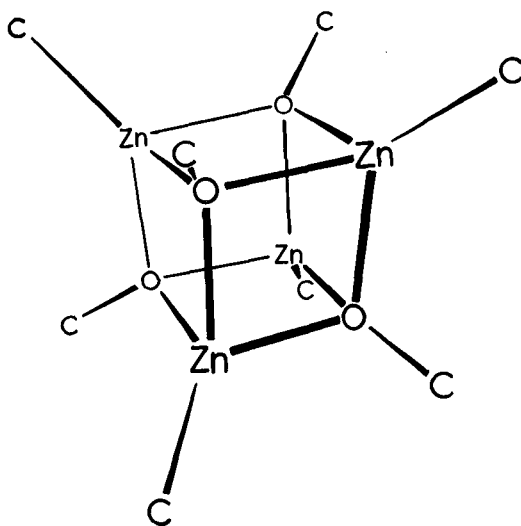
although an asymmetrically bridged structure cannot be ruled out.

b) From reactions with alcohols

The facile reaction between zinc alkyls and alcohols has been known since the first preparation of zinc alkyls by Frankland in 1849.

The oxygen atom in products of the type RMOR' has a second lone pair available for co-ordination. This enables the alkoxides to associate to form cage structures in which the metal atom achieves a preferred co-ordination number of four.

The molecular weight of methylzinc methoxide determined cryoscopically in benzene indicates that the molecule is a tetramer, $(\text{MeZnOMe})_4$. X-ray structure analysis (Shearer and Spencer, 1966) has shown that methylzinc methoxide is also tetrameric in the crystal, with zinc and oxygen atoms near the corners of a distorted cube as shown



Many other compounds $(RMOR')_4$ where M is Be, Mg, Zn or Cd have been found to be tetrameric in benzene and may be isostructural with methylzinc methoxide.

Dimeric and trimeric alkylzinc alkoxides are found when the organic groups attached to oxygen are very large.

Alkylmagnesium alkoxides have been mentioned in various connections and are discussed in a review (Wakefield, 1966). Two of them have been found to be trimeric, $(EtMgOEt)_3$ in diethyl ether (Blomberg and Vreugdenhil, 1965) and $(Bu^iMgOPr^i)_3$ in benzene (Bryce-Smith and Graham, 1966).

Since alkylmagnesium alkoxides feature in the most reasonable mechanisms for the reaction between Grignard reagents and carbonyl compounds, information bearing on their constitution is held to be of particular interest (Coates et al., 1968).

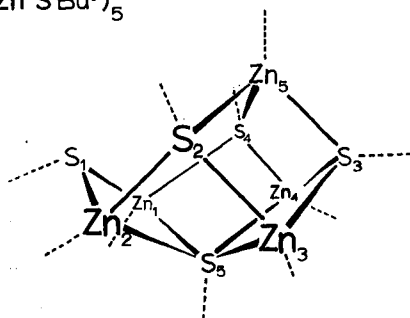
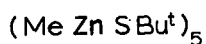
The most commonly occurring associated species when there is chain branching at the carbon α to the oxygen appears to be the tetramer as in $(EtMgOPr^i)_4$. In other cases higher degrees of association are found. Ethylmagnesium n-propoxide and isopropylmagnesium methoxide and ethoxide are oligomers which have degrees of association in benzene in the range 7-8.4. These alkoxides are probably polymeric in the crystalline state.

c) From reactions with thiols.

The thio derivatives show diverse degrees of association. Methylzinc methylsulphide is insoluble in benzene and is assumed to be polymeric

in the solid state. Other thio derivatives of methylzinc are somewhat anomalous. Methylzinc isopropyl-sulphide was found to be hexameric in benzene solution but a preliminary X-ray investigation is consistent with the existence of octamers in the crystal (Adamson and Shearer, 1967). And whereas methylcadmium t-butylsulphide is tetrameric in benzene, methylzinc t-butylsulphide is a pentamer.

A crystal structure analysis of methylzinc t-butylsulphide (Adamson and Shearer, 1966) has confirmed that the molecule is a pentamer $(\text{MeZnSBU}^t)_5$, in the crystal. The zinc atoms lie near the



Zn ₁ -S ₁	2.28 Å	Zn ₂ -S ₁	2.32 Å
Zn ₁ -S ₅	2.98	Zn ₂ -S ₅	2.71
Zn ₃ -S ₅	2.51	Zn ₄ -S ₅	2.51
All other Zn-S 2.41 - 2.47			

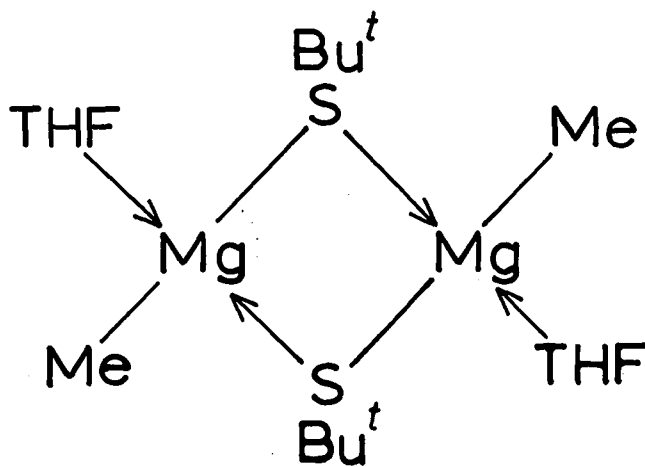
Mean values:

Zn-C 2.01, S-C 1.88, C-C 1.55

corners of a square-based pyramid with the apical atom, Zn(5), closer to Zn(3) and Zn(4). The sulphurs S(2), S(3), S(4) lie above the centres

of the triangular faces, S(1) lies above the face defined by Zn(1), Zn(2) and Zn(5), but is much further away from Zn(5). S(5) lies below the basal plane and is somewhat closer to Zn(3) and Zn(4). The arrangement results in the three zinc atoms Zn(3), Zn(4), Zn(5) and the four sulphur atoms S(2), S(3), S(4) and S(5) lying near the corners of a cube. With one methyl bonded to each zinc and one t-butyl to each sulphur all the zinc atoms and three of the sulphurs are four-coordinate whereas S(1) is three-coordinate and S(5) is five-coordinate. It is very puzzling that $(\text{MeZnSBu}^t)_5$ prefers a pentameric arrangement in which one sulphur atom is only three-coordinate to the "cubane" structure of methylzinc methoxide. There is no evidence of significant steric interactions between organic groups in $(\text{MeZnSBu}^t)_5$. The seven atoms Zn(3), Zn(4), Zn(5), S(2), S(3), S(4) and S(5) lie near the corners of a cube and on steric grounds there seems to be no reason why a MeZn moiety should not be accommodated at the eighth corner of the cube.

In the case of the thio derivatives of alkylmagnesium, the second lone pair on the sulphur atom competes unsuccessfully with ether (present as solvent during their preparation) for the fourth coordination position about the metal atom. All the complexes of this type which have been reported are etherates and are dimeric, probably with structures similar to that shown for $(\text{MeMgSBu}^t \cdot \text{THF})_2$.



d) Halides

Monomeric Grignard reagents have been found to complete the four-co-ordination of the magnesium atom by the incorporation of two coordinatively bound ether molecules per mole (Rundle and Stucky, 1964; Guggenberger and Rundle, 1964). More recently dimeric Grignard reagents have been isolated. The diethyl ether complex of *t*-butylmagnesium chloride ($\text{Bu}^t\text{MgCl} \cdot 2\text{OEt}_2$)₂ is predicted (Coates and Heslop, 1968) to have chlorine bridges and an X-ray structure analysis (Stucky and Toney, 1967) has shown that the triethylamino adduct of ethylmagnesium bromide ($\text{EtMgBr} \cdot \text{NEt}_3$)₂, which is also dimeric, has a bromine-bridged structure.

Alkoxy bridges are preferred to halogen bridges in the dimeric diethyl ether complex of t-butoxymagnesium bromide $(\text{Bu}^t\text{OMgBr}\cdot\text{OEt}_2)_2$.

The unsolvated alkylzinc halides afford examples of two different degrees of association also. Ethylzinc chloride and bromide are tetrameric in benzene solution (Boersma and Noltes, 1966) and a "cubane" structure is envisaged for these, similar to that of methylzinc methoxide. Ethylzinc iodide forms a co-ordination polymer in the crystal which extends in two dimensions and results in a layer structure. It is possible that methylzinc methylsulphide and the polymeric alkylmagnesium alkoxides mentioned earlier have similar structures.

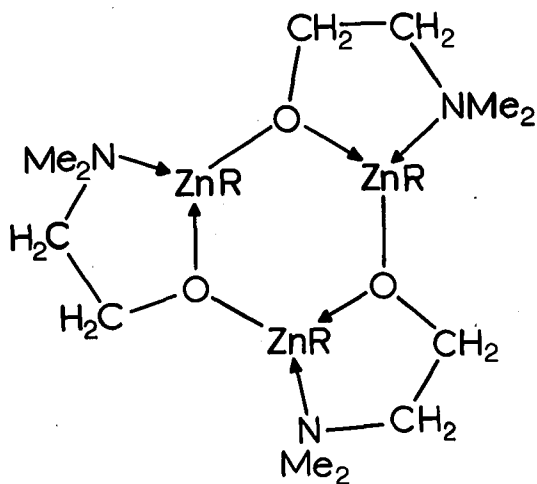
The co-ordinate bonding in unsolvated ethylzinc halides is weaker than that in the corresponding alkoxides as is apparent from their complex forming behaviour. Whereas compounds RZnOR' (with the special exception of $(\text{Bu}^t\text{OZnBu}^t)_3$ (Boersma and Noltes, 1968)) do not form complexes with pyridine (py) (Coates and Ridley, 1965), ethylzinc chloride and bromide dissolved in n-pentane form stable monomeric 1:2 complexes typified by $\text{EtZnCl}\cdot 2\text{Py}$ (Boersma and Noltes, 1966).

2.2.ii Complexes with 2-atom donor groups

When the donor group attached to metal contains two electronegative atoms a greater number of structural possibilities arise. In some cases both donor atoms are involved in co-ordination and in other cases only one.

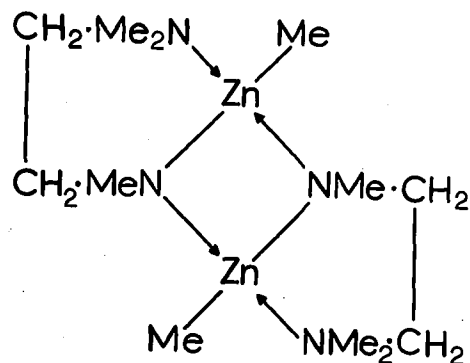
The complex formed by the reaction between 2-methoxyethanol and dimethylzinc is tetrameric $(\text{MeZnOCH}_2\text{CH}_2\text{OMe})_4$ and is believed to be like the "cubane" type tetramers because the donor strength of the oxygen bound to zinc is greater (due to the electropositive character of the metal) than that of the ether oxygen. The ether-side chains will protrude from the corners of the cube resulting in a molecule of low symmetry and this is probably responsible for the fact that methylzinc-methoxy ethoxide is a liquid.

The 2-dimethylaminoethoxy derivatives of dimethyl and diethylzinc are however both trimers. The preference for an open ring structure



in this case is probably due to the fact that the nitrogen lone pair competes successfully with the fourth valency of the relatively rarely encountered four-co-ordinate oxygen for a co-ordination site about the metal atom.

Me_2Mg and Me_2Zn form complexes with NNN'-trimethylethylenediamine-(TriMED) which are dimeric in benzene and are believed to have structures similar to that shown for $(\text{MeZnTriMED})_2$



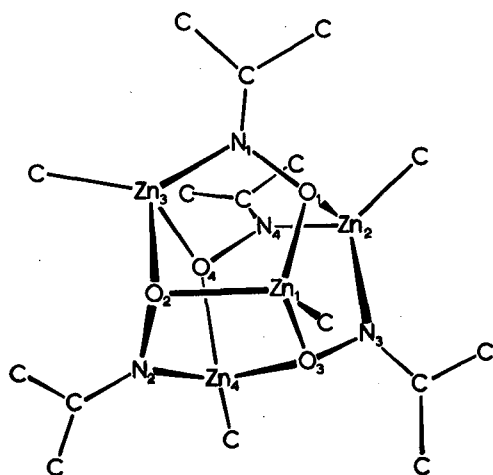
Beryllium dialkyls form a series of complexes with TriMED also (Coates and Roberts, 1968) which are dimeric when the alkyl groups are small but monomeric when the alkyl groups are large as in $(\text{Bu}^t\text{BeTriMED})_1$. The critical size of the alkyl group seems to be at

isopropyl. $(\text{Pr}^i\text{BeTriMED})_2$ is dimeric in benzene but is the only compound in the series for which the proton magnetic resonance (PMR) doublet of the isopropyl group is split to a quartet. This data is interpreted to mean that the steric interference arising from the size of the alkyl groups is allowing two isomeric forms to interconvert at a rate detectable by the PMR technique.

Zinc and beryllium hydrides form hydride complexes with TriMED. The zinc compound $(\text{HZnTriMED})_2$ is dimeric in benzene and an X-ray analysis has shown that in the crystal the structure is analogous to that shown above for $(\text{MeZnTriMED})_2$. The beryllium analogue however is trimeric in benzene and probably polymeric in the solid state (Schneider and Shearer, 1968). An X-ray structure analysis of this compound is in progress.

Also worthy of mention here is the structure of tetrameric methyl-zinc dimethylketoximate $(\text{MeZnON:CMe}_2)_4$ in which use is made of both nitrogen and oxygen for co-ordinate bonding.

A cage structure results in which, significantly, four-membered rings are avoided. There are four five-membered rings and two adjacent six-membered rings and all of the oxygen atoms are three-co-ordinate.



2.3 The Constitution of Ethylzinc Halides in Solution.

Ethylzinc halides dissolved in donor solvents do not retain the molecular structures of the solid compounds and a discussion of their constitution, parallel to the interest in Grignard reagents has continued over several years.

The empirical formula of crystalline ethylzinc iodide as prepared by the action of ethyl iodide on a Zn/Cu couple has been established as C_2H_5ZnI and at the same time it has been shown (Jander et al., 1958) that reaction between diethylzinc and zinc iodide in the absence of solvent yields the same solid material. A number of experiments have been

directed towards discovering the nature of the species existing in solutions of ethylzinc iodide and various chemical entities, based on the empirical formula C_2H_5ZnI have been postulated.

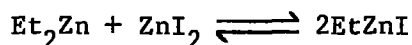
It is reported (Kocheshkov et al., 1963) that the addition of Grignard reagents $RMgX$ (where $R \neq Et$) to solution of ethylzinc iodide in ether affords high yields of unsymmetrical dialkylzincs $RZnEt$, which observation may be interpreted (Job and Reich, 1923) as being more consistent with a structure $EtZnI$ (1) than with the unsymmetrical dimer of the form $Et_2Zn \cdot ZnI_2$ (2) for ethylzinc iodide. However such data does not preclude the possibility of structures such as $(EtZnI)_2$ (3), $(EtZnI)_n$ (4) or of equilibria involving any combination of the species 1 - 4.

The proton magnetic resonance (PMR) spectra of ethereal solutions of ethylzinc iodide and diethylzinc are very similar having a sharp triplet at τ 8.95 p.p.m. and a sharp quartet at τ 9.92 p.p.m. It was originally suggested (Evans and Maher, 1962) that such similarities were more consistent with structure (2) above than with structure (1). However in the light of subsequent infra-red and Raman spectral data (Evans and Wharf, 1966) it appears that this deduction was incorrectly drawn. It is not immediately evident why PMR cannot distinguish between species such as Et_2Zn and $EtZnI$.

When 2,2'^{yl}bipyridine (bipy) is added to mixtures of zinc chloride and diethylzinc which have stood for 120 hours in solvent ether or in solvent

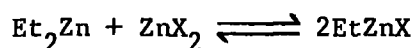
tetrahydrofuran (THF), the complex $\text{ZnCl}_2(\text{bipy})$ precipitates out. When $^{65}\text{ZnCl}_2$ is used a statistical exchange of ^{65}Zn is observed (Dessy and Coe, 1963). Molecular weight determinations on a mixture of diethylzinc and zinc chloride in solvent THF correspond either to (a) no interaction at all between diethylzinc and zinc chloride or to (b) a monomer EtZnCl . Together these two results might be quoted as evidence for a monomeric structure for ethylzinc chloride in solution in THF but it would not be correct to extrapolate and draw general conclusions about the bromide and iodide or about solutions in other solvents without more data.

Ebullioscopic measurements of solutions of ethylzinc iodide in ether and in THF respectively coupled with an experiment involving the addition of NNN'N'tetramethylethylenediamine (TMED) to precipitate the complex $\text{EtZnI}(\text{TMED})$ from each solution have demonstrated (Abraham and Rolfe, 1967) that the "Schlenk" equilibrium



lies well to the right in these two solvents.

The results of the work on the diethylzinc-zinc halide system in donor solvents may be satisfactorily expressed in terms of the general syn-proportionation/symmetrisation equilibrium



where the equilibrium probably lies strongly on the side of the syn-

proportionation species (EtZnX) for the systems examined.

In the absence of a donor solvent the properties of ethylzinc halides show some diversity (Boersma and Noltes, 1966). Ethylzinc chloride and bromide show sharp melting points and give clear solutions in aprotic non polar solvents such as n-hexane or toluene. As mentioned earlier both are tetrameric cryscopically in benzene. Ethylzinc iodide on the other hand melts with decomposition and deposits a residue of ZnI_2 when attempts are made to dissolve it in non-polar solvents. This is no doubt a reflection of the polymeric nature of the solid, there being apparently no smaller degree of association available to the iodide without solvation.

The Schlenk equilibrium for EtZnCl and EtZnBr dissolved in n-pentane or toluene lies essentially on the right at room temperature. Neither $ZnCl_2$ nor $ZnBr_2$ precipitate from solution and upon addition of 2,2'-bipyridine (bipy), the orange-red colour of $Et_2Zn.bipy$ (Noltes and Van den Hurk, 1965) is barely perceptible. This does not hold true for ethylzinc iodide as appears from the presence of insoluble ZnI_2 in hydrocarbon solvents added to solid EtZnI and from the formation of $Et_2Zn.bipy$ upon addition of 2,2'bipyridine. Thus it seems that the monomeric species EtZnI in solution requires donor ligands for stability.

Difficulties in crystallizing ethylzinc iodide from solution in ethyliodide are understandable in terms of the molecular adjustment which is required to take place



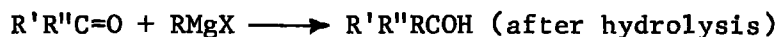
2.4 The Reaction of Grignard Reagents with Ketones.

The reactions of Grignard reagents are inevitably complex due to the complicated structure of the Grignard reagents themselves and are the more difficult to study as a result of the air sensitive nature not only of the reactants but also of some of the products. Grignard reactions have been reviewed comprehensively in two books (Yoffe and Nesmeyanov, 1957; Kharasch and Reinmuth, 1954) and two review articles (Ashby, 1967; Salinger, 1963). It would not be feasible to give more than a brief outline of the topic here.

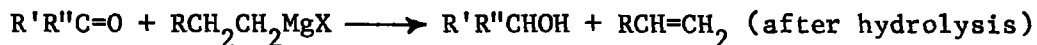
The theory that the initial step in the reaction of a ketone with a Grignard reagent is the replacement of a solvent molecule co-ordinatively bound to the Grignard, by an approaching ketone molecule (Strauss, 1912) has subsequently been supported by experiments (Pfeiffer and Blank, 1939) which show that the presence of a strong base (e.g. pyridine) in the Grignard solution inhibits reaction with ketones considerably. Subsequent steps in the reaction are less easy to elucidate and conflicting theories have differed both concerning the nature of the Grignard entity with which the ketone initially interacts and in the order of reaction with respect to Grignard.

Three products of the reaction are possible

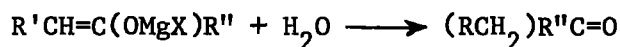
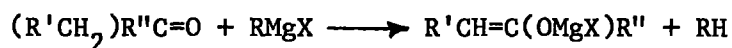
(i) Normal Addition



(ii) Reduction of the Ketone

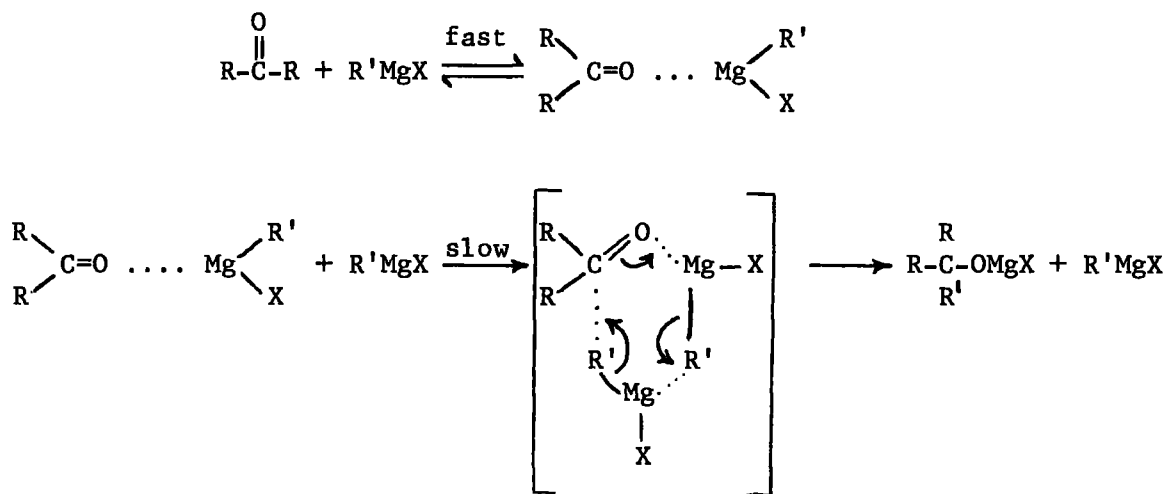


(iii) Enolate formation

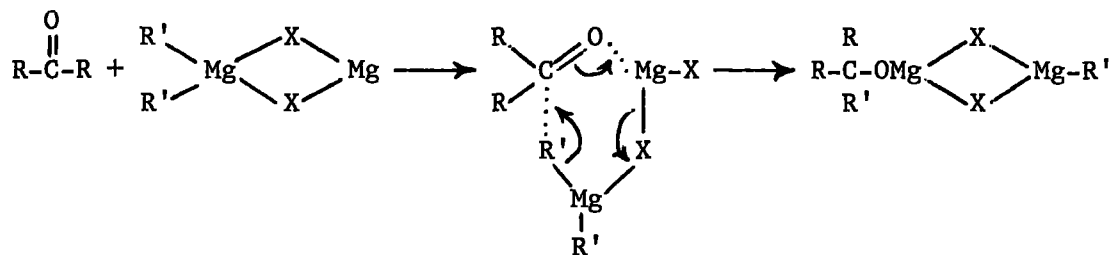


depending on reaction conditions and on which alkyl groups are represented by R, R', R''. The kinetics of the reduction reaction have been studied (Singer, Salinger and Mosher, 1967) but the normal addition reaction has received most attention.

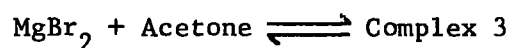
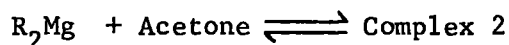
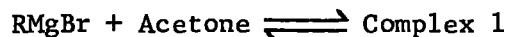
The first serious mechanistic suggestion for the addition (Swain and Boyles, 1951) was that the reaction was third order: first order in ketone and second order in Grignard reagent as follows



After 1957 when the Grignard reagent was reported to have the $R_2Mg \cdot MgX_2$ structure (Dessy et al.) a bimolecular mechanism involving one molecule of ketone and one molecule of unsymmetrical dimeric Grignard reagent was proposed (Bikales and Becker, 1962; Hamelin and Hayes, 1961; Miller et al., 1961)



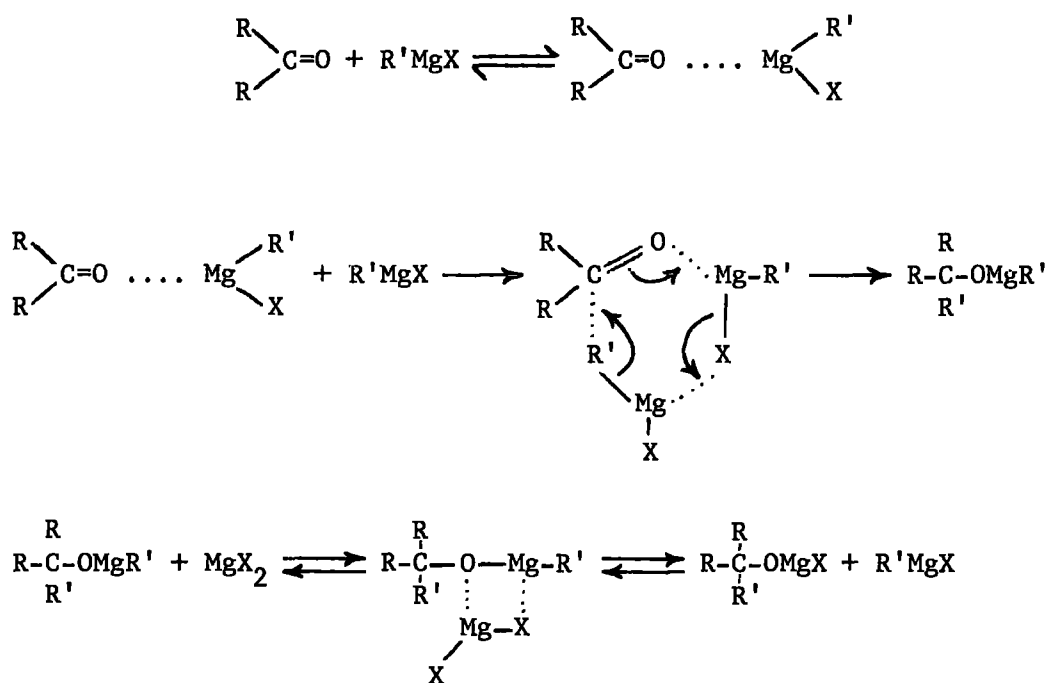
Since the return to favour of a monomeric structure for the Grignard reagent (Ashby and Smith, 1964) however the above proposal has lost headway. It has been suggested recently (Holm, 1968) that in the reaction between butylmagnesium bromide and acetone the initial step involves co-ordination of acetone to all three magnesium containing constituents of the Schlenk equilibrium



but that the equilibrium involving $RMgBr$ probably accounts for 90% of the co-ordinated acetone.

The situation may be even more complicated by the possibility that the mechanism varies from one Grignard reagent to another since it has been shown that Grignard reagents themselves may have more than one type of structure, certainly in the solid state (Stucky and Toney, 1967) and probably also in concentrated solutions (Ashby and Walker, 1967).

For the reaction of benzophenone and methylmagnesium bromide in diethyl ether kinetic results have been obtained which support a suggested mechanism (Ashby, Duke and Neumann, 1967) which resembles Swain's original scheme



To account for the drop in reaction rate observed after half of the available alkyl groups in the Grignard reagent have been consumed in

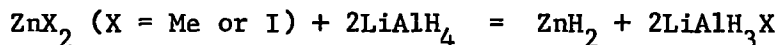
reaction with ketone the mechanism above requires that the reaction between alkylmagnesium alkoxide and magnesium halide (regenerating Grignard reagent) be slow relative to the other stages of the overall reaction. In fact it has been shown (Ashby and Arnott, 1967) that the redistribution of alkylmagnesium alkoxides and magnesium bromide to form alkoxy magnesium bromide is rapid. Thus it appears that the details of the final step are not clear even now.

The alkoxy magnesium halide product has been isolated in a number of cases (Coates et al., 1968). Often, as in the reaction between benzophenone and methylmagnesium bromide, the product is insoluble in ether, but t-butoxy magnesium bromide prepared from acetone and methylmagnesium bromide is soluble in ether and in benzene. $(\text{Bu}^t\text{OMgBr}\cdot\text{OEt}_2)_2$ is dimeric in both these solvents and also in the solid phase. An X-ray structure analysis has revealed that the dimer consists of two units of $\text{Bu}^t\text{OMgBr}\cdot\text{OEt}_2$ linked round a centre of symmetry by means of a Mg_2O_2 four-membered ring involving the butoxy oxygens. One ether molecule is co-ordinatively bound to each magnesium bringing the co-ordination number of the metal atom to four. Such a structure is consistent with current expectations of the chemical characteristics of the magnesium atom in Grignard systems.

All the questions concerning Grignard reaction mechanisms involving various alkyl groups and even in different solvents have not yet been answered but it would appear that progress is being made in the right direction.

2.5 Zinc and Magnesium Hydrides

Zinc hydride as prepared from lithium aluminium hydride and dimethylzinc or zinc iodide,



is a non volatile, insoluble material decomposing slowly at room temperature and rapidly at 90°C. It has been suggested (Mackay, 1966) that zinc hydride is probably an electron deficient-bridged polymer.

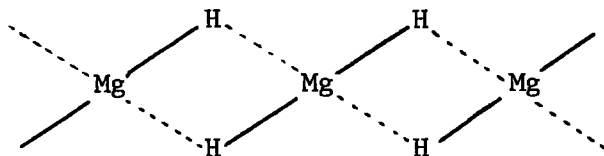
Few reactions of zinc hydride have so far been reported, no doubt due to solubility difficulties. A suspension in ether reacts with diborane to form zinc borohydride $\text{Zn}(\text{BH}_4)_2$ (Barbaras et al., 1951).

Zinc hydride reacts with NNN' trimethylethylenediamine (TriMED) to give a hydrido complex $(\text{HZnTriMED})_2$ which may be crystallised from toluene (Bell and Coates, 1968) and is dimeric both in benzene and in the crystal. An X-ray structure analysis has revealed a Zn_2N_2 four-membered ring and terminal zinc hydrogen bonds. A broad band at 1825 cm^{-1} (width at half-height ca. 120 cm^{-1}) which is beyond all reasonable doubt associated with zinc-hydrogen vibrations suggests that the Zn-H bond is predominantly covalent.

There are indications of an intermediate methylzinc hydride (Barbaras et al., 1951) and the preparation of iodozinc hydride, HZnI is reported (Wiberg et al., 1951; Wiberg et al., 1952).

Magnesium hydride is far more stable than zinc hydride and was initially prepared as long ago as 1912 (Jolibois) by the pyrolyses of

Grignard reagents. An X-ray structure analysis (Ellinger et al., 1955) has shown that the magnesium hydride crystal has the rutile structure, although the bonding involved is believed to be on the borderline between ionic and covalent (involving electron-deficient bridges). An infra-red study (Mackay, 1966) revealed as the only feature of the spectrum a broad band stretching from 900-1600 cm^{-1} which was ascribed to incipient bridge bonding



Magnesium hydride dissolves slowly in a solution of trimethylethylenediamine (Bell and Coates, 1968) in toluene and hydrolysis of the filtrate shows hydridic hydrogen to be present but no solid product analogous to $(\text{HZnTriMED})_2$ is obtained.

The hydride chemistry of neither zinc nor magnesium is developed very far and the stability of the complex $(\text{HZnTriMED})_2$ (up to a melting point of 120°C) seems to be uncharacteristic.

Chapter Three

The Crystal Structure of Ethylzinc Iodide

3.1 Introduction

Ethylzinc iodide was probably first prepared in 1849 by Frankland and subsequently there has been considerable speculation and controversy over the nature of alkylzinc halides. Indeed this study is part of a more general interest in compounds of the type RMX where M is an element of Group II and X is Cl, Br, or I. At one time it was claimed (Dessy, 1960) that except for Mercury, the Group II organometal halides exist as R_2M, MX_2 complexes rather than as RMX. Since then, convincing evidence for monomeric solvated alkylmagnesium halides has been obtained by molecular weight studies (Ashby and Smith, 1964), and crystallographic investigations of $EtMgBr.(OEt_2)_2$ (Guggenberger and Rundle, 1964) and of $PhMgBr.(OEt_2)_2$ (Rundle and Stucky, 1964).

There is now evidence for the existence of solvated monomeric alkylzinc halides also (Dessy and Coe, 1963), and, since this present structure analysis began, the tetrameric unsolvated ethylzinc chloride and bromide have been prepared (Boersma and Noltes, 1966). These latter two compounds are believed to have structures similar to that of $(MeZnOMe)_4$, (Shearer and Spencer, 1966). Significantly, Boersma and Noltes found differences in the properties of ethylzinc chloride and bromide on the one hand, and ethylzinc iodide on the other. For example attempts to dissolve ethylzinc iodide in hydrocarbons resulted in decomposition to ZnI_2 and Et_2Zn ,



and hence molecular weight measurements were not possible.

There were no crystallographic data about any of the unsolvated Group II organometal halides except those of Mercury until the work described in this chapter.

3.2 Preparation

Of four methods of preparation of RZnI reported in the literature:

Ethylzinc iodide Jander, Fischer and Winkler, 1958

Phenylzinc iodide Hilpert and Gruttner, 1913

Isopropylzinc iodide Karrer et al., 1928

Ethylzinc iodide Ridley, 1965

that due to Jander, Fischer and Winkler was found to be the most convenient for obtaining crystals: Ethylzinc iodide was prepared by refluxing pure ethyl iodide (38 grams) and zinc dust (16 grams, 1 mol.) under an atmosphere of dry, oxygen-free nitrogen at 85-90°C, for two hours, and filtering the resultant solution, while hot, from excess zinc. A clear solution was obtained which, on cooling, yielded colourless crystals in the form of thin plates. The compound may well interact with ethyl iodide in solution but no more satisfactory alternative solvent was discovered. Analysis of the crystals was in good agreement with the empirical formula of the unsolvated species [Found: Zn, 30.7; hydrolysable ethyl, 12.6%. C_2H_5ZnI requires Zn, 29.5; hydrolysable ethyl 13.1%. Melting point measured: 95°C (decomp.). Jander et al. literature value: shrinks at 95°C, decomposes at 98°C].

Repeated attempts were made to obtain a well formed single crystal but the best specimen still gave rise to two separate diffraction patterns indicating that it consisted of more than one part. It was however found possible to proceed with this, since the diffraction pattern of one portion of the crystal had intensities much greater than those of the other.

The crystals are very air sensitive and were sealed into pyrex glass capillary tubes under the dry, oxygen-free atmosphere of a glove box.

3.3 Crystal Data

Precession and Weissenberg photographs revealed an orthorhombic cell with

$$a = 21.17, \quad b = 4.33 \quad \text{and} \quad c = 5.38\overset{\circ}{\text{A}}$$

The following conditions governed the reflections observed.

$$\begin{array}{lll} 0k1 & k + 1 = 2n & h0l \text{ no conditions} \\ hk0 & h = 2n & hkl \text{ no conditions} \end{array}$$

The space group as deduced from the systematic absences was thus either $Pnma (D_{2h}^{16})$ No.62 in the International Tables for X-ray Crystallography or $Pn2_1a (C_{2v}^9)$ (corresponding to No.33, only having the b and c axes interchanged) but the subsequent structure analysis led to the adoption of the former. The density of the crystals, examined by flotation, was between 3.1 (Me_2Hg) and 2.3 (MeI) g.cm^{-3} , while the calculated density,

2.98 g.cm^{-3} , corresponds to four units of $\text{C}_2\text{H}_5\text{ZnI}$ per unit cell.

The crystal used for data collection was plate-like having the long crystal axis, a, perpendicular to its plane. The axes b and c lay in the plane but the sides of the plate were, surprisingly, developed in the 012 (width) and 021 (length) directions. The corresponding dimensions of the cross-section were $0.42 \times 0.05 \text{ mm}$ and the linear absorption coefficients, μ ,

for copper radiation ($\lambda = 1.5418\text{\AA}$), $\mu_{\text{cu}} = 557.5 \text{ cm}^{-1}$ and for molybdenum radiation ($\lambda = 0.7107\text{\AA}$), $\mu_{\text{mo}} = 112.5 \text{ cm}^{-1}$.

The unit cell dimensions were determined from precession photographs of the $hk0$ and $0kl$ nets and the statistical standard deviations of the measurements were $\pm 0.05\text{\AA}$ for a and $\pm 0.03\text{\AA}$ for b and c. The instrumental uncertainty however is probably of the order of 0.2% and hence the overall uncertainty in a should probably be increased to about $\pm 0.06\text{\AA}$.

3.4 Data Collection

The intensities of the high order reflections fell off rapidly with increasing θ and the equi-inclination Weissenberg technique was preferred to the precession method in order to collect the maximum quantity of data and also because of the higher quality of the photographs thus obtained. Partial three dimensional data were recorded using zirconium-filtered molybdenum radiation for layers $h0l$ to $h3l$.

Higher nets were of poor quality. The multiple film packs contained sheets of 0.0008" nickel foil interleaved between consecutive films. The intensities were visually estimated by comparison with a calibrated scale and correlated through a set of timed exposures of different nets. The film to film intensity reduction factor was found to be $2.82 \pm 0.02:1$ compared with the value quoted in the literature (Abrahams and Sime, 1960) of 2.65:1. Over the range of equi-inclination angle used, the obliquity factor (Rossman, 1956) is negligible and a single value (2.82) was used for all four nets.

As previously described the crystal used for data collection gave rise to two ranges of reflections on each film and although it had been possible to select one self-consistent set for estimation, it was not possible to correct for anisotropic absorption effects since it was clear that more than one piece of crystal was intersecting the path of the X-ray beam.

The 335 independent intensities were corrected for Lorentz and polarization factors and for variation in spot length, using a programme written by Dr. G.W. Adamson.

3.5 Structure Determination

(a) Heavy Atom Positions

The three dimensional Patterson function was calculated along

u at intervals of 0.35\AA ($^a/60$)

v at intervals of 0.22\AA ($^b/20$)

w at intervals of 0.27\AA ($^c/20$)

The relevant Patterson function is

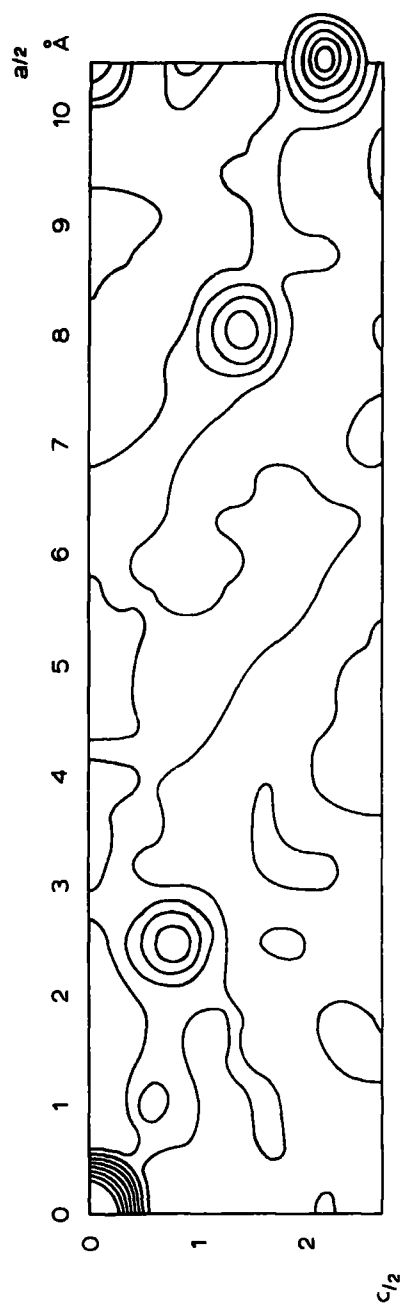
$$P(u,v,w) = \frac{8}{V} \sum_u \sum_v \sum_w w(hkl) |F_{(hkl)}|^2 \cos 2\pi(hu + kv + lw)$$

modified to allow for the multiplicities of the reflections. $w(hkl)$ is a sharpening function given the value of $\exp.2B\left(\frac{\sin\theta}{\lambda}\right)^2$. For each of the two possible space groups the symmetry of the vector set is Pmmm so that the asymmetric unit of the Patterson function appears eight times in the unit cell. The symmetry operations result in a Harker section ($2x, \frac{1}{2}, 2z$) and two Harker lines ($-\frac{1}{2} + 2x, \frac{1}{2}, \frac{1}{2}$ and $\frac{1}{2}, 0, -\frac{1}{2} + 2z$).

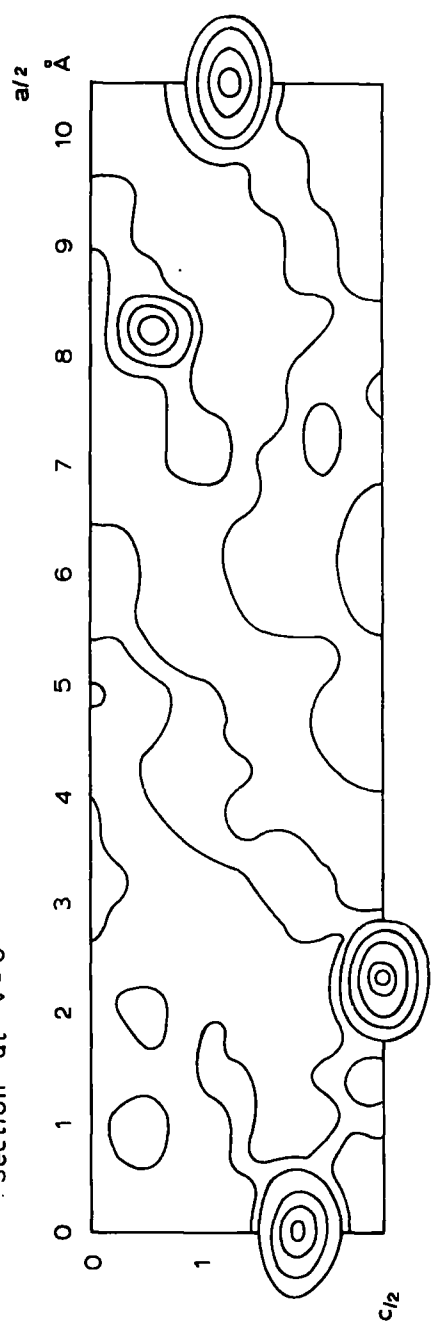
The principle peaks in the Patterson function occurred on sections at $v = 0$ and $v = \frac{1}{2}$, which are drawn out in figure 3.1. The co-ordinates of the peaks are tabulated below:

$u(^a/60)$	$v(^b/20)$	$w(^c/20)$	Relative height	assignment
30	0	8	84,5	I-I vector
23	0	5	34,0	Zn-I "
7	0	3	34,5	Zn-I "
7	10	10	84,0	I-I "
23	10	2	34,4	I-I "
0	10	7	61,6	Zn-I "
30	10	5	56,8	Zn-I "

Ethylzinc Iodide Patterson Function



Section at $v = 0$



Section at $v = 1/2$

Contours are at equal arbitrary intervals except for the peak at the origin

Figure 3-1

The heavy atoms were thus located at:

	x/a	y/b	z/c
Iodine	0.1955	0.2500	0.0534
Zinc	0.3080	0.2500	0.1885

The iodine and zinc atoms were found to have very similar values for their y-co-ordinates, indeed it was not possible to assign different values to them. Further, if these atoms have the same values for y-co-ordinates then the arrangement of zinc and iodine atoms is centrosymmetric and these atoms will lie on mirror planes at $y = \frac{1}{4}$ and $y = \frac{3}{4}$. (This corresponds to the space group Pnma).

(b) Carbon Atom Positions.

If the iodine, zinc and carbon atoms all lay on the mirror plane at $y = \frac{1}{4}$, which seemed quite possible, then the location of the two carbon atoms would be reduced to a 2-dimensional problem and sufficient information might be available in the Patterson function through the level at $v = 0$ to solve it. However, an attempt to use the vector convergence method (Robertson and Beevers, 1950) by drawing out the vector convergence density map from the Patterson function at this section, using the iodine-iodine vectors, failed to reveal coherent positions for carbon atoms and served only to confirm the previously determined sites for zinc.

Structure factors were calculated using the iodine and zinc co-ordinates given above. Since these two atoms were given the same y-co-

ordinate and thus had a centrosymmetric arrangement, the structure factors calculated at this stage correspond to the centrosymmetric space group Pnma even though this had not yet been shown to be the correct one. The reliability index R, for the structure factors was 28.4%,

$$\text{where } R = \frac{\sum |F_d - F_c|}{\sum |F_o|}$$

A three dimensional F_o synthesis was then calculated phasing on the heavy atom positions, over the range

from $x = 0$ to $x = \frac{1}{2}$ by units of 0.35\AA

from $y = 0$ to $y = \frac{1}{4}$ by units of 0.22\AA

and from $z = 0$ to $z = 1$ by units of 0.27\AA

Peaks on the iodine and zinc positions appeared with magnitudes of $163 \pm 5 \text{ e}\text{\AA}^{-3}$ and $77 \pm 2 \text{ e}\text{\AA}^{-3}$ respectively. A peak of $9.5 \text{ e}\text{\AA}^{-3}$ on the same section ($y = \frac{1}{4}$) appeared to be in a likely position for the α -carbon atom but the positions and shapes of other peaks on this level (8.8 and $8.6 \text{ e}\text{\AA}^{-3}$) did not encourage confidence and the electron density did not reach this magnitude any where else in the map. The iodine and zinc positions were then improved through two cycles of isotropic least squares refinement using the block diagonal approximation, R dropping to 19.8%. Structure factors were calculated using the new parameters and a second electron density map phased on the heavy atoms

prepared. The iodine and zinc peak heights were now 118 and 55 e\AA^{-3} respectively the scale factor having changed considerably since the previous calculation. A peak of 8.5 e\AA^{-3} was coincident with the site selected for the α -carbon on the first map and a peak of 5 e\AA^{-3} appeared on the same level ($y = \frac{1}{4}$) in an appropriate place for the β -carbon atom. There were only three other peaks of over 4 e\AA^{-3} and these appeared in positions related by symmetry to the heavy atom positions.

3.6 Structure Refinement

The positional and thermal parameters of all four atoms were then refined by full matrix least squares methods. After three cycles with isotropic and four cycles with anisotropic temperature parameters the residual, R, had improved to 11.04%.

Since in the last of these cycles the 36 parameter shifts were all small the refinement seemed almost complete and structure factors were calculated and used to compute an $F_o - F_c$ synthesis, as a check against any gross errors in the structure. The difference map showed no peaks as great as 1.5 electrons with the exceptions that electron density was still accumulated on the sites of detected atoms:

on the iodine position	12.3 e\AA^{-3}
zinc	4.3 e\AA^{-3}
carbon 1	0.7 e\AA^{-3}
carbon 2	1.5 e\AA^{-3}

It is supposed that these features together with a value of the thermal

vibrational tensor component, U_{11} , for one of the carbon atoms which was negative (albeit by less than half of the corresponding estimated standard deviation) are due to imperfections in the intensity data.

Structure factors were calculated for 139 unobserved planes and only 7 of these were greater than 1.5 times the minimum observable value.

Two more cycles of refinement on the observed planes saw R converge to a value of 10.94% and the final least squares totals together with an analysis of the effect of the weighting scheme are shown in Table 3a.

For the last two cycles the structure factors were weighted by the function w , given by

$$\sqrt{w} = \left\{ \frac{1 - e^{-R \left(\frac{\sin \theta}{\lambda} \right)^2}}{1 + P_2 |F_o| + P_3 |F_o|^2 + P_4 |F_o|^3} \right\}^{\frac{1}{2}}$$

and $P_1 = 10$, $P_2 = 0.1$, $P_3 = 0.00222$, $P_4 = 0$.

The final values of the positional and thermal parameters and their estimated standard deviations are given in Table 3b, the parameter shifts in the final cycle all being less than one third of their corresponding e.s.d. The observed and calculated structure factors are listed in Table 3c.

In this case, as with the two structures subsequently to be described, the atomic scattering curves used were those given in the International Tables for X-Ray Crystallography (1962) Volume III. The real parts of the

EtZnI TABLE 3a.

Least-Squares Totals

Number of Observed Planes 335

$\Sigma \Delta $	1848.3	$\Sigma F_o $	16901.2	$\Sigma F_c $	16637.7	R	0.109
$\Sigma w \Delta ^2$	1023.6	$\Sigma w F_o ^2$	44639.8	$\Sigma w F_c ^2$	43777.0	R'	0.023

Weighting Analysis

$w\Delta^2$ averaged in batches and the number of planes per batch

$\sin\theta/\lambda$

	0.0-0.2	0.2-0.4	0.4-0.6	0.6-0.8	TOTALS
$ F_o $					
0-6	0.00/0	0.00/0	0.00/0	0.00/0	0.00/0
6-11	0.00/0	0.00/0	0.00/0	0.00/0	0.00/0
11-22	0.00/0	2.52/17	2.62/25	9.46/7	3.56/49
22-45	1.69/3	7.36/28	3.21/85	5.60/25	4.42/141
45-89	3.42/6	2.55/42	2.29/53	2.79/2	2.47/103
89-UP	3.02/10	2.14/27	4.22/5	0.00/0	2.60/42
TOTALS	2.94/19	3.63/114	2.86/168	6.23/34	3.47/335

EtZnI TABLE 3bFinal Values of Atomic Co-ordinates and their Standard Deviations

Atom	x/a	y/b	z/c	$\sigma(x/a)$	$\sigma(y/b)$	$\sigma(z/c)$
I	0.19522	0.25000	0.04920	0.00012	0.00000	0.00053
Zn	0.31473	0.25000	0.18947	0.00025	0.00000	0.00131
C(1)	0.40197	0.25000	0.07103	0.00162	0.00000	0.01093
C(2)	0.44770	0.25000	0.26632	0.00147	0.00000	0.01513

Final Values of Anisotropic Temperature Parameters (\AA^2) and their Standard Deviations ($\text{\AA}^2 \times 10^4$ for iodine and zinc, $\text{\AA}^2 \times 10^3$ for carbon)

Atom	U_{11}	U_{22}	U_{33}	$2U_{23}$	$2U_{31}$	$2U_{12}$
I	0.0408(15)	0.0341(28)	0.0190(13)	0.0000(0)	-0.0009(22)	0.0000(0)
Zn	0.0391(27)	0.0383(49)	0.0477(36)	0.0000(0)	0.0030(42)	0.0000(0)
C(1)	-0.0049(12)	0.2152(79)	0.0502(29)	0.0000(0)	0.0381(33)	0.0000(0)
C(2)	0.0001(14)	0.3284(159)	0.0785(51)	0.0000(0)	0.0163(40)	0.0000(0)

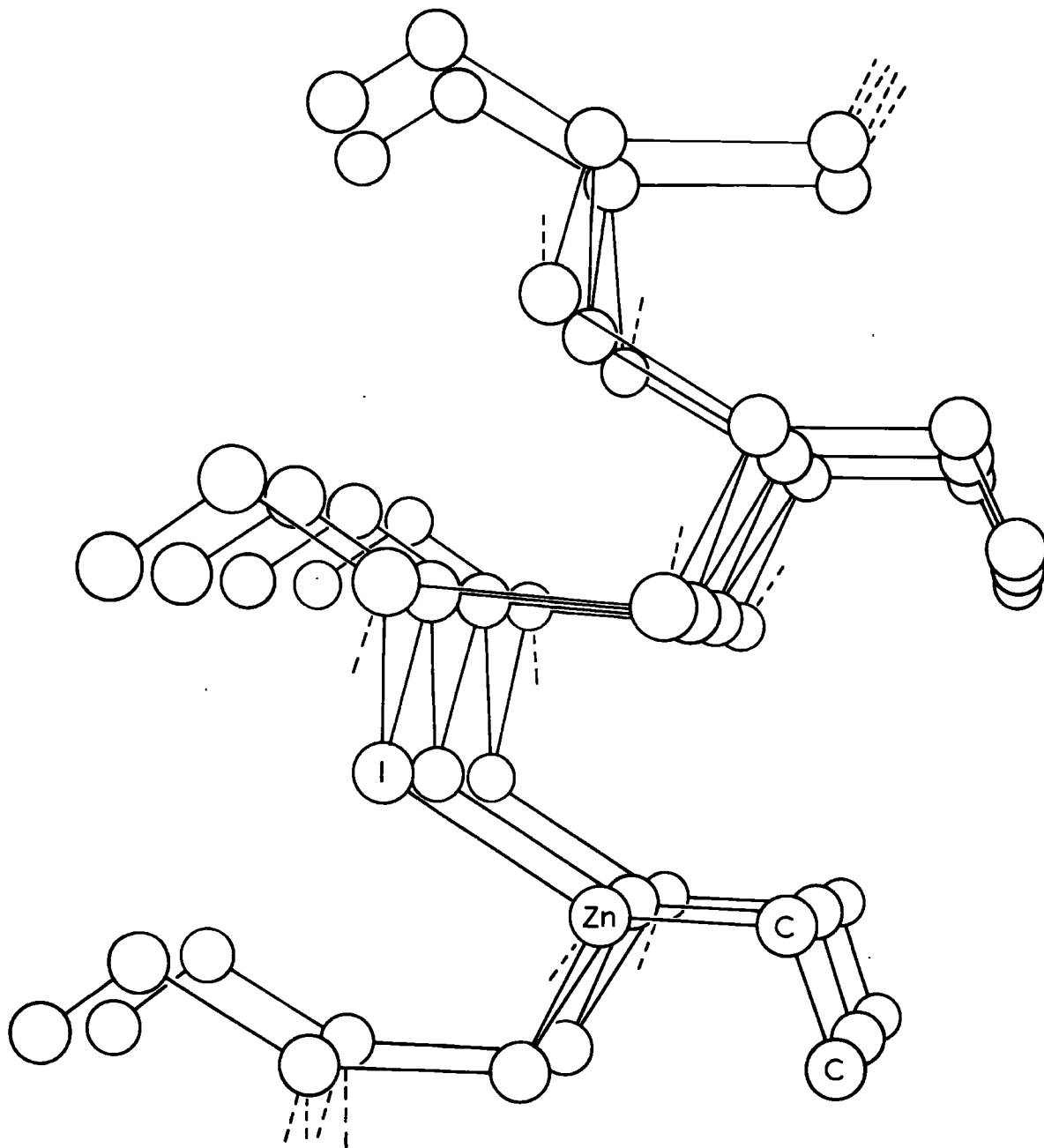
dispersion corrections were applied in the cases of the iodine and zinc atoms.

3.7 Test of the Space Group

The structure refinement above was undertaken incorporating a centre of symmetry in the space group since the implications were that a mirror plane was present at $y = \frac{1}{4}$ (and therefore also at $y = \frac{3}{4}$) on which the iodine, zinc and carbon atoms lay. In order to test the validity of this assumption a separate refinement, parallel to that described, was performed using the non-centric space group $Pn2_1a$. This manoeuvre however produced results which were less satisfactory from several aspects. The carbon atoms persistently jumped from one side of the plane at $y = \frac{1}{4}$ to the other between successive cycles, despite a partial shift factor of 0.8, and their thermal vibrational tensor components, U_{33} , would not refine. Also the reliability index, R , only improved to 17.8%. This relative failure indicated that $Pnma$ was the correct space group and that the former refinement was valid.

3.8 Description of Structure

The structure takes the form of a co-ordination polymer, the iodine and zinc linkages giving rise to layers as shown in figure 3.2. The four units of C_2H_5ZnI which occupy the unit cell are situated on mirror planes at $y = 0.25$ and 0.75 . Each iodine atom is at a distance of $2.64\overset{\circ}{\text{A}}$ from a zinc atom lying in the same mirror plane, the I-Zn-C(1)



Fragment of the Ethylzinc Iodide Polymer

Figure 3.2

angle in the plane (144.4°) having a value approximately half-way between the tetrahedral and the linear. In addition, each iodine is 2.91\AA from two other zinc atoms, which lie on adjacent mirror planes half a unit cell length above and below it respectively. Estimates of the iodine-zinc bond length based on the tetrahedral atomic radii quoted by Pauling (1960) are, 2.59\AA for covalent bonds, and 2.70\AA for ionic bonds. Perhaps the most relevant comparison available in the literature is that afforded by the crystallographic examination of zinc iodide (Oswald, 1960) where the bond length is 2.62\AA . Although Oswald does not quote e.s.d.'s this value is probably in good agreement with the shorter of the two zinc-iodine bond lengths found in ethylzinc iodide.

There are no other zinc atoms at a distance of less than 4\AA . Thus each iodine forms two long and one more normal bond to zinc and has a nearly pyramidal environment. The bond angles at iodine (105° , 105° and 96°) are all less than the tetrahedral so that the stereochemistry is as would be predicted for an atom making use of one direction in space to accommodate a lone pair (Gillespie and Nyholm, 1957).

The arrangement at zinc departs considerably from the tetrahedral and the I-Zn-C(1) angle (144.4°) might be interpreted as representing a situation intermediate between a polymer on the one hand and discrete, non-interacting monomers on the other. The structure may be compared with that of mercury(II) cyanide (Hvolsef, 1958) where almost linear

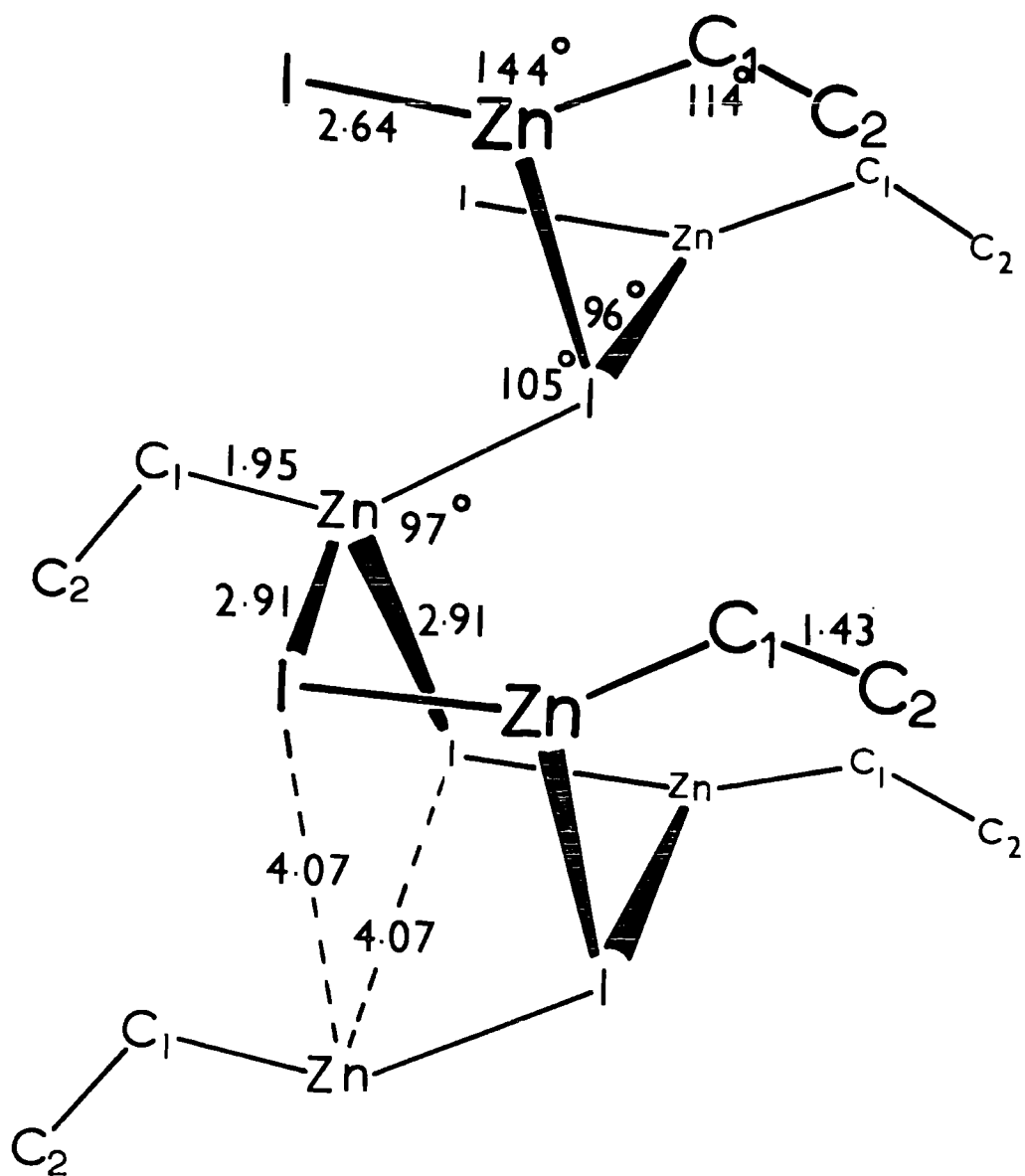
$\text{Hg}(\text{CN})_2$ molecules are linked together by long Hg-N bonds.

The Zn-C(1) distance of $1.95\overset{\circ}{\text{Å}}$ is less than the sum ($2.08\overset{\circ}{\text{Å}}$) of the Pauling tetrahedral covalent radii but agrees closely with the length of $1.94\overset{\circ}{\text{Å}}$ found in dimethylzinc (Rundle, 196~~2~~³). A shortening of the Zn-C bond in dimethylzinc was explained by invoking hyperconjugation involving the empty 4p orbitals on zinc. It is interesting to note that the change from a formally 2-co-ordinate zinc atom in dimethylzinc through 3 co-ordinate zinc in $(\text{MeZnNPh}_2)_2$ (Shearer and Spencer, 1967) to 4 co-ordinate zinc in $(\text{MeZnOMe})_4$ (Shearer and Spencer, 1966) and $(\text{MeZnON:CMe}_2)_4$ (Shearer and Spencer, 1967) has little effect on the length of the zinc-carbon bond. The mean values of the Zn-C bond lengths found for these three compounds are:

$(\text{MeZnOMe})_4$	-	$1.948\overset{\circ}{\text{Å}}$
$(\text{MeZnNPh}_2)_2$	-	$1.949\overset{\circ}{\text{Å}}$
$(\text{MeZnON:CMe}_2)_4$	-	$1.950\overset{\circ}{\text{Å}}$

The C(1)-C(2) bond length ($1.43 \pm 0.08\overset{\circ}{\text{Å}}$) does not differ significantly from that found in diamond ($1.54\overset{\circ}{\text{Å}}$). The thermal vibration tensor components, U_{22} , of the carbon atoms (in the direction normal to the mirror planes) are very large however, and some apparent shortening of the length of the bond would be expected.

The final bond lengths and bond angles are shown in figure 3.3 and are listed, together with their respective standard deviations as calculated from the estimated standard deviations of the positional parameters, in Table 3d.



EtZnI

Bond Lengths and Angles

Figure 3.3

EtZnI TABLE 3dBond lengths (\AA) and their Standard Deviations ($\text{\AA} \times 10^3$)

I-Zn	2.640(6)
I-Zn'	2.911(6)
Zn-C(1)	1.954(38)
C(1)-C(2)	1.428(80)

Zn' is the atom at $\frac{1}{2}-x, \frac{3}{4}, \frac{1}{2} + z$ in the cell (0, 0, -1)

Bond Angles with their Standard Deviations

	Angle	e. s. d.
I-Zn-C(1)	144.4 $^\circ$	1.7 $^\circ$
Zn-C(1)-C(2)	113.6 $^\circ$	4.1 $^\circ$
Zn-I-Zn'	105.0 $^\circ$	0.8 $^\circ$
Zn'-I-Zn''	96.1 $^\circ$	0.8 $^\circ$
I-Zn-I'	96.9 $^\circ$	0.8 $^\circ$

Zn'' is the atom at $\frac{1}{2}-x, \frac{3}{4}, \frac{1}{2} + z$ in the cell (0, -1, -1)

I' is the atom at $\frac{1}{2}-x, \frac{3}{4}, \frac{1}{2} + z$ in the cell (0, 0, 0)

The non-bonding interatomic distances less than the shortest unit cell translation ($b = 4.33\text{\AA}$) are shown in Table 3e.

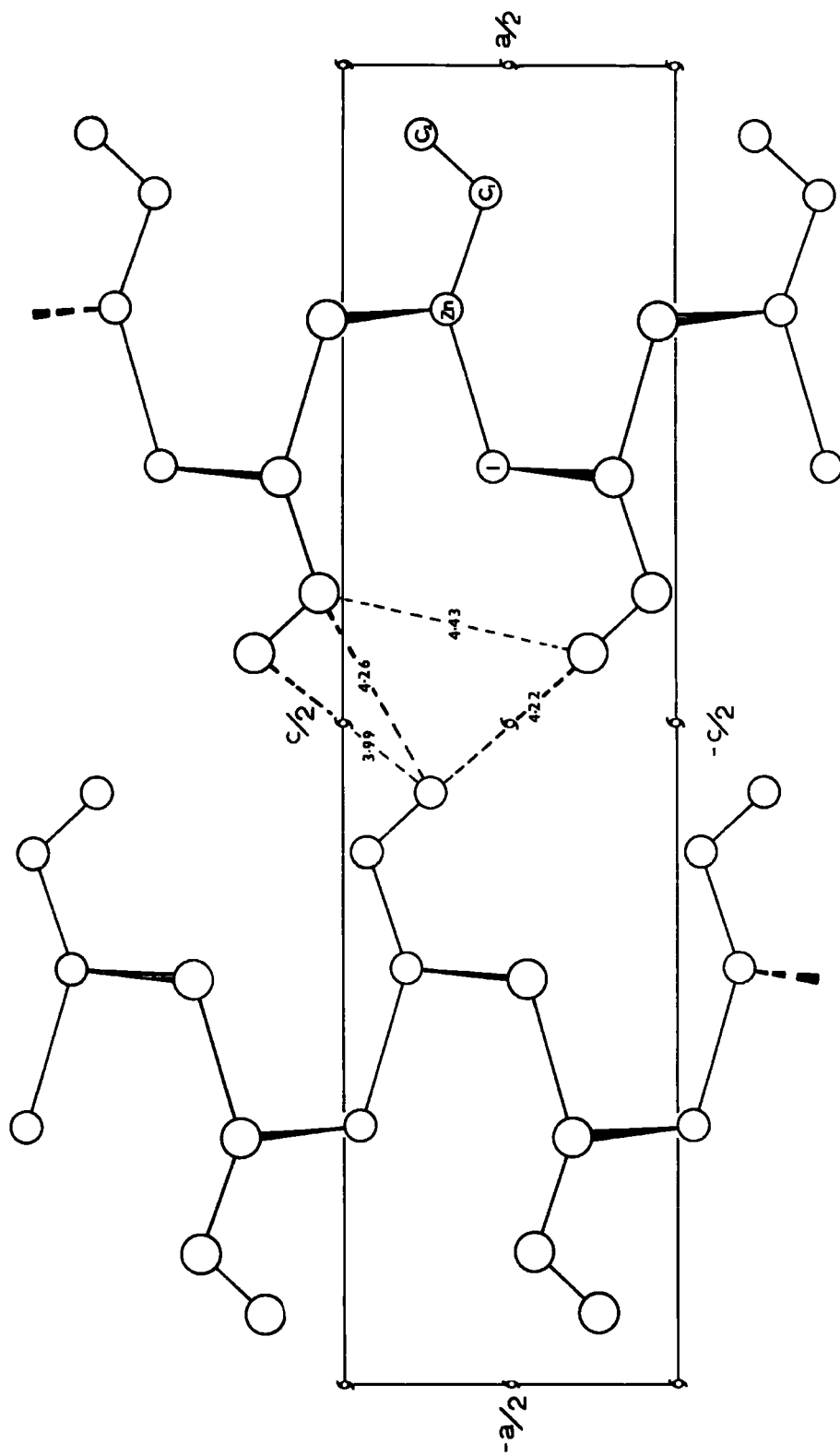
The shortest contact between non bonded carbon atoms is 3.99\AA so that neighbouring layers appear to pack easily together. Figure 3.4 shows the packing between layers and the relevant non-bonding separations, and is a projection along \underline{b} . The average values of B rise from about $2.0-2.5\text{\AA}^2$ for the iodine and zinc atoms through 6\AA^2 for carbon (1) to about 8\AA^2 for carbon (2) - a predictable gradation which represents the greater thermal motion of the lighter less rigidly bound atoms.

The exact values of B, however, are viewed with a certain amount of circumspection, since, as Bradley (1935) has pointed out, while absorption effects reduce observed intensities much more at low than at high angles, the reduction of intensities due to thermal motions depends on θ in the opposite sense. A consequence of this is that unless a correction is made for absorption, the resulting systematic errors will be largely taken up in the temperature factors during refinement. Thus although the refinement of the positional parameters of ethylzinc iodide may not have suffered generally as a result of the high absorption exhibited by this compound, it is highly likely that the isotropic temperature factors will be somewhat in error and further that the U_{ij} 's will have been affected in the specific directions in which absorption is most marked.

EtZnI TABLE 3eNon-bonding Intermolecular Contacts less than 4.33^oÅ

Equivalent Position Number 1	x,	y,	z
Equivalent Position Number 2	$\frac{1}{2}+x,$	$\frac{1}{2}-y,$	$\frac{1}{2}-z,$
Equivalent Position Number 3	\bar{x}	$\frac{1}{2}-y,$	$\bar{z},$
Equivalent Position Number 4	$\frac{1}{2}-x,$	$\bar{y},$	$\frac{1}{2}+z,$

Atom A	Atom B	Equivalent Position	Cell	A-B Angstroms
I	C(1)	4	(0, 0, -1)	3.94
I	C(2)	4	(0, 0, -1)	4.02
I	Zn	4	(0, 0, 0)	4.07
I	C(1)	4	(0, 0, 0)	4.10
I	I	4	(0, 0, 0)	4.16
C(1)	C(2)	3	(0, 0, -1)	4.26
C(2)	C(2)	3	(0, 0, 0)	3.99
C(2)	C(2)	3	(0, 0, -1)	4.22



EtZnI projection on the 010 plane

Figure 3.4

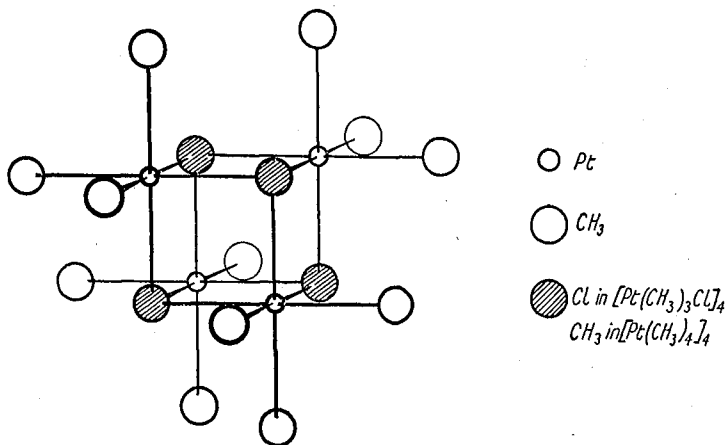
3.9 The Polymerisation of Unsolvated Alkyl group IIB halides

Polymerisation in alkyl group IIB halides is a manifestation of the tendency of the metal atom to expand its covalency by co-ordination with more electronegative atoms. Entropy considerations of course favour the lowest possible degree of association but discrete monomer units have only been found so far in the compounds of mercury, where lone pair effects undoubtedly play a permissive role.

Microwave data indicate (Gordy and Sheridan, 1954) that in the vapour, methylmercury chloride and bromide are linear monomeric molecules, and X-ray crystal studies (Grdenich, and Kitaigorodskii, 1949) show that for methylmercury chloride at least this situation persists into the solid phase. More recently Mills and Kennard (1967) have found that methylmercury(II) cyanide crystallises in the same space group as ethylzinc iodide, but in this case too the C-Hg-C skeleton is linear, which would not be the case if there were any interaction between the mercury atom and neighbouring pseudo halogen groups.

There is little data available concerning the cadmium compounds but the zinc analogues have been the object of some study. Following the general trend up the group, it would be expected that association would be more pronounced for alkylzinc halides than for compounds of the heavier metals and indeed ethylzinc chloride and bromide are reported (Boersma and Noltes, 1966) to be tetrameric in benzene solution. A cubane like structure is proposed for these compounds, the main

associative interactions taking place between metal and halogen atoms as in $(Me_3PtCl)_4$.



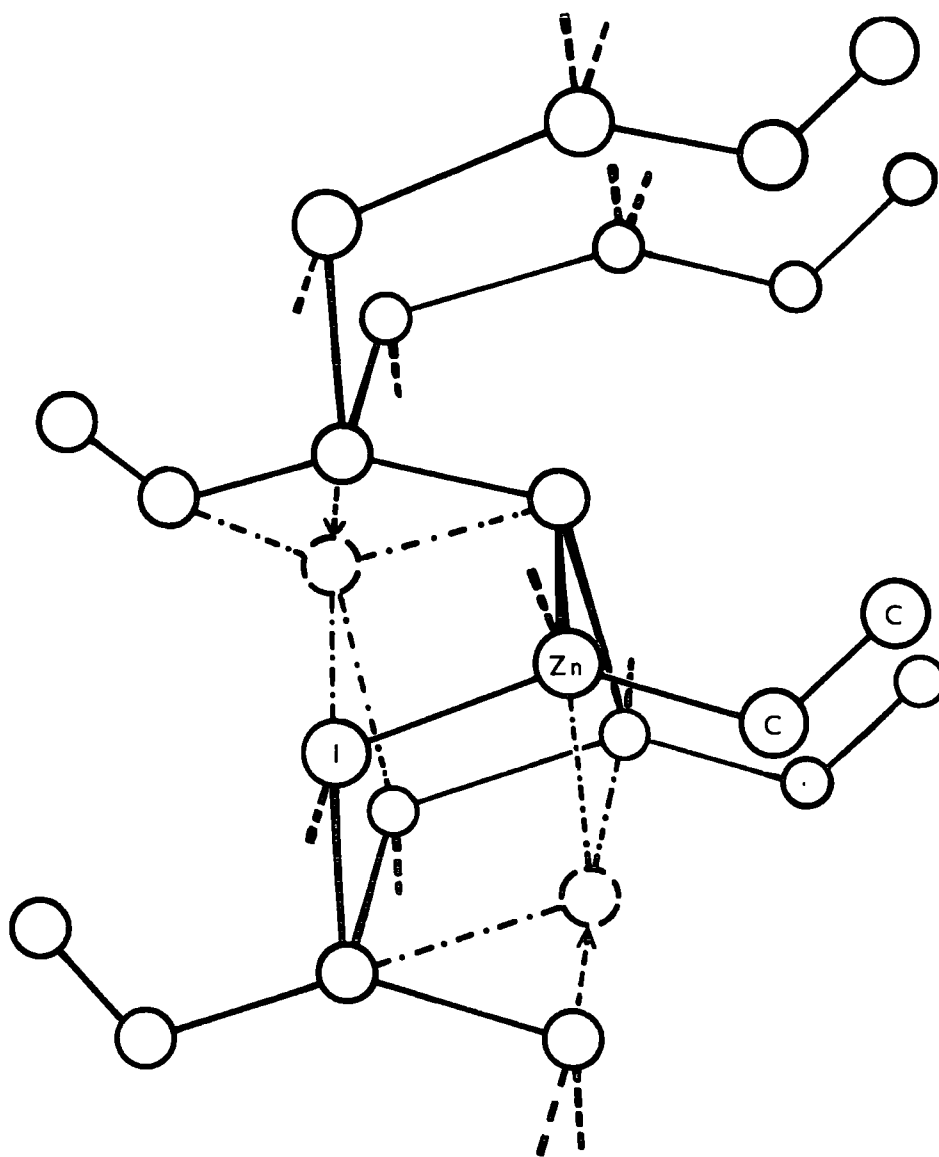
The structure of the tetrameric molecules $[Pt(CH_3)_3Cl]_4$ and $[Pt(CH_3)_4]_4$ (idealized).

Some versatility of the cubane structure is indicated by the range of compounds for which it obtains, $[(MeZnOMe)_4]$, (Shearer and Spencer, 1966); $(TiOMe)_4$, (Dahl et al., 1962); $(Ti(OEt)_4)_4$, (Gaughlan and Watenpaugh, 1967); etc.] and this type of tetramer appears to represent the smallest reasonable structural unit that allows the metal atom of RMX to be four co-ordinate. There are limitations inherent in this form, however, imposed by the essential presence of a four membered ring, since optimum bond angles in the ring will be 90° and a large discrepancy

between the sizes of the two atom types would cause serious inner core repulsions. In extreme cases these will be prohibitive and Rundle (1963) explains the monomeric nature of dimethylzinc in these terms.

The origins of the ethylzinc iodide polymer may in part be rooted in the lower electronegativity of the halogen attached to zinc but the polymer is also consistent with an inability to form a four-membered zinc iodine ring. The relationship between the polymer and a theoretical tetrameric alternative is illustrated in figure 3.5 where it will be seen that in a representative fragment of the status quo only two atoms would need to be constrained to make 2 bonds each in an opposite sense in order to obtain the pseudo cubane structure. It seems, however to be energetically favourable for quasi monomer units to be loosely linked together by long bonds in a way which reduces the entropy of the system but imposes less strain on the backbone of the molecule.

The establishment of this structure for ethylzinc iodide has led to an interest in the dissolved species. Molecular weight measurements have therefore been carried out on solutions of ethylzinc iodide in ethyliodide, using the Signer method of isopiestic distillation (Steyermark, 1961) and the results obtained were consistent with monomers in this case. The practical details of the method are outlined in Appendix 1.



EtZnI

Figure 3.5

Relationship between the polymer and a theoretical tetrameric
alternative

EtZnI TABLE 3c

Final Values of the Observed and Calculated
Structure Factors. Some unobserved planes
(signified by negative values of $|F_o|$) are
included.

Chapter Four

The Crystal Structure of the Diethyl Ether Complex of t-Butoxymagnesium Bromide

4.1 Introduction

Despite the considerable effort which has been devoted to the study not only of the constitution of Grignard reagents but also of the kinetics of their reactions with carbonyl compounds (Ashby, 1967), there is little information about the nature of the products of these reactions that are present before the usual hydrolysis is performed. Further, although proposed reaction mechanisms (Kharasch and Reinmuth, 1954) have involved specific entities such as $R_2R'COMgX$, "intermediate" products of this type have only rarely been isolated (Nesmeyanov and Sazonova, 1941), (Coates and Ridley, 1966a). The present structure analysis was undertaken to provide information about this phase of the reaction.

The etherate of tertiarybutoxymagnesium bromide is obtained when a diethyl ether solution of acetone is slowly added to methyl magnesium bromide, also in ether, at $-78^{\circ}C$ and the reaction mixture is allowed to warm to room temperature. Recrystallisation from the ether solution yields the product as colourless parallelepipedal plates which shrink at $90^{\circ}C$ and soften at $200^{\circ}C$. Cryoscopic measurements showed that tertiarybutoxymagnesium bromide etherate is dimeric in benzene solution - $(Bu^tOMgBr.OEt_2)_2$ (Coates and Ridley, 1966), and ebullioscopic measurements indicated the same degree of association in ether solution (Coates et al., 1968). Crystals for X-ray examination were sealed in pyrex capillaries under an atmosphere of dry, oxygen-free nitrogen.

4.2 Crystal Data

Zero-level precession photographs, with Mo K_{α} radiation ($\lambda = 0.7107\text{\AA}$) gave the following unit cell dimensions:

Monoclinic:

$$a = 9.68, \quad b = 11.10, \quad c = 15.10\text{\AA};$$

$$\beta = 129^{\circ} 8';$$

$$U = 1258.5\text{\AA}^3; \quad Z = 2 \text{ units of } (\text{Bu}^t\text{OMgBr.OEt}_2)_2;$$

$$D_{\text{calc.}} = 1.327 \text{ gm.cm}^{-3}; \quad \text{M.W. of } (\text{C}_4\text{H}_9\text{OMgBr.OC}_4\text{H}_{10})_2 = 502.92$$

Absorption Coefficient for Mo K_{α} radiation,

$$\mu = 35 \text{ cm}^{-1}.$$

The density of the crystals was measured by flotation using a mixture of 2-bromopropane ($\rho = 1.31 \text{ gm.cm}^{-3}$) and bromoethane ($\rho = 1.46 \text{ gm.cm}^{-3}$) and the value obtained was $D_{\text{obs.}} = 1.3 \text{ gm.cm}^{-3}$.

The space group was unambiguously determined by the conditions limiting the observed reflections;

$$0k0: \quad k = 2n,$$

$$h0l: \quad l = 2n,$$

as Number 14, $P2_1/c$, (C_2^h).

The statistical standard deviations in unit cell lengths were 0.01\AA in a, b and c and the uncertainty in β is of the order of $15'$.

Systematic errors are probably about 0.2% so that the overall uncertainty in the unit cell lengths is of the order of 0.02\AA .

4.3 Data Collection and Correction

Three dimensional intensity data were recorded photographically using the precession technique for nets hkn, $n = 0-5$ and hnl, $n = 0-4$. Intensities were observed to fall off rapidly at high values of θ . The use of the precession method meant that absorption effects were minimal and the collection of data up two axes allowed good net to net correlation.

The intensities were estimated visually using a calibrated scale compiled on the precession camera, and were corrected for Lorentz and polarisation factors. In view of the camera geometry involved in the precession method, anisotropic absorption errors were expected to be small and no correction was made for these.

The intensity data from individual nets were correlated on to a common scale using a least-squares method (Monahan, Schiffer and Schiffer, 1966) and where two values of the intensity for a reflection had been estimated, the mean value was adopted.

The crystal used for data collection was a parallelepipedal plate having the axes a and b in the plane of the plate, with the {110} faces well developed. The cross-section of the plate had dimensions 0.4 mm. x 0.2 mm.

4.4 The Patterson Function

The observed structure factors were multiplied by a weighting function w where $w = \exp\left(4\sin^2\theta/\lambda^2\right)$. This weighting function was not

permitted to exceed a value of 2.718 (i.e. e^1). This allowed the weighting function to take a constant value for reflections with $\sin\theta/\lambda \geq 0.5$. The Patterson function was then calculated using the squares of the weighted structure factors as fourier coefficients:

$$P(u,v,w) = \frac{4}{V} \sum_0^h \sum_0^k \sum_{-1}^1 \left(w(hkl) |F_{(hkl)}|^2 \right) (\cos 2\pi hu.$$

$$\cos 2\pi lw - \sin 2\pi hu \sin 2\pi lw) \cos 2\pi kv$$

The symmetry of the vector set is $P2/m$. The Patterson function was calculated over one quarter of the unit cell; 'u' at intervals of 0.323\AA to $a/2$, 'v' at intervals of 0.278\AA to $b/2$ and 'w' at intervals of 0.302\AA to c.

The Patterson function includes a Harker section at $(u, \frac{1}{2}, w)$ which contains vectors between atoms related by the two fold screw axis, and a Harker line at $(0, v, \frac{1}{2})$ containing vectors between atoms related by the axial glide plane. A double weight Br-Br vector is expected on each Harker section, and both the line $P(0, v, \frac{1}{2})$ and the section $P(u, \frac{1}{2}, w)$ contained only one peak large enough to accommodate a vector of the expected height. The values of x, y and z for the bromine atom were deduced from the positions of these two peaks and confirmed by the discovery of a single weight peak at $(2x, 2y, 2z)$ corresponding to the vector between bromine atoms related by the centre.

The next four peaks in order of magnitude were of heights expected

for double weight Bromine-Magnesium vectors and one of these was at a distance from the origin roughly corresponding to a Mg-Br bond length ($\sim 2.5\text{\AA}$). Hence values of x , y and z for the magnesium atom were deduced which were consistent with all four of these peaks representing Bromine-Magnesium vectors and the positions of Magnesium-Magnesium vectors were also successfully predicted.

The co-ordinates of the bromine and magnesium atoms were obtained as:

	x/a	y/b	z/c
Br	0.2400	0.2700	0.0480
Mg	0.0123	0.1325	-0.0040

At this stage it was already apparent that the magnesium atoms were situated in pairs round centres of symmetry close enough to be part of four membered rings and that the bromine atoms would be terminal rather than bridging.

4.5 Light Atom Positions

Structure factors were calculated on the basis of the positions of the bromine and magnesium atoms ($R = 0.323$) and were used to calculate an F_o synthesis. The function was evaluated for x at intervals of 0.323\AA to a , y at intervals of 0.278\AA to $b/2$ and z at intervals of 0.302\AA to $c/2$.

The two oxygen atoms in the asymmetric unit were located immediately and the peak heights corresponding to the four heaviest atoms,

which were the largest features on the map, were as follows: bromine 36, magnesium 14, O(1) 5.4 and O(2) 6.9 $\text{e}\text{\AA}^{-3}$, respectively. Eighteen other peaks of 2 $\text{e}\text{\AA}^{-3}$ or greater were found, and of these, four were grouped as would be expected for a t-butyl group attached to O(1).

The co-ordinates of these eight atoms were then improved through one cycle of refinement, using arbitrary initial values for the isotropic temperature parameters, and 'R' improved to 0.226. Structure factors were calculated using the improved atomic parameters and an $F_o - F_c$ synthesis computed. The difference synthesis showed regions of positive electron density on the sites of previously detected atoms. Aside from these, the largest features were four peaks (of heights 1.6, 1.7, 1.3 and 1.6 $\text{e}\text{\AA}^{-3}$ respectively) which were identified as arising from the ether carbon atoms.

4.6 Refinement

The structure was refined by the method of least squares using the block diagonal approximation. For two cycles, isotropic temperature factors were used, R improving to 0.165. There followed three cycles with all of the atoms having anisotropic temperature factors and R became 0.102. Finally an improved weighting scheme was adopted to bring the values of $w\Delta^2$ as nearly as possible uniform for all the averaged batches of F_o and three more cycles of anisotropic refinement saw R converge to 0.0986.

The parameter shifts in the final cycle were all less than one third of the corresponding estimated standard deviation (e.s.d.). The final values of the positional and thermal parameters together with their e.s.d.'s are given in Tables 4a and 4b.

Structure factors were calculated based on the final atomic parameters and used to compute a final $F_o - F_c$ synthesis as a check against any feature of the structure being overlooked. Small positive peaks were again observed on the atomic sites ranging in intensity from $3.5 \text{ eA}^{\circ-3}$ on the site of the bromine atom to about $0.5 \text{ eA}^{\circ-3}$ on the sites of the carbon atoms. These were the largest features and in only a few other regions did the background reach a height of $0.4 \text{ eA}^{\circ-3}$.

During the final cycles of refinement the structure factors were weighted by the same function that was used in the refinement of ethylzinc iodide. In the present case the following parameters were used:

$$P_1 = 15 \quad P_2 = 0.1667 \quad P_3 = 0.0037 \quad P_4 = 0$$

The final least squares totals together with an analysis of the effect of the weighting scheme are shown in Table 4c.

The observed and calculated structure factors are given in Table 4d. During the refinement unobserved planes were given zero weighting and when structure factors were calculated for 481 of these, only three had values of 1.7 times greater than the minimum observable value F_{Min} .

(Bu^tOMgBr.OEt₂)₂ TABLE 4aFinal values of Atomic Co-ordinates and their Standard Deviations

Atom	x/a	y/b	z/c	$\sigma(x/a)$	$\sigma(y/b)$	$\sigma(z/c)$
Br	0.24564	0.26974	0.05261	0.00031	0.00025	0.00022
Mg	0.01282	0.12794	0.00004	0.00083	0.00060	0.00058
O(1)	0.05611	0.00298	0.10192	0.00170	0.00113	0.00115
O(2)	-0.20346	0.22558	-0.05597	0.00167	0.00144	0.00124
C(1)	0.11801	0.00904	0.21775	0.00272	0.00185	0.00164
C(2)	0.31065	-0.03279	0.29753	0.00526	0.00410	0.00251
C(3)	0.10954	0.14373	0.23676	0.00761	0.00326	0.00397
C(4)	-0.01709	-0.05957	0.22177	0.00735	0.00581	0.00334
C(5)	-0.26127	0.39509	-0.17196	0.00472	0.00270	0.00342
C(6)	-0.21459	0.35612	-0.06147	0.00388	0.00237	0.00285
C(7)	-0.37194	0.16365	-0.10316	0.00370	0.00343	0.00311
C(8)	-0.42634	0.17292	-0.03146	0.00567	0.00546	0.00427

Final values of Anisotropic Temperature Parameters (\AA^2) and their Standard Deviations

Atom	U_{11}	U_{22}	U_{33}	$2U_{23}$	$2U_{31}$	$2U_{12}$
Br	0.0594(11)	0.0677(14)	0.0643(13)	-0.0098(36)	0.0585(21)	-0.0483(24)
Mg	0.0480(33)	0.0360(35)	0.0338(32)	-0.0167(73)	0.0478(57)	-0.0030(51)
O(1)	0.059(8)	0.029(7)	0.049(8)	-0.032(15)	0.073(14)	0.001(11)
O(2)	0.052(8)	0.054(8)	0.063(9)	-0.034(21)	0.060(15)	-0.014(12)
C(1)	0.067(13)	0.038(11)	0.034(10)	0.001(24)	0.070(21)	-0.019(18)
C(2)	0.126(25)	0.157(34)	0.053(17)	0.084(47)	0.064(35)	0.155(47)
C(3)	0.251(51)	0.093(27)	0.119(31)	-0.109(59)	0.241(71)	0.063(55)
C(4)	0.216(46)	0.200(50)	0.089(25)	-0.062(65)	0.223(61)	-0.203(83)
C(5)	0.136(26)	0.047(16)	0.128(27)	-0.013(42)	0.178(46)	0.034(29)
C(6)	0.100(21)	0.049(16)	0.087(22)	0.033(36)	0.079(35)	0.050(26)
C(7)	0.071(16)	0.127(25)	0.117(26)	0.075(51)	0.123(37)	0.068(34)
C(8)	0.130(31)	0.177(40)	0.155(38)	0.039(78)	0.194(62)	-0.025(58)

(Bu^tOMgBr.OEt₂)₂ TABLE 4c

LEAST-SQUARES TOTALS

Number of observed planes 672

$\Sigma \Delta $	2153.1	$\Sigma F_o $	21845.8	$\Sigma F_c $	21294.8	R	0.0986
$\Sigma w \Delta ^2$	784.8	$\Sigma w F_o ^2$	47566.0	$\Sigma w F_c ^2$	46722.2	R'	0.0165

WEIGHTING ANALYSIS

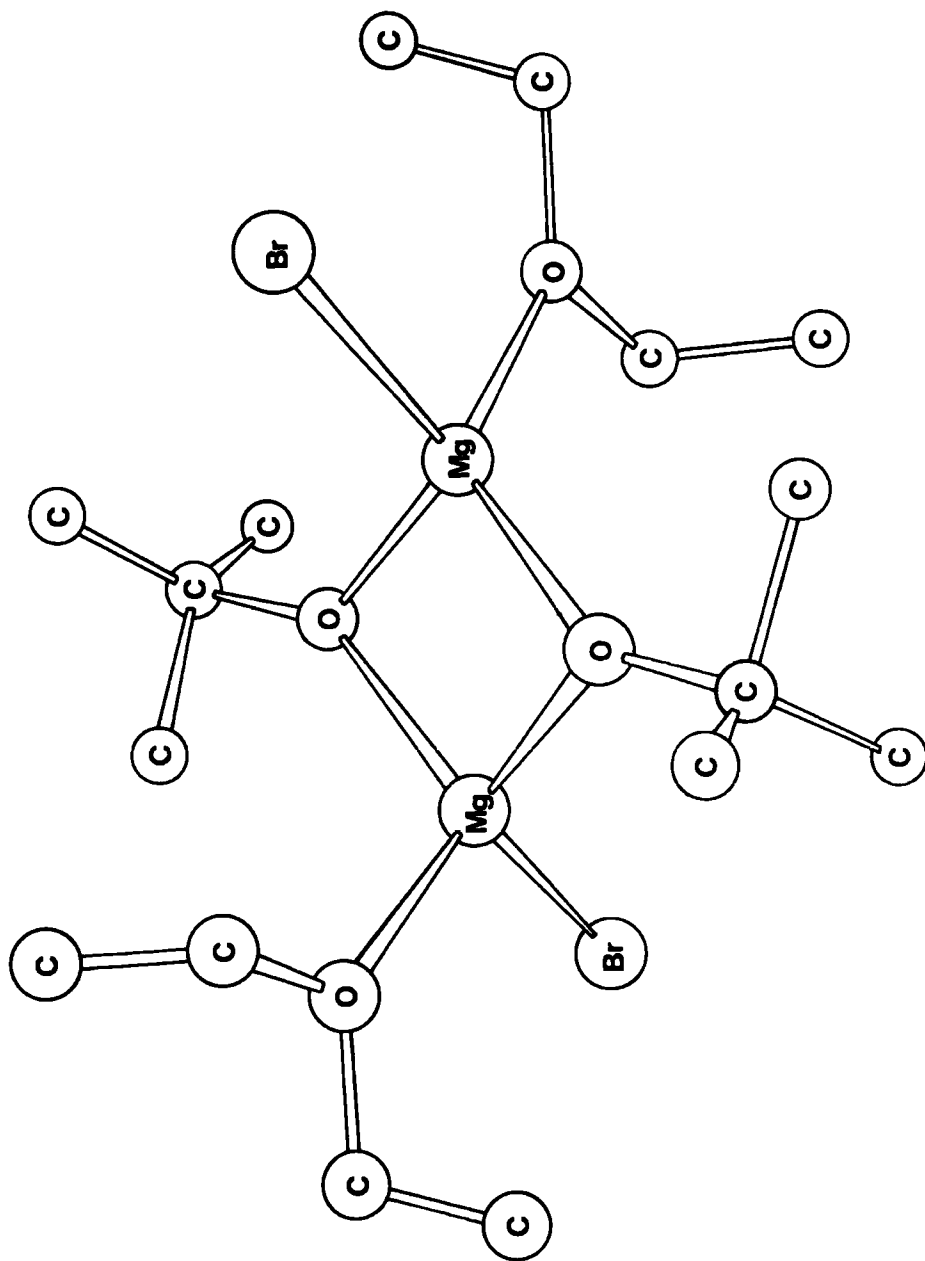
$w\Delta^2$ averaged in batches and the number of planes per batch

	sin θ/λ				
	0.0-0.2	0.2-0.4	0.4-0.6	0.6-0.8	TOTALS
$ F_o $					
0-7	0.00/0	0.00/0	0.00/0	0.00/0	0.00/0
7-14	0.47/3	1.40/38	2.26/26	0.00/0	1.69/67
14-28	1.31/9	0.80/117	1.19/199	1.25/1	1.06/326
28-55	0.96/16	1.07/143	1.10/42	0.00/0	1.07/201
55-111	0.95/22	1.64/48	0.00/0	0.00/0	1.42/70
111-UP	0.26/5	3.84/3	0.00/0	0.00/0	1.60/8
TOTALS	0.92/55	1.12/349	1.28/267	1.26/1	1.17/672

4.7 Description and Discussion of Structure

The molecular arrangement is shown in Figure 4.1. The compound is dimeric by virtue of a four-membered Mg-O ring which allows the magnesium atom to become four co-ordinate and the butoxy oxygen atom to become three co-ordinate.

Two features of the structure invite particular scrutiny. First, it is established that although three co-ordinate, all the oxygen atoms are coplanar with their three attached atoms within the limits of experimental error. The ring oxygen atoms, the magnesiums and the tertiary carbon atoms of the t-butyl groups all deviate by less than $0.01\overset{\circ}{\text{Å}}$ from their mean plane and the situation with respect to the oxygen and α -carbon atoms of the ether molecule and to the magnesium is scarcely less precise. Details of the mean planes are given in Table 4e. The second feature, which may be related to the first, is the presence of two different Mg-O distances. While the Mg-O length ($2.01\overset{\circ}{\text{Å}}$) involving the ether oxygens compares well with values found in crystalline $\text{PhMgBr}\cdot 2\text{Et}_2\text{O}$ (2.01 and $2.06\overset{\circ}{\text{Å}}$; - Rundle and Stucky, 1964) and in $\text{EtMgBr}\cdot 2\text{Et}_2\text{O}$ (2.03 and $2.06\overset{\circ}{\text{Å}}$; - Guggenberger and Rundle, 1964) the Mg-O distances (1.91 and $1.91\overset{\circ}{\text{Å}}$) in the ring are significantly shorter. These points and the general stereochemistry of the molecule are discussed further in section 4.8 but it may be mentioned here that although magnesium 3d orbitals are normally regarded as relatively diffuse and of high energy, some appreciable $d\pi$ - $p\pi$ interaction as suggested in



$(\text{Bu}^t\text{OMgBr}\cdot\text{OEt}_2)_2$

Figure 4.1

(Bu^tOMgBr.OEt₂)₂ TABLE 4eSummary of mean planes through the oxygen atoms and
the atoms bonded to oxygen

Atoms in Plane 1	Orthogonal Co-ordinates in Å			Distance of Atom from plane in Å
	x'	y	z'	
C(1)	0.8861	0.1003	2.5671	-0.0035
O(1)	0.4213	0.0331	1.1962	0.0074
Mg	0.0963	1.4201	-0.0777	0.0001

$$\text{Equation of Plane 1: } 0.9427 x' - 0.0816 y - 0.3236 z' = 0$$

Atoms in Plane 2	Orthogonal Co-ordinates in Å			Distance of Atom from plane in Å
	x'	y	z'	
C(7)	-2.7928	1.8165	0.7146	0.0082
O(2)	-1.5277	2.5039	0.3978	-0.0239
C(6)	-1.6113	3.9529	0.3828	0.0089
Mg	0.0963	1.4201	-0.0777	0.0067

$$\text{Equation of Plane 2: } -0.2653 x' - 0.0027 y - 0.9642 z' = 0.0389$$

$$\text{Dihedral angle between plane 1 and plane 2} = 86.4^\circ$$

connection with the $(\text{Bu}^n\text{MgOPr}^i)_3$ trimer (Bryce-Smith and Graham, 1966), would be facilitated by the presence of electronegative atoms bonded to magnesium and may possibly contribute to the bond shortening in the Mg_2O_2 ring.

The final values for bond lengths and bond angles together with their standard deviations are given in Tables 4f and 4g. Some bond lengths are also shown on Figure 4.2.

The Br-Mg bond length ($2.44\overset{\circ}{\text{A}}$) is seen to be in good agreement with the value ($2.44\overset{\circ}{\text{A}}$) found in $\text{PhMgBr}\cdot 2\text{Et}_2\text{O}$. The bond angles at magnesium however are considerably removed from the normal tetrahedral value and probably at least three factors make contributions affecting this situation. Participation in the four-membered ring of course requires that the angle in the ring (83.3°) be much less than the others. Also, the discrepancy in size between the atoms bonded to the metal is probably responsible for the remaining two O-Mg-O angles ($\text{O}(1)\text{-Mg-O}(2) = 112^\circ$, $\text{O}(1')\text{-Mg-O}(2) = 109^\circ$) being less than the mean value of the O-Mg-Br angles (117°). Of the three O-Mg-Br angles, that involving O(2) (107°) is by far the smallest, due, at least in part, to the fact that the Mg-O(2) bond is 5% longer than the other two Mg-O bond lengths.

In the Mg_2O_2 ring the angle at oxygen (96.7°) is larger than that at Magnesium, the shape of the ring being consistent with both the state of hybridisation of the constituent atoms and with their relative sizes.

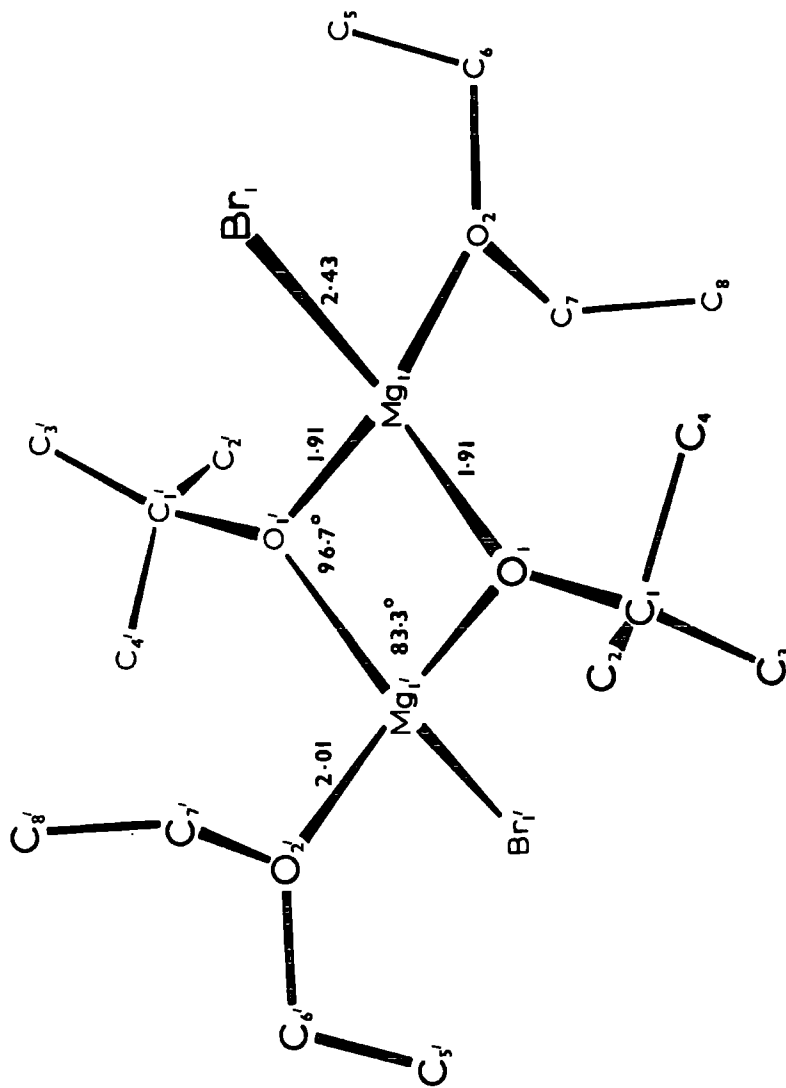
(Bu^tOMgBr.OEt₂)₂ TABLE 4f

Bond lengths (Å) and their Standard Deviations (Å x 10³)

Br - Mg	2.435 (7)
Mg - O(1)	1.911(15)
Mg - O(1')	1.905(15)
Mg - O(2)	2.010(15)
O(1) - C(1)	1.449(25)
O(2) - C(6)	1.452(31)
O(2) - C(7)	1.474(34)
C(1) - C(2)	1.519(45)
C(1) - C(3)	1.534(42)
C(1) - C(4)	1.547(56)
C(5) - C(6)	1.491(56)
C(7) - C(8)	1.476(63)

(Bu^tOMgBr.OEt₂)₂ TABLE 4gBond Angles with their Standard Deviations

	Angle	e.s.d.
O(1) - Mg - O(2)	111.8 ^o	0.7 ^o
O(1) - Mg - Br	121.3	0.5
O(2) - Mg - Br	107.0	0.5
O(1') - Mg - Br	122.5	0.5
O(1') - Mg - O(2)	109.3	0.7
O(1') - Mg - O(1)	83.3	0.7
Mg - O(1) - Mg'	96.7	0.6
Mg - O(1) - C(1)	130.7	1.2
Mg' - O(1) - C(1)	132.7	1.2
Mg - O(2) - C(6)	125.6	1.5
Mg - O(2) - C(7)	119.5	1.7
C(6) - O(2) - C(7)	114.7	2.0
O(1) - C(1) - C(2)	108.0	2.0
O(1) - C(1) - C(3)	103.9	2.3
O(1) - C(1) - C(4)	108.0	2.1
C(2) - C(1) - C(3)	109.5	3.0
C(2) - C(1) - C(4)	117.6	3.0
C(3) - C(1) - C(4)	109.0	3.2
O(2) - C(6) - C(5)	108.2	2.6
O(2) - C(7) - C(8)	114.3	3.1



$(\text{Bu}^t\text{OMgBr}\cdot\text{OEt}_2)_2$

Some Bond Lengths and Angles

Figure 4.2

The C-O bond lengths do not differ significantly from one another and their mean ($1.46\overset{\circ}{\text{Å}}$) is not significantly longer than the value ($1.43 \pm 0.03\overset{\circ}{\text{Å}}$) found in dimethyl ether (Kimura and Kubo, 1959). The mean C-C bond length of the t-butyl group is $1.53\overset{\circ}{\text{Å}}$ and that of the ether molecule is $1.48\overset{\circ}{\text{Å}}$. Their difference is not significant and none of the C-C bonds differ significantly from the bond length found in diamond ($1.54\overset{\circ}{\text{Å}}$).

Three of the bond angles at carbon atoms are considerably removed from the tetrahedral value. The large value for C(2)-C(1)-C(4) (118°) and the small value for O(1)-C(1)-C(3) (104°) represent a distortion of the tertiary butyl group away from the ether molecule on the other half of the dimer. It would seem most likely that these irregularities originate in intramolecular steric interference, particularly in view of the fact that the shortest non-bonding carbon-carbon contact between peripheral groups ($3.64\overset{\circ}{\text{Å}}$) involves C(2) and C(7') where C(7') is the atom related to C(7) by the centre of symmetry. Further evidence in accord with this theory is the slight enlargement of the angle O(2)-C(7)-C(8) (114°) which also represents a movement to relieve the short contact between C(2) and C(7').

Table 4h shows the non-bonding intramolecular contacts of less than $4\overset{\circ}{\text{Å}}$. Aside from the short contacts between pairs of atoms belonging to the same ether molecule or t-butyl group there are eleven contacts between peripheral non-bonding atoms of from 3.5 to $4.0\overset{\circ}{\text{Å}}$. These contacts

(Bu^tOMgBr.OEt₂)₂ TABLE 4h

Intramolecular non-bonding contacts less than 4^oÅ

Equivalent Position 1 x, y, z;
 Equivalent Position 2 -x, -y, -z;

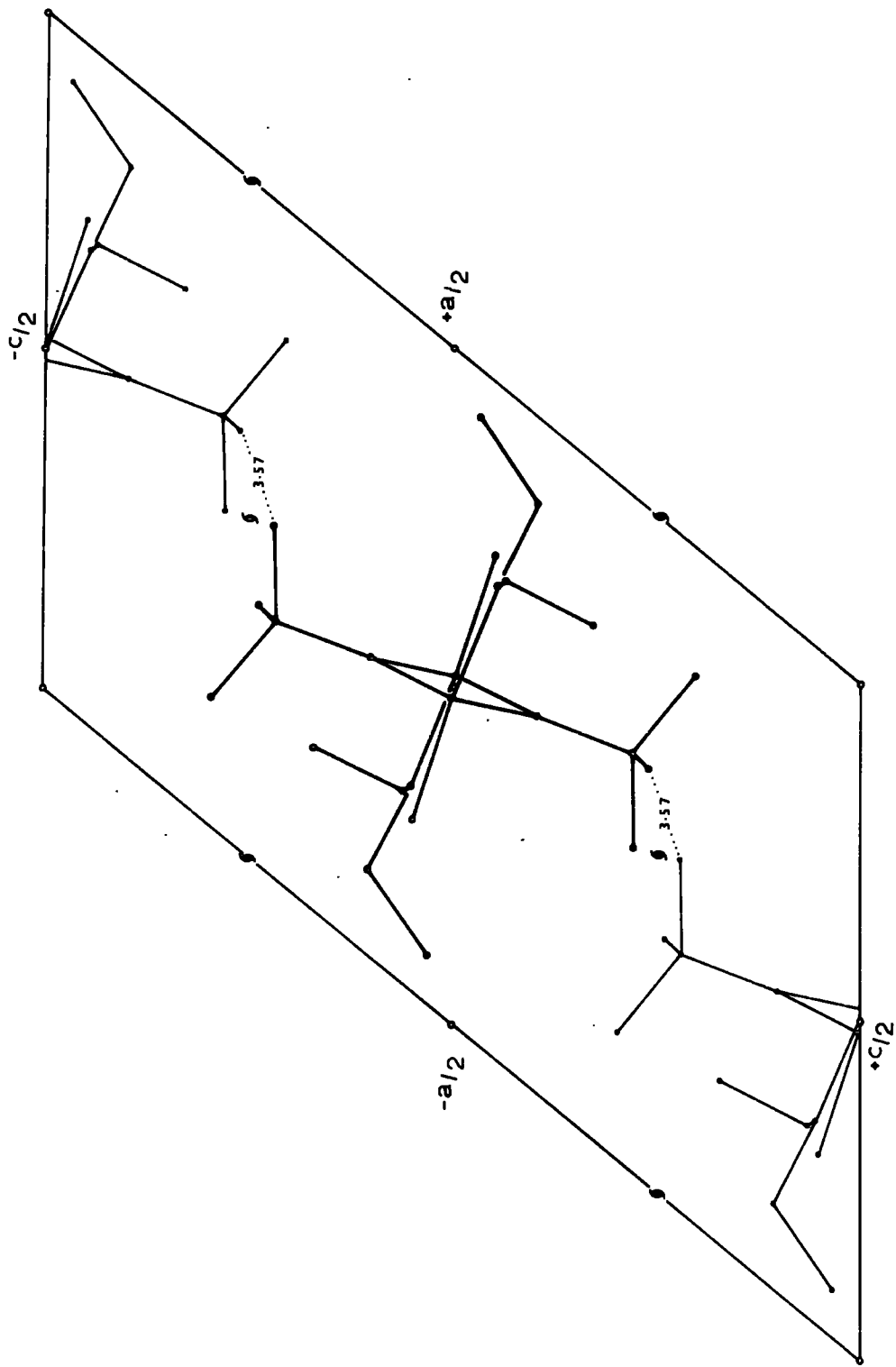
Atom B	Atom B	Equivalent Position	A-B Angstroms
Br	O(2)	1	3.582
Br	C(6)	1	3.748
Br	O(1)	1	3.796
Br	O(1)	2	3.813
Br	C(4)	2	3.992
Mg	Mg	2	2.851
O(1)	C(7)	2	3.563
O(1)	C(7)	1	3.707
O(2)	C(3)	1	3.555
O(2)	C(2)	2	3.766
O(2)	C(1)	2	3.998
C(2)	C(7)	2	3.643
C(5)	C(7)	1	3.199
C(6)	C(8)	1	3.117
O(1)	O(1)	2	2.537

occur all round the dimeric unit and the general impression which they afford is of a molecule whose constituent groups pack well together. The magnesium-magnesium contact across the Mg_2O_2 ring (2.85\AA) is only slightly greater than the sum (2.80\AA) of the tetrahedral covalent radii for two magnesium atoms (Pauling, 1960).

Figure 4.3 shows the packing of the dimeric units together in the unit cell in the projection along \underline{b} .

The only non-bonding intermolecular contact less than 4\AA is between C(3) at x, y, z and C(4) at $-x, \frac{1}{2} + y, \frac{1}{2} - z$ in the same unit cell. These atoms are 3.57\AA apart, and although this contact is not considered to be unduly short, it will be recognised that C(4) is also one of the atoms involved in the most distorted angle found in the *t*-butyl group. Further, a movement of C(4) to reduce the intermolecular contact to C(3) would be such as to increase the distortion of angle C(2)-C(1)-C(4) and is thus discouraged.

The mean values of B for the various atom types are Br 5, Mg 3, O 4 and C 9\AA^2 . As would be expected the more tightly bound magnesium and oxygen atoms are vibrating less than the atoms situated further from the molecular centre.



(Bu^tOMgBr.OEt₂)₂ projection on the (010) plane

Figure 4.3

4.8 Stereochemistry of Compounds $(\text{Bu}^t\text{OMBr.OEt}_2)_2$ (where M is Mg or Be)

Although the X-ray investigation of the crystal structure of the diethyl ether complex of t-butoxymagnesium bromide was initially undertaken to provide information about the reaction of Grignard reagents with ketones, the emergence of the previously unpredicted structural features mentioned earlier provokes further interest in the stereochemistry of the molecule. The preference for trigonal geometry at the oxygen atoms over a pyramidal alternative which would provide one direction in space free to accommodate a lone pair of electrons not used in bonding appears to contrast with the general predictions (Gillespie and Nyholm, 1957) that have been made about atoms in this sort of environment. The crystal structures of Grignard reagents provide examples of both trigonally $(\text{EtMgBr}(\text{OEt}_2)_2$; Guggenberger and Rundle, 1964) and tetrahedrally co-ordinated $(\text{PhMgBr}(\text{OEt}_2)_2$; Rundle and Stucky, 1964) ether oxygen atoms, and Rundle points out that the trigonal configuration is more characteristic of expectations for ionic than for covalent bonding. However, in the case of the ring oxygens in $(\text{Bu}^t\text{OMgBr.OEt}_2)_2$ the very short Mg-O bond lengths (in crystalline magnesium oxide $\text{Mg}-\overset{\text{O}}{\text{O}} = 2.1\text{\AA}$; Brock, 1927) are consistent with a bond order of greater than one and a synergic bonding system as mentioned earlier could be envisaged which would also require trigonal oxygen atoms.

The situation may be more complicated than this however as appears from preliminary molecular orbital calculations on the four ring atoms

(Clark, 1968). An initial interaction matrix suggests that there is an interaction between the 3 dxy and 3 dxz orbitals of the magnesium atoms across the ring which is energetically more important than any involving the $2p_z$ orbitals of the oxygen. According to Pauling's proposed equation dealing with fractional bonds (1947) the Mg-Mg separation corresponds to a bond order of 0.83.

The physical meaning of these calculations is not easy to envisage. More tangible is the possibility that steric interference between peripheral groups might also contribute to the preference for the structure actually adopted. The molecule certainly appears to pack well together with trigonal oxygens and an alternative configuration could well be less favourable in terms of non-bonding contacts.

The distortion of bond angles mentioned previously and the lack of disordering of the co-ordinatively bound ether molecules (cf. $Mg_4Br_6O(OEt_2)_4$; Rundle and Stucky, 1964a and $Na_2Be_2Et_4H_2(OEt_2)_2$; Adamson and Shearer, 1965) lend weight to the theory that considerations of steric interference do play a part in dictating the shape of the $(Bu^tOMgBr.OEt_2)_2$ dimer.

Features of the proton magnetic resonance spectrum have prompted the suggestion (Coates et al., 1968) that a geometrical isomer of $(Bu^tOMgBr.OEt_2)_2$ is available in solution, but it is expected that this would involve a cis arrangement of the bromine atoms rather than pyramidal ring oxygens.

In view of the possibility that a combination of factors affect the

conformation adopted by $(\text{Bu}^t\text{OMgBr.OEt}_2)_2$ an X-ray structure study has been made of the beryllium analogue $(\text{Bu}^t\text{OBeBr.OEt}_2)_2$ (Shearer and Twiss, 1968) which is also dimeric in the solid phase. Here it is expected that any possibility of metal-oxygen, $d\pi-p\pi$ interaction would be precluded and indeed it has been established that the Be-O bonds in the ring are not shorter than the beryllium bonds to the ether oxygens. Other features of the structure of $(\text{Bu}^t\text{OBeBr.OEt}_2)_2$ parallel those found in the magnesium compound and the coplanarity of the three-coordinate oxygen atoms is true to the same degree.

Thus it appears that the steric effects alone are important enough to impose an unusual electronic situation on the oxygen atoms and although it must be realised that these effects will be more pronounced in the case of the molecule based on the smaller central ring, it is quite possible that the molecular shape of both compounds arises from such considerations and that any extra bonding in the magnesium compounds occurs as a secondary consequence of the relevant atoms finding themselves with a suitable geometry.

(Bu^tOMgBr.OEt₂)₂ TABLE 4d

Final Values of Observed and Calculated Structure Factors

Chapter Five

The Crystal Structure of Dimeric 2-dimethylamino-
ethylmethylaminozinc Hydride

5.1 Introduction

When zinc hydride is stirred with NNN' trimethylethylenediamine (TriMED) in toluene at 60°C, for 12 hours, one mole of hydrogen is evolved and a solution is obtained which, on standing, yields colourless crystals. Analyses of the crystals for hydrolysable H and for Zn are in accord with the empirical formula $ZnN_2C_5H_{14}$ and cryoscopic molecular weight measurements indicate that the molecule is dimeric in benzene solution (Bell and Coates, 1968).

The preparation of RMTriMED has been reported for M = Be, Mg or Zn and where R is any one of a variety of alkyl groups (Coates and Heslop, 1968; Coates and Roberts, 1968). Such compounds are frequently dimeric and structures have been suggested for them, but up to the time when the present work began no crystal structure data were available concerning either these compounds or the related species HMTriMED, where M = Be, Zn. Furthermore no crystalline compound containing a zinc-hydrogen bond had previously been available for examination by diffraction techniques.

Crystals for X-ray examination were sealed in pyrex capillaries under the dry, oxygen-free, atmosphere of a glove box.

5.2 Crystal Data

Zero level precession photographs, with Mo K_{α} radiation, showed the following unit cell dimensions:

Monoclinic: broad needles elongated along a.

$$a = 6.372, \quad b = 11.316, \quad c = 11.977 \text{ \AA};$$

$$\beta = 111^\circ 45'$$

$$U = 802.1 \text{ \AA}^3; \quad Z = 2 \text{ units of } \left(\text{HZnN}(\text{Me})\text{C}_2\text{H}_4\text{NMe}_2 \right)_2;$$

$$D_{\text{calc.}} = 1.386 \text{ gm.cm}^{-3}; \quad \text{M.W. of } (\text{ZnN}_2\text{C}_5\text{H}_{14})_2 = 335.1;$$

Absorption coefficient for Cu K_α radiation $\mu = 36.7 \text{ cm}^{-1}$.

The density of the crystals was measured by flotation using mixtures of perfluorobutylamine ($\rho = 1.86 \text{ gm.cm}^{-3}$) and benzotrifluoride ($\rho = 1.17 \text{ gm.cm}^{-3}$). The observed value was $1.39\text{--}1.41 \text{ gm.cm}^{-3}$.

As with $(\text{Bu}^t\text{OMgBr.OEt}_2)_2$ the space group was unambiguously determined from the conditions limiting the observed reflections

$$0k0: \quad k = 2n,$$

$$h0l: \quad l = 2n$$

as Number 14, $P2_1/c$, (C_{2h}^5) .

The statistical standard deviations on the unit cell dimensions are 0.003 \AA on a, 0.005 \AA on b and c, and $5'$ on β , but when systematic errors are taken into consideration the overall uncertainties are probably of the order of 0.2% .

5.3 Data Collection and Correction

Three dimensional intensity data were recorded by the equi-inclination Weissenberg technique using nickel-filtered copper radiation for nkl type



nets $n = 0-4$, and were found to persist well out to high values of θ . The intensities were estimated visually by comparison with a calibrated scale and film to film ratios were employed which increased with inclination angle (Rossmann, 1956).

In the case of high order reflections which were split owing to the resolution of the $K\alpha_1$, $K\alpha_2$ doublet, the intensity of the reflection due to the $K\alpha_1$ component alone was estimated and was multiplied by an empirical correcting factor of 1.32.

Corrections were made for Lorentz and polarisation factors, and for spot length effects in the case of the upper levels. Initially no correction was made for absorption as the requisite computer programme was incomplete. The investigation was continued without this correction however in the anticipation that it would be applied later.

The intensity data were correlated onto a common scale by exposing several nets on to different sections of the same piece of film for an equal period of time. As a precaution against the inadequacies of this method however an individual scale factor was used for each net during the later stages of the refinement.

The dimensions of the crystal used for data collection were 0.24 by 0.52 mm (cross-section) by 1.5 mm (length). The needle axis corresponded to a but, curiously, the developed planes of the cross-section appeared to be of fairly high order.

5.4 Patterson Function

The observed structure factors were multiplied by the weighting function w where $w = \exp. \left(4 \sin^2 \theta / \lambda^2 \right)$.

The weighting function was not allowed to exceed a value of 2.718 so that reflections with $\sin \theta / \lambda \geq 0.5$ were given a constant weight. The Patterson function was then calculated using the squares of the weighted structure factors as fourier coefficients:

$$P(u,v,w) = \frac{4}{V} \sum_0^h \sum_0^k \sum_{-1}^l \left(w(hkl) |F(hkl)| \right)^2 \cos 2\pi kv$$

$$(\cos 2\pi hu \cos 2\pi lw - \sin 2\pi hu \sin 2\pi lw)$$

Since the symmetry of the vector set is P2/m the Patterson function was calculated over one quarter of the unit cell, 'u' at intervals of $0.319 \overset{\circ}{\text{Å}}$ to $\frac{a}{2}$, 'v' at intervals of $0.283 \overset{\circ}{\text{Å}}$ to $\frac{b}{2}$ and 'w' at intervals of $0.299 \overset{\circ}{\text{Å}}$ to $\frac{c}{2}$.

The Patterson function, as described for $(\text{Bu}^{\text{t}}\text{OMgBr.OEt}_2)_2$, includes a Harker section at $(u, \frac{1}{2}, w)$ and a Harker line at $(0, v, \frac{1}{2})$ in the quadrant computed. Accordingly one peak large enough to correspond to a double weight zinc-zinc vector was detected as the largest feature on both the line $P(0, v, \frac{1}{2})$ and also on the section $P(u, \frac{1}{2}, w)$. The zinc position was deduced from these and confirmed by the location of a single weight peak at $2x, 2y, 2z$.

The co-ordinates of the zinc position were obtained as

x/a	y/b	z/c
0.0900	0.0990	-0.0334

The positions of this zinc atom and the one related to it by the centre of symmetry at the origin were seen to be close enough to be part of the same four-membered ring.

No attempt was made to locate any of the lighter atoms from the Patterson function.

5.5 Light Atom Positions

Structure factors were calculated phased on the zinc atom ($R = 0.366$) and were used to compute an F_o synthesis. The function was evaluated for x at intervals of $0.319\overset{\circ}{\text{A}}$ to \underline{a} , y at intervals of $0.283\overset{\circ}{\text{A}}$ to $\frac{b}{2}$ and z at intervals of $0.299\overset{\circ}{\text{A}}$ to $\frac{c}{2}$.

The positions of the nitrogen and carbon atoms were revealed by the seven peaks on the electron density map which were next in order of magnitude after the peak corresponding to the zinc atom. It was possible to decide the identity of each atom individually by inspection of its stereochemistry. The electron density at the site of the zinc atom reached a peak height of $40 \text{ e}\overset{\circ}{\text{A}}^{-3}$ and the mean peak heights for the nitrogen and carbon atoms were 4.2 and $3.4 \text{ e}\overset{\circ}{\text{A}}^{-3}$ respectively.

5.6 Refinement

The structure was refined by the method of least squares using the full matrix of the normal equations. For the first three cycles all the atoms were refined with isotropic temperature parameters and an elementary weighting scheme was used which was designed to give a constant

weight to the small planes. The R factor stood at 0.169 at this stage and structure factors were prepared and used to compute an $F_o - F_c$ synthesis. The difference map showed no peaks greater than $1.1 \text{ e}\overset{\circ}{\text{A}}^{-3}$ other than at the sites of detected atoms, but a peak of $0.6 \text{ e}\overset{\circ}{\text{A}}^{-3}$ at a distance of $1.7\overset{\circ}{\text{A}}$ from the zinc atom was in a suitable position to represent a hydrogen atom.

The refinement was continued for three cycles, without inclusion of the hydrogen atom, but with the eight atoms given anisotropic temperature parameters. The reliability index R improved to 0.120 and at this stage a second difference map was computed. The greatest peak height away from atomic sites had fallen to $0.52 \text{ e}\overset{\circ}{\text{A}}^{-3}$ but the hydrogen atom peak near zinc persisted at $0.5 \text{ e}\overset{\circ}{\text{A}}^{-3}$ albeit shifted $0.2\overset{\circ}{\text{A}}$ from its previous position to give a Zn-H distance of $\sim 1.8\overset{\circ}{\text{A}}$.

Convergence of the structure refinement was achieved after four further cycles, refining an individual scale factor for each net. The weighting scheme used in the closing stages employed the same function as was used in the refinement of ethylzinc iodide but with the following parameters:

$$P_1 = 15 \qquad P_2 = 0.417 \qquad P_3 = 0.0083 \qquad P_4 = 0$$

The parameter shifts in the final cycle were all less than 1/8 of the corresponding estimated standard deviation (e.s.d.). The final values of the positional and thermal parameters together with their e.s.d.'s are given in Tables 5a and 5b.

(HZnN(Me)C₂H₄NMe₂)₂ TABLE 5aFinal values of Atomic Co-ordinates and their Standard Deviations

Atom	x/a	y/b	z/c	$\sigma(x/a)$	$\sigma(y/b)$	$\sigma(z/c)$
Zn	0.09568	0.10123	-0.03511	0.00030	0.00013	0.00012
N(1)	0.14524	0.02152	0.12736	0.00191	0.00083	0.00075
N(2)	-0.05557	0.24281	0.03419	0.00214	0.00094	0.00089
C(1)	0.06019	0.09895	0.20083	0.00298	0.00111	0.00094
C(2)	-0.12688	0.17916	0.12294	0.00330	0.00121	0.00126
C(3)	-0.25275	0.31157	-0.05085	0.00335	0.00138	0.00148
C(4)	0.13915	0.32331	0.09249	0.00306	0.00145	0.00169
C(5)	0.36867	-0.02308	0.19953	0.00295	0.00141	0.00131
H(a)	0.24750	0.17600	-0.10750			
H(b)	0.28000	0.18000	-0.09500			

H(a) and H(b) represent the peaks on the first and second difference maps which might be assigned to the hydrogen atom attached to zinc.

Final values of Anisotropic Temperature Parameters (\AA^2) and their Standard Deviations

($\text{\AA}^2 \times 10^4$ for Zn, $\text{\AA}^2 \times 10^3$ for N and C)

Atom	U_{11}	U_{22}	U_{33}	$2U_{23}$	$2U_{31}$	$2U_{12}$
Zn	0.0722(16)	0.0566(8)	0.0353(7)	0.0002(12)	0.0355(15)	-0.0087(14)
N(1)	0.0760(8)	0.0550(5)	0.0268(4)	-0.0101(7)	0.0155(8)	0.0034(9)
N(2)	0.0837(9)	0.0546(5)	0.0449(5)	-0.0018(8)	0.0366(10)	0.0064(10)
C(1)	0.1054(13)	0.0662(7)	0.0235(5)	-0.0041(8)	0.0460(11)	0.0191(13)
C(2)	0.1225(14)	0.0596(7)	0.0529(7)	0.0184(11)	0.0885(16)	0.0254(15)
C(3)	0.1120(14)	0.0671(8)	0.0687(9)	0.0241(13)	0.0426(18)	0.0414(16)
C(4)	0.0733(12)	0.0827(10)	0.0926(11)	-0.0382(16)	0.0744(18)	-0.0339(16)
C(5)	0.0829(12)	0.0782(9)	0.0525(8)	0.0032(12)	-0.0048(14)	-0.0016(15)

The final least squares totals together with an analysis of the effect of the weighting scheme are shown in Table 5c and the observed and calculated structure factors are given in Table 5d.

Unobserved planes were given zero weight during the refinement and when structure factors were calculated for 198 of these, only one had a value greater than twice the minimum observable value F_{Min} .

5.7 Absorption Correction

An absorption correction programme based on Busing and Levy's method (1957) became available after the above refinement was complete and an attempt was made to obtain some improvement in the results by correcting the observed structure factors.

The direction parallel to the rotation axis was divided into eight intervals and the directions contained in the cross-section were divided into four and two intervals respectively.

The corrected structure factors were used to repeat the final stages of the refinement described in § 5.6. The only modification made was to the parameters used in the weighting scheme. The new values were;

$$P_1 = 5, \quad P_2 = 0.216, \quad P_3 = 0.0024, \quad P_4 = 0.$$

The block diagonal approximation was employed for one cycle of refinement while the scale factors shifted appreciably. Thereafter the full matrix was used for four further cycles until the parameters shifts were all less than one tenth of their corresponding e.s.d.'s.

(HZnN(Me)C₂H₄NMe₂)₂ TABLE 5c

LEAST-SQUARES TOTALS

Number of observed planes 1000

$\Sigma \Delta $	1805.87	$\Sigma F_o $	16534.37	$\Sigma F_c $	16190.97	R	0.1092
$\Sigma w \Delta ^2$	437.60	$\Sigma w F_o ^2$	22356.42	$\Sigma w F_c ^2$	21910.83	R'	0.0196

WEIGHTING ANALYSIS

$w\Delta^2$ averaged in batches and the number of planes per batch

$\sin\theta/\lambda$

	0.0-0.2	0.2-0.4	0.4-0.6	0.6-0.8	TOTALS
$ F_o $					
0-5	1.24/3	0.46/31	0.22/103	0.37/44	0.32/181
5-9	0.62/6	0.64/62	0.18/196	0.55/34	0.33/298
9-18	0.76/7	0.61/85	0.31/174	0.86/5	0.43/271
18-36	0.77/16	0.76/124	0.40/46	0.00/0	0.67/186
36-72	0.41/13	0.82/44	0.00/0	0.00/0	0.73/57
72-UP	0.10/6	0.10/1	0.00/0	0.00/0	0.10/7
TOTALS	0.61/51	0.68/347	0.25/519	0.47/83	0.44/1000

The new positional parameters and e.s.d.'s together with the discrepancies between these and the values obtained using the uncorrected data are listed in Table 5a*. The maximum discrepancy in any co-ordinate is $0.01\overset{\circ}{\text{Å}}$ which is less than half of the corresponding e.s.d., although most were much less than this. The mean discrepancies in atomic co-ordinates are $0.0002\overset{\circ}{\text{Å}}$ for zinc, $0.002\overset{\circ}{\text{Å}}$ for nitrogen and $0.005\overset{\circ}{\text{Å}}$ for carbon.

The thermal parameters show a greater disparity, as might be expected and these are shown in Table 5b*. Six of the individual discrepancies (Δ) are greater than the corresponding e.s.d.'s. Only in the case of the zinc atom however is the mean discrepancy ($0.0026\overset{\circ}{\text{Å}}^2$) greater than the mean value ($0.0016\overset{\circ}{\text{Å}}^2$) of the e.s.d.'s. For the nitrogens the mean discrepancy is $0.0032\overset{\circ}{\text{Å}}^2$ and the mean e.s.d. is $0.009\overset{\circ}{\text{Å}}^2$ while for the carbons the mean discrepancy is $0.004\overset{\circ}{\text{Å}}^2$ and the mean e.s.d. is $0.015\overset{\circ}{\text{Å}}^2$.

The reliability index, R, has converged at a slightly higher value (0.119) and all of the e.s.d.'s for the positional and the thermal parameters are larger than those given by the uncorrected data.

The two sets of positional parameters are the same within the limits of experimental error and the following discussion and the tables of bond lengths and angles refer to the results obtained from the uncorrected data.

(HZnN(Me)C₂H₄NMe₂)₂ TABLE 5a*Atomic Co-ordinates and their Standard Deviations derived from data
corrected for absorption

Δ represents the difference in individual parameters
and e.s.d.'s from the uncorrected results in Table 5

Atom	x/a	y/b	z/c	σ(x/a)	σ(y/b)	σ(z/c)
Zn	0.09564	0.10123	-0.03513	0.00039	0.00016	0.00016
Δ	-0.00004	0.00000	-0.00002	+0.00009	+0.00003	+0.00004
N(1)	0.14526	0.02134	0.12723	0.00254	0.00101	0.00092
Δ	+0.00002	-0.00018	-0.00013	+0.00063	+0.00018	+0.00017
N(2)	-0.05662	0.24315	0.03423	0.00276	0.00111	0.00113
Δ	-0.00105	+0.00034	+0.00004	+0.00062	+0.00017	+0.00024
C(1)	0.06105	0.09845	0.20086	0.00384	0.00141	0.00113
Δ	+0.00086	-0.00050	+0.00003	+0.00086	+0.00030	+0.00019
C(2)	-0.12815	0.17914	0.12247	0.00439	0.00153	0.00157
Δ	-0.00127	-0.00002	-0.00047	+0.00109	+0.00032	+0.00031
C(3)	-0.25220	0.31203	-0.05016	0.00435	0.00172	0.00188
Δ	+0.00055	+0.00046	+0.00069	+0.00100	+0.00034	+0.00040
C(4)	0.13716	0.32329	0.09170	0.00399	0.00182	0.00218
Δ	-0.00199	-0.00002	-0.00079	+0.00093	+0.00037	+0.00049
C(5)	0.36715	-0.02323	0.19875	0.00383	0.00168	0.00167
Δ	-0.00152	-0.00015	-0.00078	+0.00088	+0.00027	+0.00036

Anisotropic Temperature Parameters (\AA^2) and their Standard Deviations ($\text{\AA}^2 \times 10^4$ for Zn, $\text{\AA}^2 \times 10^3$ for N and C) derived from data corrected for absorption

Δ represents the difference in individual parameters
and e.s.d.'s from the uncorrected results in Table 5b.

Atom	U ₁₁	U ₂₂	U ₃₃	2U ₁₂	2U ₁₃	2U ₂₃
Zn	0.0725(21)	0.0490(11)	0.0385(11)	-0.0002(15)	0.0318(19)	-0.0091(17)
Δ	+0.0003(5)	-0.0076(3)	+0.0032(4)	-0.0004(3)	-0.0037(4)	-0.0004(3)
N(1)	0.0819(11)	0.0477(6)	0.0267(5)	-0.0136(8)	0.0097(10)	0.0030(11)
Δ	+0.0059(3)	-0.0073(1)	-0.0001(1)	-0.0035(1)	-0.0058(2)	-0.0004(2)
N(2)	0.0822(11)	0.0478(6)	0.0488(6)	0.0004(10)	0.0368(12)	0.0058(12)
Δ	-0.0015(2)	-0.0068(1)	+0.0039(1)	+0.0022(2)	+0.0002(2)	-0.0006(2)
C(1)	0.1146(17)	0.0591(8)	0.0253(6)	-0.0042(10)	0.0427(14)	0.0167(17)
Δ	+0.0092(4)	-0.0071(1)	+0.0018(1)	-0.0001(2)	-0.0033(3)	-0.0024(4)
C(2)	0.1243(19)	0.0567(9)	0.0542(8)	0.0181(13)	0.0848(20)	0.0316(19)
Δ	+0.0018(5)	-0.0029(2)	+0.0013(1)	-0.0003(2)	-0.0037(4)	+0.0062(14)
C(3)	0.1054(18)	0.0600(10)	0.0742(11)	0.0246(16)	0.0413(22)	0.0387(20)
Δ	-0.0066(4)	-0.0071(2)	+0.0055(2)	+0.0005(3)	-0.0013(4)	-0.0027(4)
C(4)	0.0724(16)	0.0723(11)	0.0977(14)	-0.0438(20)	0.0670(23)	-0.0316(19)
Δ	-0.0009(4)	-0.0104(1)	+0.0051(3)	-0.0056(4)	-0.0074(5)	+0.0023(3)
C(5)	0.0840(15)	0.0654(10)	0.0582(10)	0.0027(14)	-0.0083(18)	-0.0022(18)
Δ	+0.0011(3)	-0.0128(1)	+0.0057(2)	-0.0005(2)	-0.0035(4)	-0.0006(3)

5.8 Description and Discussion of Structure

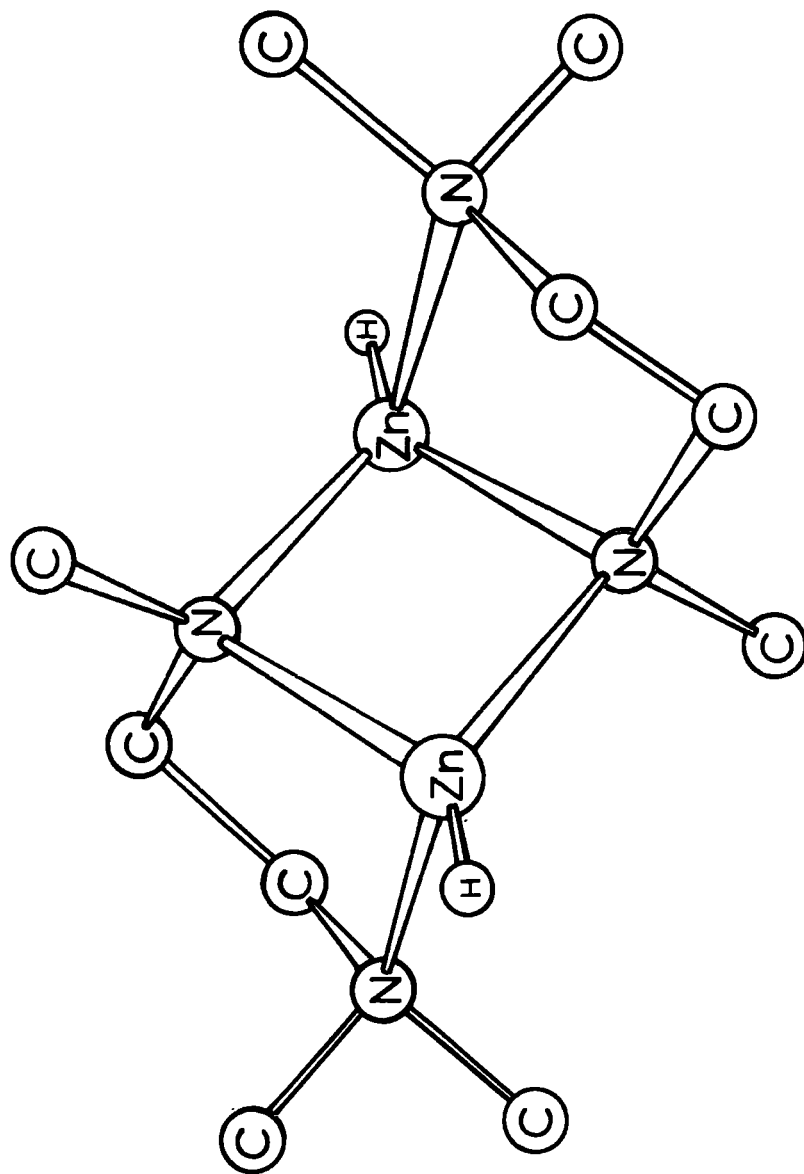
The molecular arrangement of the $(\text{HZnN}(\text{Me})\text{C}_2\text{H}_4\text{NMe}_2)_2$ dimer is shown in figure 5.1. The zinc atoms achieve four-co-ordinate status by participating in two co-ordinate bonds each with nitrogen, the one involving N(1) resulting in a four-membered ring about the centre of symmetry and the other involving N(2) giving rise to two five-membered rings.

The atoms N(1), C(1) and C(5) all lie within $0.01\overset{\circ}{\text{A}}$ of a plane through the origin which is almost at right angles to the plane of the Zn_2N_2 ring. The details of these planes are given in Table 5e.

The final values of the bond lengths and bond angles together with their standard deviations are given in Table 5f and Table 5g. Some bond lengths are also shown on Figure 5.2.

The zinc-nitrogen bond lengths in the four-membered ring (2.06 and $2.06\overset{\circ}{\text{A}}$) are not significantly different from the bond lengths (mean $2.07\overset{\circ}{\text{A}}$) found in the Zn_2N_2 ring in $(\text{MeZnNPh}_2)_2$ (Shearer and Spencer, 1967) but are shorter than the zinc-nitrogen bond length in the five-membered ring ($2.19\overset{\circ}{\text{A}}$). It is interesting to compare this situation with the structures of compounds $(\text{Bu}^t\text{OMBr.OEt}_2)_2$ where the M-O ring bonds are shorter than the M-O bond not involved in the ring when $\text{M} = \text{Mg}$, but not when $\text{M} = \text{Be}$.

Apparently the bond involving N(2) is the least strong. The possibility that this is due to steric effects involving the two methyl groups attached to N(2) is discussed later.



$(\text{HZnNMe}\cdot\text{C}_2\text{H}_4\cdot\text{NMe}_2)_2$

Figure 5.1

(HZnN(Me)C₂H₄NMe₂)₂ TABLE 5e

Equations of Least Squares Planes referred to the crystal axes

Atoms in Plane 1	Orthogonal Co-ordinates in Å			Distance of Atom from Plane in Å
	x'	y	z'	
N(1)	0.8596	0.2436	1.1825	0.0064
C(1)	0.3563	1.1197	2.2632	-0.0019
C(5)	2.1820	-0.2613	1.5194	-0.0022

Equation of Plane 1: $0.4111 x' + 0.7893 y - 0.4561 z' = 0$

Atoms in Plane 2	Orthogonal Co-ordinates in Å		
	x'	y	z'
Zn	0.5663	1.1455	-0.6464
N(1)	0.8596	0.2436	1.1825

Equation of Plane 2: $0.7124 x' - 0.5773 y - 0.3990 z' = 0$

Dihedral angle between plane 1 and plane 2 = 88.9°

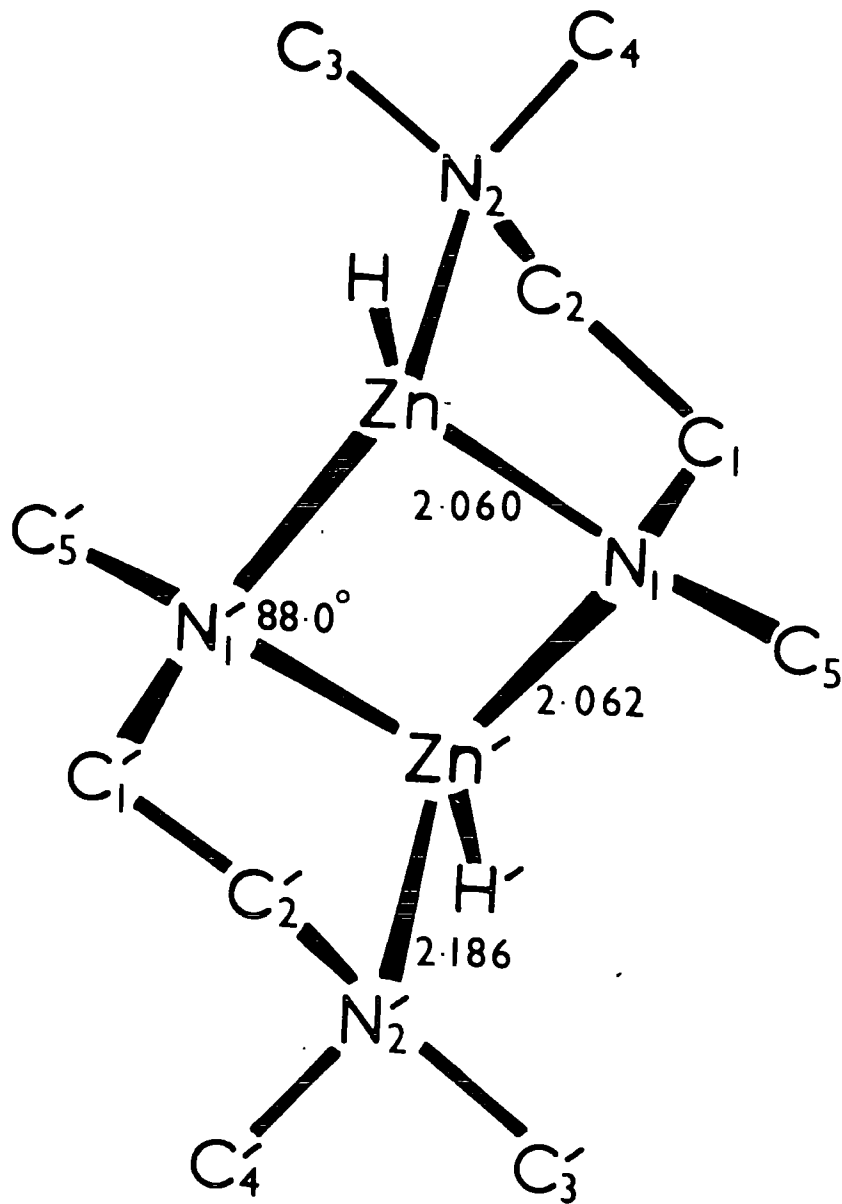
(HZnN(Me)C₂H₄NMe₂)₂ TABLE 5fBond lengths (Å) and their Standard Deviations (Å × 10³)

Zn - N(1)	2.060(10)
Zn - N(1')	2.062(11)
Zn - N(2)	2.186(11)
N(1) - C(1)	1.479(16)
N(1) - C(5)	1.455(21)
N(2) - C(2)	1.488(18)
N(2) - C(3)	1.507(22)
N(2) - C(4)	1.488(22)
C(1) - C(2)	1.514(23)
Zn - H(a)	1.72
Zn - H(b)	1.82

H(a) and H(b) represent the peaks on the first and second difference maps which might be assigned to the hydrogen atom attached to zinc.

(HZnN(Me)₂C₂H₄NMe₂)₂ TABLE 5gBond Angles with their Standard Deviations

	Angle	e. s. d.
N(1) - Zn - N(1')	92.0 ^o	0.4 ^o
N(1) - Zn - N(2)	84.1	0.4
N(1') - Zn - N(2)	110.6	0.5
C(1) - N(1) - C(5)	110.2	1.1
Zn - N(1) - C(5)	119.1	0.9
Zn' - N(1) - C(5)	117.1	0.9
Zn - N(1) - C(1)	109.9	0.7
Zn' - N(1) - C(1)	110.7	0.9
Zn - N(1) - Zn'	88.0	0.4
C(2) - N(2) - C(4)	112.5	1.2
C(2) - N(2) - C(3)	109.6	1.3
C(2) - N(2) - Zn	102.2	0.8
C(3) - N(2) - C(4)	109.9	1.2
C(4) - N(2) - Zn	102.6	1.0
C(3) - N(2) - Zn	119.8	0.9
N(1) - C(1) - C(2)	111.5	1.0
N(2) - C(2) - C(1)	110.6	1.4
H(a) - Zn - N(1)	140.5 ^o	
H(a) - Zn - N(1')	119.9	
H(a) - Zn - N(2)	103.3	
H(b) - Zn - N(1)	133.7	
H(b) - Zn - N(1')	125.4	
H(b) - Zn - N(2)	103.3	



$(\text{HZnN}(\text{Me}) \cdot \text{C}_2\text{H}_4 \cdot \text{NMe}_2)_2$
Some Bond Lengths and Angles

Figure 5.2

The sum of the Pauling covalent radii for zinc and nitrogen is 2.01\AA but purely covalent bonding in $(\text{HZnN}(\text{Me})\text{C}_2\text{H}_4\text{NMe}_2)_2$ would place formal charges of +1 on the nitrogen atoms and -2 on the zinc atom. The observed Zn-N distances are consistent with the Zn-N bonds having a little polar character.

The N-C bond lengths are all the same within the limits of experimental error, with a mean value of 1.48\AA . This compares well with the bond lengths found in ethylamine (1.47\AA) (Allen and Sutton, 1950) and in the tetramethylethylenediamine (TMED) moiety in AlH_3TMED (mean value 1.48\AA) (Palenik, 1964).

The C-C bond length (1.51\AA) also appears to be normal since it is not significantly different from the value (1.54\AA) found in diamond.

Both kinds of atoms involved in the central ring are four-coordinate and in terms of covalent bonding would formally be considered to be sp^3 hybridized. The N(1) - Zn - N(1)' angle in the ring is greater than the Zn - N(1) - Zn' angle (88.0°) but it is not easy to draw conclusions from this as distortions of the bond angles at zinc are to be expected as a consequence of the presence of the sterically unambitious hydrogen in one co-ordination position. The picture is further complicated by the simultaneous participation of the atoms Zn, N(1) in both a four-membered and a five-membered ring.

The two angles Zn - N(1) - C(5) and Zn' - N(1) - C(5) (119.1° and 117.1°) are considerably greater than the tetrahedral value, which is no

doubt a result of the Zn - N(1) - Zn' angle being constrained to 88.0° . The other three angles at N(1) do not differ significantly from the tetrahedral value.

A greater range of bond angles is found at N(2); C(3) - N(2) - Zn (120°) and C(2) - N(2) - C(4) (113°) are greater, while C(2) - N(2) - Zn (102°) and C(4) - N(2) - Zn (103°) are smaller than the tetrahedral value. These distortions are understandable in terms of a movement to alleviate the shortest non-bonding carbon-carbon contact (2.98\AA), namely that between C(4) and C(1).

Steric interferences involving C(3) and/or C(4) may also contribute to the lengthening of the Zn-N(2) bond. The intramolecular and intermolecular non-bonding contacts less than 4\AA are given in Table 5h. Contacts between carbons bonded to a common atom are not included.

The zinc-zinc separation (2.86\AA) is greater than the sum (2.62\AA) of the Pauling tetrahedral covalent radii. The shortest contact that the zinc atom makes with a methyl carbon (2.90\AA) is that involving C(4) and it will be apparent that this situation would be made worse by a shortening of the Zn-N(2) bond.

The short nitrogen-nitrogen contacts (2.85 and 2.96\AA) are those across the four-membered and five-membered rings respectively. Both are much greater than the sum (1.40\AA) of the tetrahedral covalent radii of two nitrogen atoms.

The intermolecular packing is shown in figure 5.3 which is in

(HZnN(Me)C₂H₄NMe₂)₂ TABLE 5h

Intramolecular non-bonding contacts less than 4Å^o

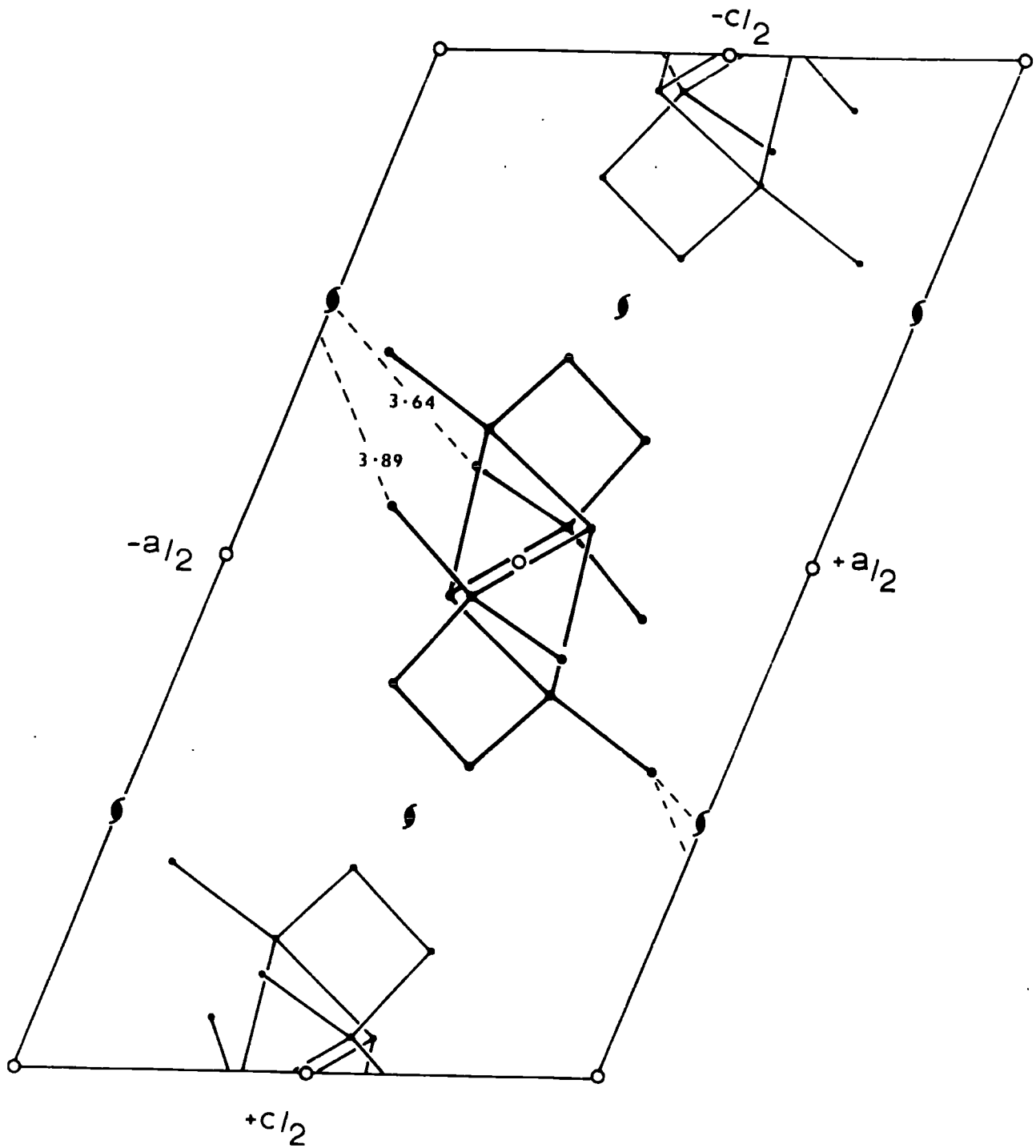
Equivalent Position 1	x,	y,	z;
Equivalent Position 2	-x,	$\frac{1}{2} + y,$	$\frac{1}{2} - z;$
Equivalent Position 3	-x,	-y,	-z;
Equivalent Position 4	x,	$-\frac{1}{2} - y,$	$-\frac{1}{2} + z;$

Atom A	Atom B	Equivalent Position	A-B Angstroms
Zn	Zn	3	2.864
Zn	C(4)	1	2.901
Zn	C(1)	3	2.932
Zn	C(5)	3	3.016
Zn	C(5)	1	3.046
Zn	C(3)	1	3.213
Zn	C(2)	3	3.372
Zn	N(2)	3	3.902
N(1)	N(2)	1	2.845
N(1)	N(1)	3	2.964
C(1)	C(4)	1	2.978
C(3)	C(5)	3	3.662

Intermolecular non-bonding contacts less 4Å^o

Atom A	Atom B	Equivalent Position	Cell	A-B Angstroms
C(3)	C(5)	4	(-1, 1, 0)	3.891
C(4)	C(5)	2	(1, 0, 0)	3.643

Unless otherwise stated the Equivalent position refers to the cell (0, 0, 0).



$(\text{HZnNMe} \cdot \text{C}_2\text{H}_4 \cdot \text{NMe}_2)_2$ projection
on the (010) plane

Figure 5.3

projection along b. Only two of the approach distances are less than 4.0\AA and both of these are greater than 3.6\AA so that there does not appear to be any significant interaction between separate dimeric molecules.

As mentioned earlier the temperature parameters are probably less reliable than the atomic co-ordinates. However the mean B values for each atom are the same to two decimal places whether derived from the data corrected for absorption or from that not corrected. The B values for the zinc and nitrogen atoms are about 4.5\AA^2 and the mean value for the carbon atoms is 6\AA^2 . These results are similar to those normally encountered (Shearer and Spencer, 1967).

5.9 The Zinc-Hydrogen Bond

Peaks on the two difference maps give an approximate position for the hydrogen atom attached to zinc, leading to values of $1.7-1.8\text{\AA}$ for the Zn-H bond length. A subsequent neutron diffraction study (Shearer and Spencer, 1968) has provided what is probably a more accurate position for this hydrogen in very much the same region but representing a rather shorter Zn-H bond length (1.61\AA).

The length of the Zn-H bond suggests that it is predominantly covalent in character since the sum of the covalent radii (1.62\AA) is very much less than the value expected for an ionic bond (the radius of the H^- ion in lithium hydride is 1.26 and the radius for zinc would certainly be greater than 0.74 , the radius of the Zn^{++} ion, so that an ionic

Zn-H bond would probably be at least $2\overset{\circ}{\text{Å}}$ long). The classification of ZnH_2 as a borderline covalent hydride (Cotton and Wilkinson, 1962) is consistent with this observation.

The hydrogen atom attached to zinc was the one most easily distinguished by X-ray diffraction and this factor is consistent with the Zn-H bond having some polar character.

The Zn-H bond length from the neutron study is not significantly longer than the value ($1.59\overset{\circ}{\text{Å}}$) obtained for a shortlived species by spectroscopic methods (Herzberg, 1950).

There can be no question of hydrogen-bridging between zinc atoms of different dimeric units since the shortest contact between zinc atoms not of the same dimer is greater than $5\overset{\circ}{\text{Å}}$.

(HZnN(Me)C₂H₄NMe₂)₂ TABLE 5d

Final Values of Observed and Calculated Structure Factors

APPENDICES

APPENDIX 1

Isothermal Molecular Weight Measurement

The molecular weight of ethylzinc iodide was measured, using ethyl iodide as solvent, in the apparatus shown in figure A1. Initially the apparatus was placed in a specially designed oven, evacuated through a tap attached to one of the cones, A, and baked at 380°C for 12 hours to remove traces of water. It was then filled with nitrogen via the other cone and allowed to cool to room temperature. A solution of ethylzinc iodide in ethyl iodide was syringed, against a counter current of nitrogen, into one of the bulbs, B, and a solution of triphenylmethane, as standard, into the other. The apparatus was then inverted and the volumes of the solutions measured by allowing them to run into the graduated pipettes, C.

Thus a known weight of both standard and unknown was introduced into the apparatus.

The solutions were allowed to run back into the bulbs which were then cooled to -196°C (to freeze the solutions). The apparatus was evacuated through the cones, sealed at the constrictions, D, and allowed to warm to room temperature, after which it was kept in a draught-free cupboard.

Solvent distilled from the solution of lower molarity to the more concentrated one until the two were equimolar. The molecular weight

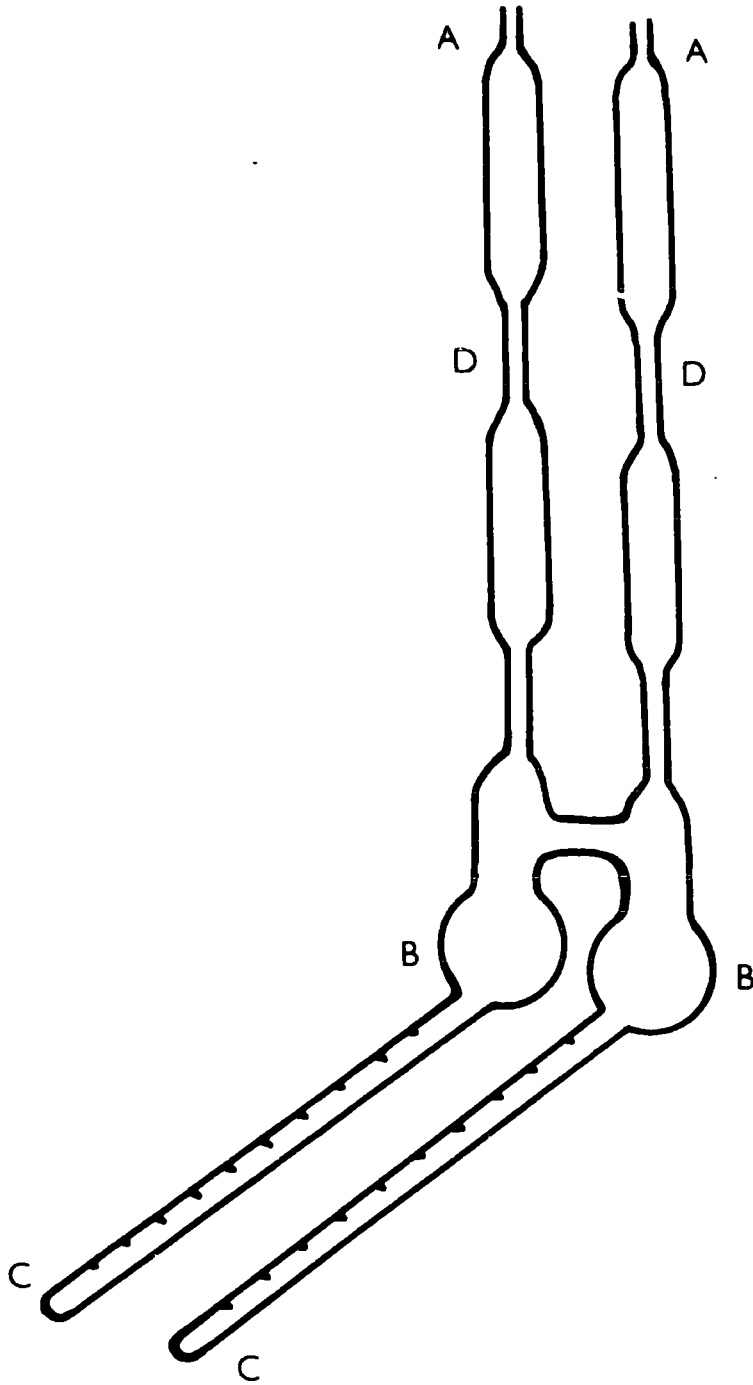


FIGURE A I

of the ethylzinc iodide species was then given by the relationship

$$M_1 = \frac{G_1 M V}{G V_1}$$

where G_1 is the weight of ethylzinc iodide, V_1 is the volume of the solution of ethylzinc iodide at equilibrium. G , V and M are the weight, final volume of solution and molecular weight of the standard (triphenylmethane).

Runs were made in duplicate and any which showed a precipitate were rejected. An example of the variation of the volumes of the two solutions in a successful run is shown in figure A2.

$$G_1 = 0.0012 \text{ grams, } G = 0.023 \text{ grams;}$$

$$M_1 \text{ calculated for } (C_2H_5ZnI) = 221.5, M_1 \text{ observed} = 227.0.$$

The method is based on that described by Steyermark (1961).

EtZnI : Molecular weight in Ethyl Iodide

Variation of volumes during isopiestic distillation

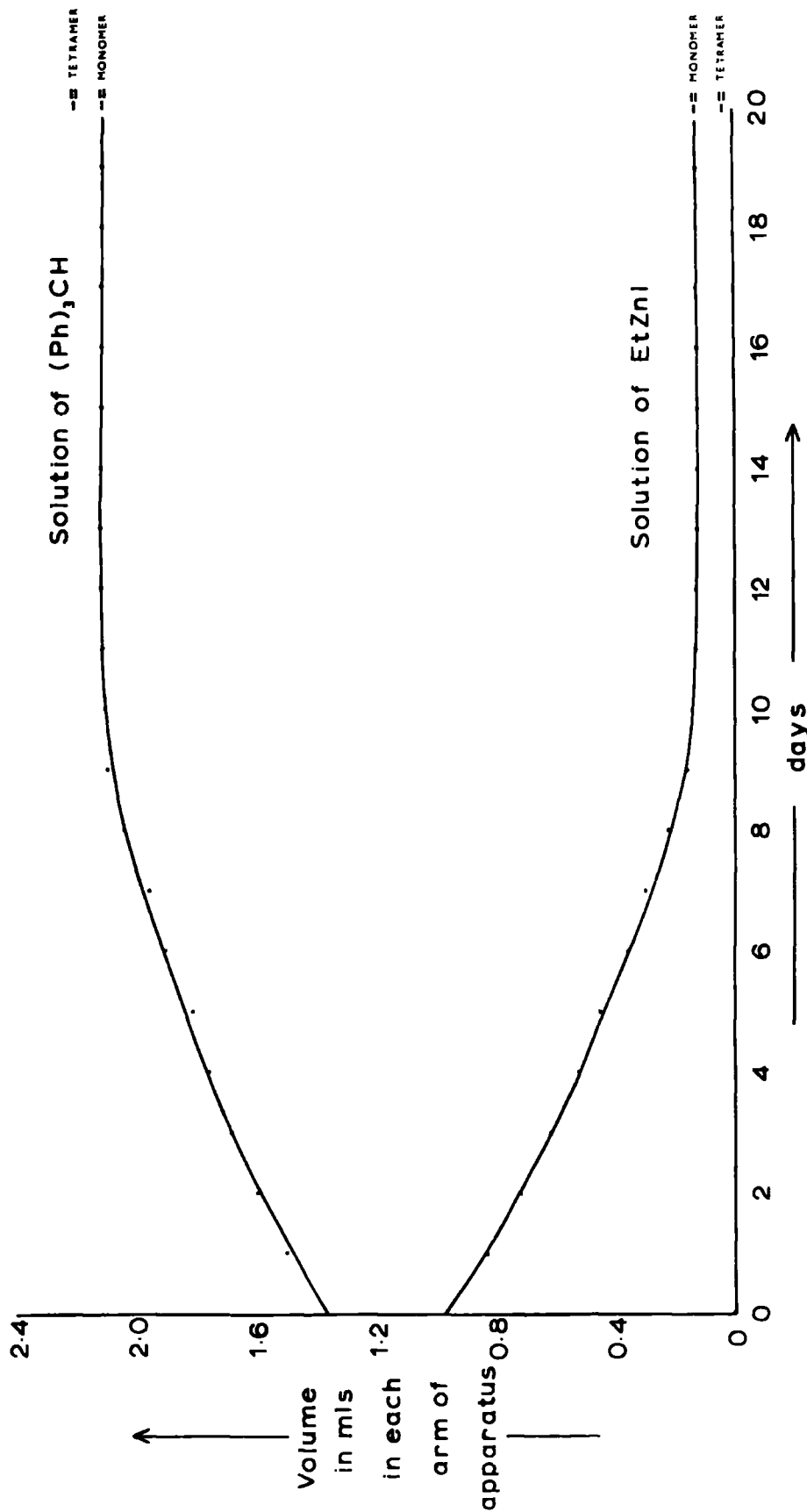


Figure A2

APPENDIX 2

Computer Programmes

Calculations were performed on the Elliott 803B computer here in Durham, the English Electric KDF9 computer in the University of Newcastle and on the Northern Universities Multiple Access computer. Thanks are due to the staffs of the computer units in Durham and in Newcastle for their assistance in running programmes.

I am indebted to Professor D.W.J. Cruickshank, Dr. J. Sime, and their associates, for making available the system of programmes written by the Glasgow group. The Mark II (November, 1965) version of the Glasgow structure factor-least squares programme, the Fourier programme written by Dr. Sime, and the several programmes to calculate molecular parameters, were found to be particularly useful.

I am also grateful to Dr. G.W. Adamson whose data correction programme I used for Lorentz, polarisation and spot length corrections on Weissenberg data, and to Mr. J. Twiss whose programmes corrected precession data for Lorentz and polarisation factors and Weissenberg data for absorption.

Various small programmes were written to meet sundry needs such as data format adjustment and the preparation of structure factor tables.

REFERENCES

- Abraham, M.H. and Rolfe, P.H., (1967), J. Organometallic Chem., 7, 35.
- Abrahams, S.C. and Sime, J.G., (1960), Acta Cryst., 13, 1.
- Adamson, G.W. and Shearer, H.M.M., (1965), Chem. Comm., 240.
- Adamson, G.W. and Shearer, H.M.M., (1966), Acta Cryst., Supplement,
7th (Moscow) Congress, Abstract 9.2.
- Adamson, G.W. and Shearer, H.M.M., (1967), personal communication.
- Allen, P.W. and Sutton, L.E., (1950), Acta Cryst., 3, 46.
- Ashby, E.C., (1967), Quart. Rev., 21, 259.
- Ashby, E.C. and Arnott, R., (1967), unpublished results.
- Ashby, E.C., Duke, R. and Neumann, H.M., (1967), J. Amer. Chem. Soc.,
89, 1964.
- Ashby, E.C. and Smith, W.B., (1964), J. Amer. Chem. Soc., 86, 4363.
- Ashby, E.C. and Walker, F., (1967), J. Organometallic Chem., 7, P17.
- Barbaras, G.D., Dillard, C., Finholt, A.E., Wartik, T., Wilzbach, K.E.
and Schlesinger, H.I., (1951), J. Amer. Chem. Soc., 73, 4585.
- Beachley, O.T. and Coates, G.E., (1965), J. Chem. Soc., 3241.
- Bell, N.A. and Coates, G.E., (1968), J. Chem. Soc.(A), 823.
- Bikales, N.M. and Becker, E.I., (1962), Canad. J. Chem., 41, 1329.
- Blomberg, C. and Vreugdenhil, A.D., (1965), Rec. Trav. Chim., 84, 39.
- Boersma, J. and Noltés, J.G., (1968), J. Organometallic Chem., 13, 291.
idem, (1966), Tetrahedron Letters, 1521.
- Bradley, A.J., (1935), Proc. Phys. Soc., 47, 879.
- Broch, E., (1927), Zeits. Phys. Chem., 127, 446.

- Bryce-Smith, D. and Graham, I.F., (1966), Chem. Comm., 559.
- Busing, W.R. and Levy, H.A., (1957), Acta Cryst., 10, 180.
- Caughlan, C.N. and Watenpaugh, K., (1967), Chem. Comm., 76.
- Clark, D., (1968), personal communication.
- Coates, G.E., Heslop, J.A., Redwood, M.E. and Ridley, D., (1968),
J. Chem. Soc.(A), 1118.
- Coates, G.E. and Heslop, J.A., (1966), J. Chem. Soc.(A); 26.
- idem, (1968), *ibid*, 514.
- Coates, G.E. and Ridley, D., (1965), J. Chem. Soc., 1870.
- idem, (1966), J. Chem. Soc.(A), 1064.
- idem, (1966a), Chem. Comm., 560.
- idem, (1967), J. Chem. Soc.(A), 56.
- Coates, G.E. and Roberts, P.D. (1968), J. Chem. Soc.(A), in press.
- Coates, G.E. and Wade, K., "Organometallic Compounds", Volume I; The
Main Group Elements, Methuen, (1968).
- Cotton, F.A. and Wilkinson, G., (1962), "Advanced Inorganic Chemistry",
Interscience.
- Cruickshank, D.W.J., Pilling, D.E., Bujosa, A., Lovell, F.M. and
Truter, M.R., (1961), "Computing Methods and the Phase Problem in
X-ray Crystal Analysis", p.32. Oxford, Pergamon.
- Dahl, L.F., Davis, G.L., Wampler, D.L. and West, R., (1962), J. Inorg.
and Nucl. Chem., 24, 357.
- de Meulenaer, J. and Tompa, H., (1965), Acta Cryst., 19, 1014.
- Dessy, R.E. (1960), J. Amer. Chem. Soc., 82, 1580.

- Dessy, R.E., Handler, G.S., Wotiz, J.H. and Hollingsworth, C.A., (1957), J. Amer. Chem. Soc., 79, 3476.
- Dessy, R.E. and Coe, G.R., (1963), J. Org. Chem., 28, 3592.
- Ellinger, F.H., Holley, C.E., McInteer, B.B. Pavone, D., Potter, R.M., Staritzky, E. and Zachariasen, W.H., (1955), J. Amer. Chem. Soc., 77, 2647.
- Evans, D.F. and Maher, J.P., (1962), J. Chem. Soc., 5125.
- Evans, D.F. and Wharf, I., (1966), J. Organometallic Chem., 5, 108;
see also, idem, (1968), J. Chem. Soc.(A), 783.
- Frankland, E., (1849), Annalen, 71, 171.
- Gillespie, R.J., (1960), J. Amer. Chem. Soc., 82, 5978.
- Gillespie, R.J. and Nyholm, R.S., (1957), Quart. Rev., 11, 339.
- Gordy, W. and Sheridan, J., (1954), J. Chem. Phys., 22, 92.
- Grdenich, D.R. and Kitaigorodskii, A.I., (1949), Zhur. Fiz. Khim., 23, 1161.
- Guggenberger, L.J. and Rundle, R.E., (1964), J. Amer. Chem. Soc., 86, 5344.
- Hamelin, R. and Hayes, S., (1961), Compt. rend., 252, 1616.
- Herzberg, G., (1950), "Molecular Spectra and Molecular Structure. Infrared Spectra of Diatomic Molecules", van Nostrand Co., New York. 2nd Edition.
- Hilpert, S. and Gruttner, G., (1913), Ber., 46, 1675.
- Hodgson, L.I. and Rollett, J.S., (1963), Acta Cryst., 16, 329.
- Holm, T., (1968), Acta. Chem. Scand., 21, 2753.
- Hvolfsef, J., (1958), Acta Chem. Scand., 12, 1568.
- Jander, G., Fischer, L. and Winkler, G., (1958), Z. Elektrochem., 62, 971.

- Jellinek, F., (1958), Acta Cryst., 11, 677.
- Job, A. and Reich, R., (1923), Bull. Soc. Chim. France, 33, 1414.
- Jolibois, P., (1912), Compt. rend., 155, 353.
- Karrer, P., Canal, F., Zohner, K. and Widmer, R., (1928), Helv. Chim. Acta., 11, 1083.
- Kimura, K. and Kubo, M., (1959), J. Chem. Phys., 30, 151.
- Kharasch, M.S. and Reinmuth, O., (1954), "Grignard Reactions of Non-Metallic Substances", Constable and Co., London.
- Kocheshkov, K.A., Sheverdina, N.I. and Paleeva, J.E., (1963), Bull. Soc. Chim. France, 1472.
- Mackay, K.M., (1966), "Hydrogen Compounds of the Metallic Elements", Spon, London.
- Miller, J., Gregarion, G. and Mosher, H.S., (1961), J. Amer. Chem. Soc., 83, 3955.
- Mills, J.C. and Kennard, C.H.L., (1967), Chem. Comm., 834.
- Monahan, J.E., Schiffer, M. and Schiffer, J.P., (1967), Acta Cryst., 22, 322.
- Nesmeyanov, A.N. and Sazonova, V.A., (1941), Izvest. Akad. Nauk. S.S.S.R., Org. Khim. Nauk., 499 (translated in "Selected Works in Organic Chemistry", A.N. Nesmeyanov, pp.252-276, Pergamon Press, Oxford, 1963).
- Noltes, J.G. and Van Den Hurk, J.W.G., (1965), J. Organometallic Chem., 3, 228.
- Oswald, von H.R., (1960), Helv. Chim. Acta, 43, 77.
- Palenik, G.J., (1964), Acta Cryst., 17, 1573.

Pauling, L., (1947), J. Amer. Chem. Soc., 69, 542.

Pauling, L., (1960), "The Nature of the Chemical Bond" 3rd Edition,
Cornell University Press.

Pfeiffer, P. and Blank, H., (1939), J. Prakt. Chem., [2], 153, 242.

Ridley, D., (1965) - Ph.D. Thesis, Durham.

Robertson, J.H. and Beevers, C.A., (1950), Acta Cryst., 3, 164.

Rossmann, M., (1956), Acta Cryst., 9, 819.

Rundle, R.E., (1963), "A Survey of Progress in Chemistry", Ed. A.I.

Scott, Academic Press, p.81ff.

Rundle, R.E. and Stucky, G.D., (1964), J. Amer. Chem. Soc., 86, 4825.

idem, *ibid*, (1964a), 86, 4821.

Salinger, R.M., (1963), "A Survey of Progress in Chemistry", Ed. A.I.

Scott, Academic Press, p.301ff.

Schneider, M.L. and Shearer, H.M.M., (1968), personal communication.

Shearer, H.M.M. and Spencer, C.B., (1966), Chem. Comm., 194.

Shearer, H.M.M. and Spencer, C.B., (1967), - C.B. Spencer - Ph.D. Thesis,
Durham.

Shearer, H.M.M. and Spencer, C.B., (1968), personal communication.

Shearer, H.M.M. and Twiss, J., (1968), personal communication.

Sim, G.A., (1961), "Computing Methods and the Phase Problem in X-ray
Crystal Analysis", Oxford Pergamon Press.

Singer, M.S., Salinger, R.M. and Mosher, H.S., (1967), J. Org. Chem.,
32, 3821.

- Steyermark, L., (1961), "Quantitative Organic Microanalysis",
Academic Press, pp.535-9; see also Signer, R., (1930), Annalen,
478, 246.
- Strauss, F., (1912), Ann. Chem., 393, 235.
- Stucky, G.D. and Toney, J., (1967), Chem. Comm., 1168.
- Swain, C.G. and Boyles, H.B., (1951), J. Amer. Chem. Soc., 73, 870.
- Wakefield, B.J., (1966), Organometallic Chem. Rev., 1, 131.
- Wiberg, E., Henle, W. and Bauer, R., (1951), Zeit. Naturf., 6b, 393.
- Wiberg, E. and Henle, W., (1952), ibid., 7b, 249.
- Woolfson, M.M., (1956), Acta Cryst., 9, 804.
- Yoffe, S.T. and Nesmeyanov, A.N., (1957), "Handbook of Magnesium-
Organic Compounds", 3 vols., Pergamon Press, London.

LIBRARY
- 3 MAY 1969
L. B. GRANT